BRNO FACULTY OF CIVIL UNIVERSITY ENGINEERING OF TECHNOLOGY

BRNO UNIVERSITY OF TECHNOLOGY

FACULTY OF CIVIL ENGINEERING

INSTITUTE OF STRUCTURAL MECHANICS

NUMERICAL ANALYSIS OF STRESS FIELDS IN SELECTED CROSS-SECTIONS OF STEEL BEAMS WITH INITIATED CRACKS

BACHELOR THESIS

AUTHOR   Jorge Álvarez Morán

SUPERVISOR   Doc. Ing. Stanislav Seitl, Ph.D
SUPERVISOR SPECIALIST: Ing. Petr Miarka

BRNO 2020

ABSTRACT

In this Bachelor Thesis, a numerical and parametrical analysis for different cross-sections of beams with initiated cracks is developed. Structural components used in different civil or mechanical constructions contain defects, like cracks. In this sense, it must be studied how these cracks affect the behaviour of the structure and how they evolve in time under applied loads. The stress fields in front of the crack tip three-point bending test is studied for three main cross-sections: I profile, IPE profile and UPE profile. In order to do this, these specimens are modelled in ANSYS, a finite element method software. It will be analysed how different crack lengths, profile dimensions and material properties influence the stress distribution in the structural element. The models are based on linear elastic fracture mechanics and, therefore, the main aim will be the determination of the stress intensity factor, as it is the main parameter for the description of the stress fields in front of the crack tip.

KEYWORDS

Fracture mechanics, stress intensity factor, finite element method, crack, Poisson's ratio, three-point bending test, beam profiles

RESUMEN

En este Trabajo fin de grado se lleva a cabo un análisis numérico y paramétrico para diferentes secciones de vigas con grietas iniciadas. Muchos componentes estructurales usados en la ingeniería civil o mecánica contienen defectos, como grietas. Por ello, debe ser estudiado como estas grietas afectan al comportamiento de la estructura y cómo evolucionan y crecen con el tiempo bajo una carga aplicada. El campo de tensiones en el frente de la grieta en un ensayo de flexión a tres puntos es analizado para tres secciones: perfil I, perfil IPE y perfil UPE. Con este objetivo, los tres perfiles son modelados mediante ANSYS, un software de elementos finitos. Se analizará como las diferentes longitudes de grieta, dimensiones de los perfiles y propiedades de los materiales influencian la distribución de tensiones en el componente. El análisis se basa en la mecánica de la fractura elástica lineal. Por lo tanto, el principal objetivo será la determinación del factor intensidad de tensiones, ya que es el parámetro más representativo para la descripción de las tensiones en el frente de la grieta.

PALABRAS CLAVE

Mecánica de fractura, factor intensidad de tensiones, método de elementos finitos, grieta, coeficiente de Poisson, prueba de flexión de tres puntos, perfiles de vigas

BIBLIOGRAPHIC CITATION

ACKNOWLEDGEMENT

TABLE OF CONTENTS

1. Introduction

Structures found in engineering and construction are built from elements which must bear the loads applied on them. However, these components have defects that could affect the service lifetime of the structure [14] . Fracture mechanics analyses how these defects affect the material's behaviour. During the life of the structure defects and cracks appear due to imperfections, scratch or material inhomogeneity. These cracks can start to propagate under cyclic loads which can result in a catastrophic failure of the structure. So, it is very important to have knowledge about the fatigue crack propagation during the lifetime of a given component [18].

In this sense, the study on how these cracks grow and develop over time is crucial in the design of any engineering component. Therefore, determining crack growth is one of the main objectives of fracture mechanic [14]. The main parameter of fracture mechanics is the stress intensity factor (K) which defines the stress fields in front of the crack tip, moreover, when it reaches to a critical value, called fracture toughness (K_C), the breakage takes place [22].

In this thesis the determination of the stress intensity factor in beams with different cross sections [20] and initiated cracks is developed. It is analysed how the different geometries, crack lengths and material properties affect the stress fields in front of the crack tip. The parametrical study has been performed by means of a three-point bending test in which the specimens have a crack at the middle of the span.

The models were simulated in ANSYS [3], a finite element software. The software provided data of stresses in front of the crack tip which are used to calculate the stress intensity factor for the different cross sections of beams and combinations with crack length. All the data obtained in this parametrical study is summarized by graphical representations such as tables and graphs.

2. Aims

The aim of this thesis is to compare the stress field description by means of the stress intensity factor (SIF) in different cross-sections of steel beams with short edge-initiated cracks under bending load.

The analysis will be performed initially to an I-shape profile with varying crack length, material properties and web thicknesses with constant flange width and thickness. Moreover, results for this profile will be compared to a rectangular cross-section profile.

Then different IPE and UPE profiles, see [9], will be analysed to determine its stress fields for different crack lengths and, finally, calibration curves will be obtained for these profiles. In addition, a comparison with rectangular profiles will also be developed.

It is important to remark that the numerical analysis will be developed by means of the Finite Element Method Software, ANSYS.

3. Theoretical Background

3.1 Fracture Mechanics

Fracture mechanics analyses how the fracture and breakage mechanisms occur in various materials. Its aim is predicting the mechanical behaviour of structural components when they are subjected to external loads. It is considered that materials are not perfectly solid and uniform, but that they have cracks or imperfections with variable size. Fracture mechanics is based on the use of three main parameters which are related among them: size of the crack or defect, applied tension and fracture toughness [2].

There are two main criteria for the fracture analysis, which are mainly equivalent:

- The energy criterion affirms that the crack growth takes place when the energy (generated by the external forces) in the material is higher than the own resistance of the material.

- The stress intensity approach states that the stress components in the crack tip are proportional to a constant, K_I, which is called stress intensity factor (SIF). Therefore, this constant gives the entire stress distribution in front of the crack tip. Figure 1 shows the stress components in the crack tip and the equations which are used to calculate them.

$$\sigma_{xx} = \frac{K_I}{\sqrt{2\pi r}} \cos\left(\frac{\theta}{2}\right)\left[1 - \sin\left(\frac{\theta}{2}\right)\sin\left(\frac{3\theta}{2}\right)\right]$$

$$\sigma_{yy} = \frac{K_I}{\sqrt{2\pi r}} \cos\left(\frac{\theta}{2}\right)\left[1 + \sin\left(\frac{\theta}{2}\right)\sin\left(\frac{3\theta}{2}\right)\right]$$

$$\tau_{xy} = \frac{K_I}{\sqrt{2\pi r}} \cos\left(\frac{\theta}{2}\right)\sin\left(\frac{\theta}{2}\right)\cos\left(\frac{3\theta}{2}\right)$$
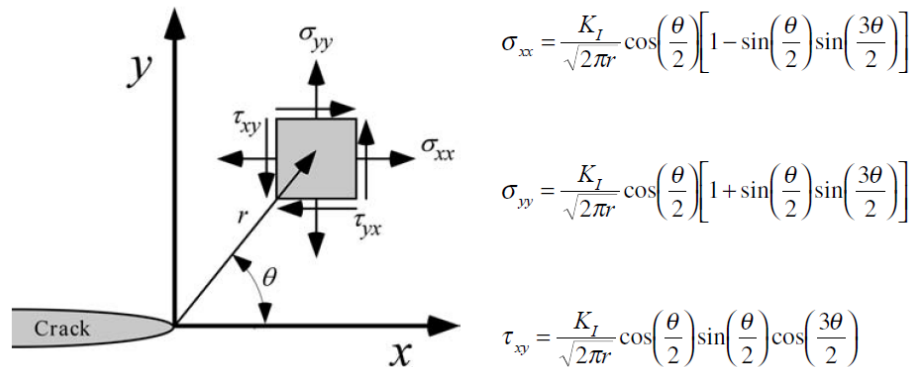
Figure 1: Coordination system with start in crack tip and description of stress fields for 2D, retaken from [2]

It is important to remark that in this approach the fracture occurs when the stress intensity factor reaches a critical value, called K_{IC}, which is a property of the material and a measure of fracture toughness.

There are two basic theories which try to explain fracture mechanics: linear elastic fracture mechanics (LEFM) and elastic-plastic fracture mechanics (EPFM). In this thesis, the analysis is performed using LEFM as the main theory [2].

3.2 Linear Elastic Fracture Mechanics

This theory was developed before the second half of the XX century. It is only applicable to materials which fulfil Hooke's law, therefore, the plastic region in front of the crack tip is considered to be negligible. In case that there is certain plasticity (non-linear material behaviour) in this region this theory cannot be used, and elastic-plastic fracture mechanics

should be used. Figure 2 shows the applicability of the theories in function of the plastic region developed in front of the crack tip.
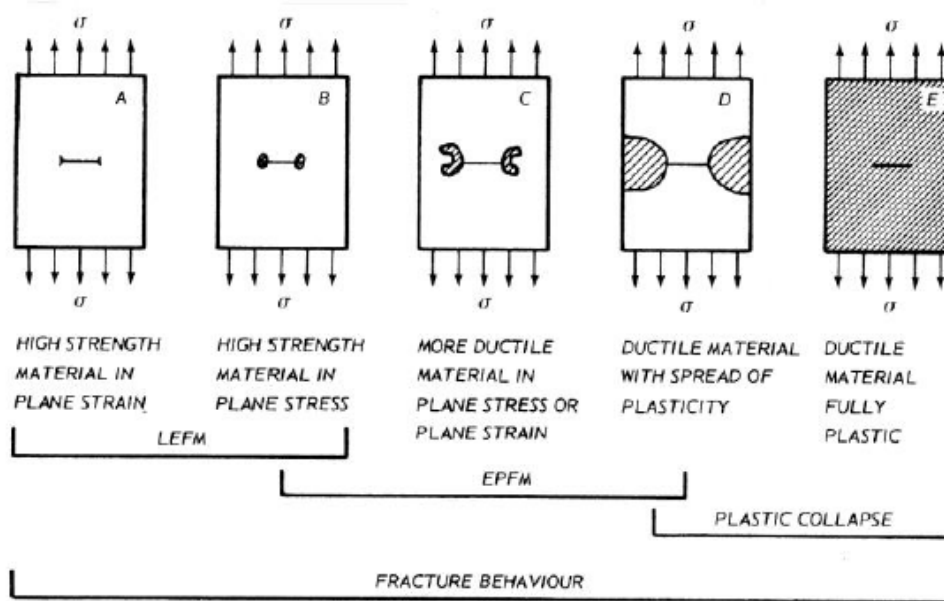
Figure 2: Plastic region in different materials, retaken [2]

Some expressions can be derived for the stresses in a body (assuming isotropic linear elastic behaviour of the material) for a cracked solid subjected to external forces [10]. By defining a polar coordinate system with the origin of coordinates located at the crack tip, the stress field is defined as follows:

$$\sigma_{ij} = \left(\frac{k}{\sqrt{r}}\right) f_{ij}(\theta) + \sum_{m=0}^{\infty} A_m r^{\frac{m}{2}} g_{ij}{}^{(m)}(\theta) \tag{1}$$

where σ_{ij} is the stress tensor, r is the radius, θ is the angle, k is a constant, f_{ij} is a dimensionless function of θ, A_m is the amplitude and g_{ij} is a dimensionless function depending on θ. The leading term of the equation is $1/\sqrt{r}$. In this sense when r tends to 0, the stress tends to infinity, what leads to a singularity for $r=0$.

3.3 Stress Intensity Factor

There are three types of loading which can act individually or combined over a solid which has a crack, they will be defined as follows [2]:

- Mode I: the stress is applied in a normal direction to the fracture plane. Opening of the crack.

- Mode II: the shear stress is applied in a normal direction to the front of the crack. One crack slide with respect to the other.

- Mode III: shear stress is applied in a parallel direction to the front of the crack.

Figure 3 describes the mentioned three modes.
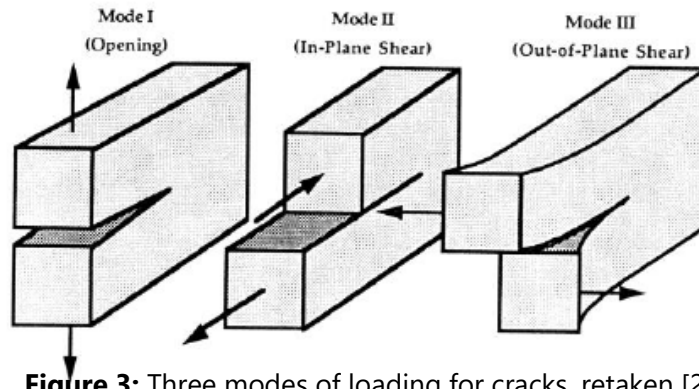

| Mode I | Mode II | Mode III |
| (Opening) | (In-Plane Shear) | (Out-of-Plane Shear) |

Figure 3: Three modes of loading for cracks, retaken [2]

The constants k and f_{ij} depend on the mode of loading. The proportionality constant k can be replaced by the stress intensity factor [2]:

$$K = k\sqrt{2\pi} \qquad (2)$$

Moreover, the stress intensity factor depends on the mode of loading, so a sub-index is used to indicate the mode: K_I, K_{II} and K_{III}. When under a cracked solid there is a mixed mode of loading (more than one mode of loading is applied simultaneously), the stress tensor is obtained by adding the individual contributions of each mode:

$$\sigma_{ij} = \sigma_{ij}{}^{(I)} + \sigma_{ij}{}^{(II)} + \sigma_{ij}{}^{(III)} \qquad (3)$$

In case of a mode I on a crack plane with $\theta = 0°$, the shear stress τ_{xy} becomes zero and the stresses in the x and y direction are equal:

$$\sigma_{xx} = \sigma_{yy} = \frac{K_I}{\sqrt{2\pi r}} \qquad (4)$$

This equation is only valid for a region close to the crack tip, it is important to remark that r is the distance to the crack tip. Therefore, a zone is defined near the crack tip where the stresses in all the points are directly proportional to the stress intensity factor (singularity-dominated zone). In this sense, once the SIF is known all the stress distribution in this region can be known. Figure 4 expresses the variation of the stress, σ_{yy}, which is perpendicular to the crack plane and shows the singularity-dominated zone:
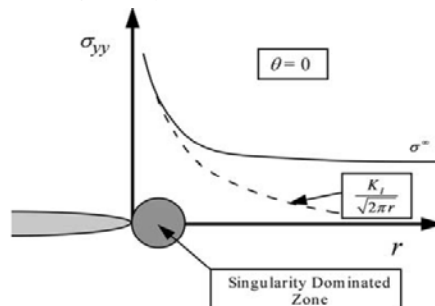

Figure 4: The course of the stress in the yy direction, $\boldsymbol{\sigma_{yy}}$, perpendicular to crack plane, retaken [2]

The parametric description of the region near the crack tip depending in only one variable is one of the most relevant concepts in fracture mechanics. In this sense, the SIF is a parameter that allows to carry out this description and to parametrically parametrise this region. Moreover, the stress intensity factor, K, depends on the applied stress, σ, the size/length of the crack, a, and the geometry being considered, C:

$$K = C\sigma\sqrt{\pi a} \tag{5}$$

The value of the function C depends on the geometry of the crack and specimen under study. Many studies have been carried out to calculate the values of C for different configurations which are common in engineering. Such as superficial elliptical cracks, initiated cracks on holes or cracks located in containers subjected to internal pressure.

3.4 Fatigue Crack Propagation

Usually structures and its components contain cracks and therefore it is crucial to determine if those flaws will grow and at what rate will they grow to determine the lifetime of the given structure. When subjected to cyclic loads the crack tends to propagate and, therefore, it is very important to know about the growing of the crack. Linear elastic fracture mechanics is a method used for the explanation of the propagation of a crack in case of small-scale yield. The Paris-Erdogan's law [17] relates the rate of propagation *da/dN* of the crack with the variation of the stress intensity factor, ΔK, in the crack tip:

$$\frac{da}{dN} = C(\Delta K)^m \tag{6}$$

C and m are material constants, N Is the number of loading cycles and ΔK the range of the stress intensity factor. ΔK can be defined as follows:

$$\Delta K = \Delta\sigma\sqrt{\pi a}f(\frac{a}{W}) \tag{7}$$

$\Delta\sigma$ is stress range, a is the length of the crack, W is the height of the profile under study and, finally, *f(a/W)* is the calibration curve which is a function that reflects the boundary conditions.

One of the goals of the thesis will be to determine the calibration curves for various standard profiles in a three-point bending test. Calibration curves are polynomials which depend on the ratio *a/W*, in case of standard specimens and known configurations these calibration curves are stated in [16].

Calibration curves are very useful as an input for software in order to predict, in a more accurate way, the fatigue life of a structural component. The analysis of the calibration curves is usually done for ratios of *a/W* ranging from 0.2 to 0.8. In this thesis, the calibration curves will be analysed for rather short cracks (ranging from 0.002 to 0.08).

3.5 Three-Point Bending Test

The three-point bending test (3PBT) is one of the most common flexural tests, in this final thesis it will be the test used. In it the specimen is supported by two rollers and a force is applied at half of the span, S, between both supports. Moreover, in half of the span and in the opposite side to the face where the load is applied there is an initiated crack with a given length, a. Figure 5 represents graphically the 3PBT:
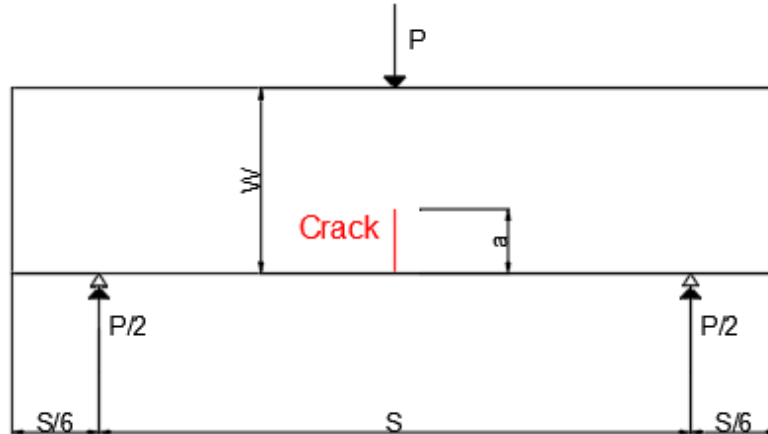

Figure 5: Three-point bending test diagram

The distribution of stresses in the cross-section containing the crack, in case of a three- point bending, is disrupted due to the proximity and presence of the load application point. This causes a strees gradient at the free surface opposite to the load and a deviating extreme fibre stress [19]. Therefore, the stress distribution differs a little from the one that could take place in a pure bending test, which is determined by simply applying the elastic beam theory.

3.6 Material - Steel

The steel is one of the most used materials in construction and engineering, it is an alloy made up, mainly, of iron and carbon. The percentage of iron is very high while the percentage of carbon never exceeds 2-2.5%, other elements can be present in the alloy (but in a small percentage) such as: sulphur, manganese or nickel. It is important to remark, that the steel alloys vary a lot in composition, and therefore, in properties. Depending on the usage of the alloy the composition of steel varies accordingly.

Pure iron (Fe) is soft and useless as a material for engineering applications. However, when adding carbon (C) in small amounts increases the strength and coverts iron into steel. When steel is solid carbon can be found in steel as: austenite, ferrite or carbide (it can be cementite, Fe_3C). In this sense, the percentage of carbon in the steel varies the microstructure and, therefore, the properties of the alloy. The effects of carbon (as well as the temperature) in steel are very well explained by the iron-carbon diagram, Figure 6.

The main advantages of steel main advantages are the: high strength/weight ratio, ductility, fatigue strength and quality of construction. However, in the other hand, the strength of steel is reduced a lot in case of fire or high temperatures, it is more costly than other materials and it is quite susceptible to corrosion.
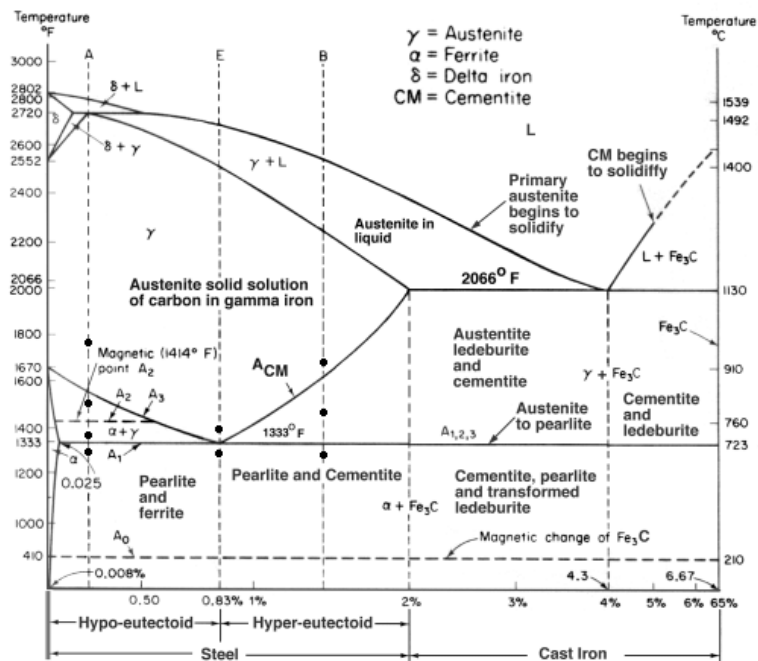

Figure 6: Iron-carbon diagram, retaken [7]

3.7 Finite Element Method

The Finite Element Method (FEM) is a numerical technique used for the simulation of a physical phenomenon such as structural, thermal or fluid behaviour. These phenomena are defined by means of partial differential equations, which are hard to solve by computers. In this sense, numerical methods had to be developed and one of the most important is the Finite Element Method. This method was developed in the second half of the XX century in order to solve structural problems related to the structural engineering.

Engineering mechanics face many problems in which it is required to solve partial differential equations to determine the behaviour of structures (such as determining stresses or displacements). These equations are really hard to compute and to solve, so the finite element method is basically a numerical technique to obtain an approximate solution of these partial differential equations. Nowadays, the use of this method is very widely spread as it helps engineers to optimize and improve their design.

The simulations developed in FEM are based in the creation of a mesh formed by a huge number of elements with recreate the shape of the structural part under study, Figure 7 represents a mesh over a structural profile. In each element calculations are performed, so by combining the results of all the elements, the global behaviour of the component can be obtained. Therefore, values are only known at certain points in the structure, these points are called nodal points. In this sense, the calculations of variables in regions between nodal points is carried out by means of polynomial approximations which can be linear, quadratic, cubic…
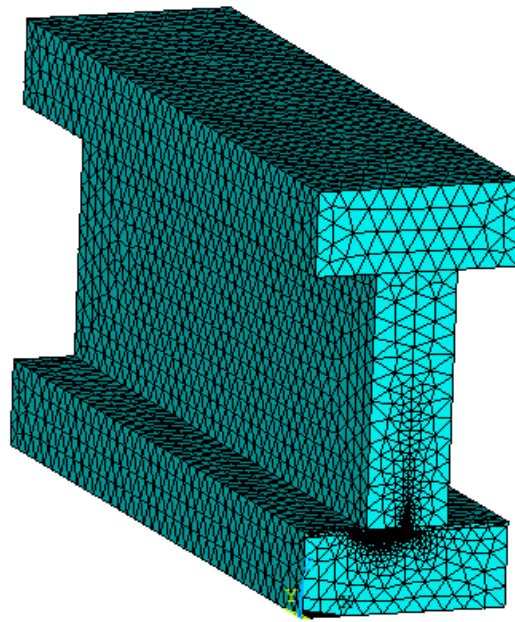
Figure 7: Mesh example of the FEM applied to a structural profile in software ANSYS

Therefore, with the FEM it is possible to convert a system with an infinite number of unknowns (continuous system) into a system with a finite number of unknowns (discrete system). Moreover, one of the biggest advantages of the FEM is that the mesh can be discretized in different sizes according to the region. For example, very fine element size can be used in regions closed to the crack tip and more coarsely far away from the crack tip. So, a good approximation can be obtained in zones with high gradients of stress, like in the crack tip.

In this thesis the results will be obtained by applying this method to a three-point bending test for different profiles with initiated cracks.

4. Numerical Model

The 3D numerical models developed in this final thesis are mainly three, they simulate a three-point bending test in three different cross-sections, they are the following:

- I cross-section profile
- IPE cross-section profile (according to European Standards)
- UPE cross-section profile (according to European Standards)

In order to model them ANSYS [3] was the finite element software used. In the following pages these models will be explained in further detail.

Some other models simulating rectangular cross section beams where also developed as a way of comparison between them and 3 selected profiles under study.

4.1 Cross-sections under Study

First of all, a description of the profiles will be developed to show the shape of the different profiles as well as their different parts. It is important to remark that these profiles are composed of too clearly differentiated parts: the web is the central part of the profile and the flange is the part of the profile that is located at the sides in order to resist the bending moments. Moreover, the parameters that describe the profiles are: the height, W, the width, B, the flange thickness, t, the web thickness, e, and the radius, R.

IPE and UPE profiles are standard ones, their dimensions are stated by European and International Standards (EU 19-57 for IPE and DIN 1026-2: 2002-10 for UPE). They are widely used for construction and engineering purposes.

Now, the different profiles will be described. Figure 8, Figure 9 and Figure 10 show their shape and dimensions.
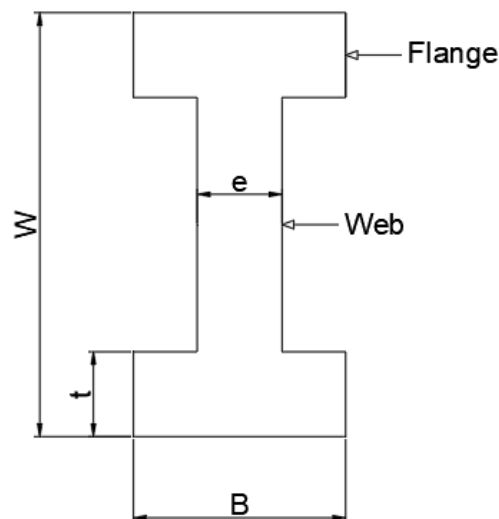
- I-cross section:

Figure 8: I-cross section profile description

- IPE cross-section profile (according to European Standards):
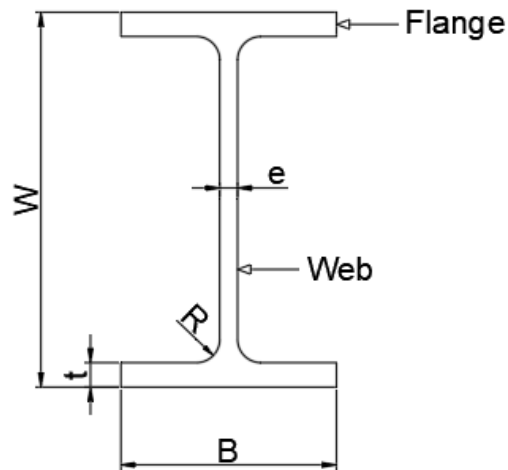
Figure 9: IPE profile description

- UPE cross-section profile (according to European Standards):
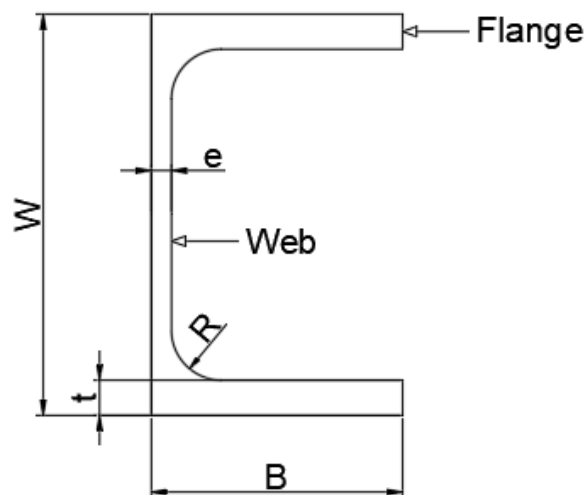
Figure 10: UPE profile description

4.2 Boundary Conditions and Loading in 3PBT

The thesis is mainly based on the stress field analysis to beams subjected to a 3PBT, therefore the boundary conditions and loading of this test must be applied to the specimens. To simulate the effect of a support the displacements in the lateral and vertical direction (x-axis and z-axis) must be restricted at the location of the support.

The loading is applied as a distributed load in the upper flange of the profile at half of the span. Its direction is pointing downwards the z-axis.

One of the problems of the 3D simulation is that it can results in a very high number of nodes and, hence, the computation time increases. To avoid this, boundary conditions can be applied to the beam in order to study only half of the model (in case of the I profile and the UPE profile) or in one quarter of the model (in case of the IPE profile).

When half of the beam is considered in the model, apart from the boundary condition at the support, another one must be introduced at half the span to consider the symmetry

conditions so that the displacement in the longitudinal direction (y-axis) is zero. It is important to remark that at this section the crack is located; therefore, the crack should not have any boundary conditions applied on it. Regarding the loading, as only half of the model is considered, the value of the load should be reduced by one half.

Figure 11 and Figure 12 show the boundary conditions (light blue) for the I and the UPE profile, respectively. Red arrows represent the forces applied at half of the span. It can be seen that the crack (shown as a red rectangle in both figures) has no restrictions applied.
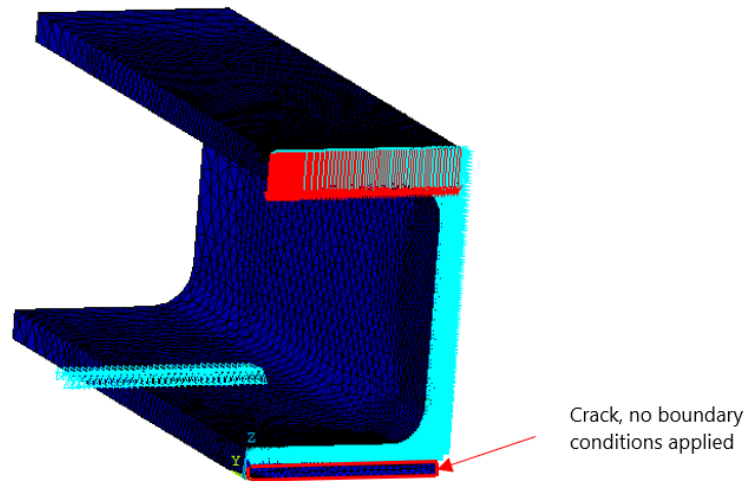
Figure 11: UPE profile and applied boundary conditions for 3PBT
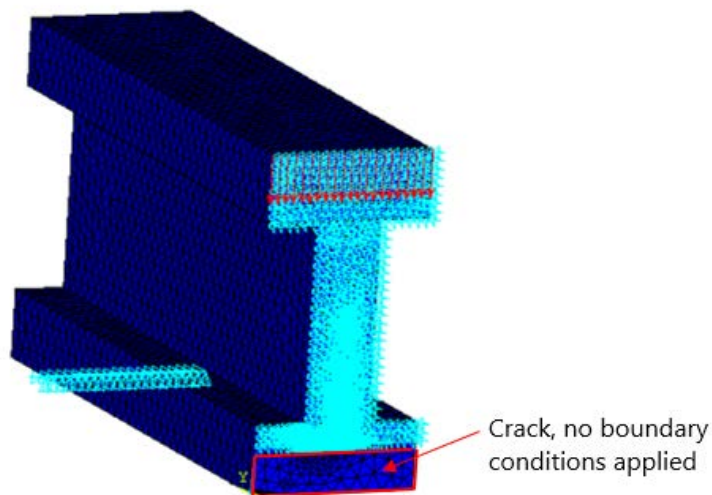
Figure 12: I profile and applied boundary conditions for 3PBT

In case of a quarter of the beam, the boundary conditions in the support and the symmetry condition in the section of half of the span should also be applied. In addition, another symmetry condition must be applied in the model, the internal longitudinal face must have its displacements in the lateral direction (x-axis) restricted. In terms of the load, only one quarter of it must be considered. Figure 13 shows the boundary conditions and loading for the IPE profile, where it can be seen that the internal longitudinal face has its displacements restricted (Ux=0).
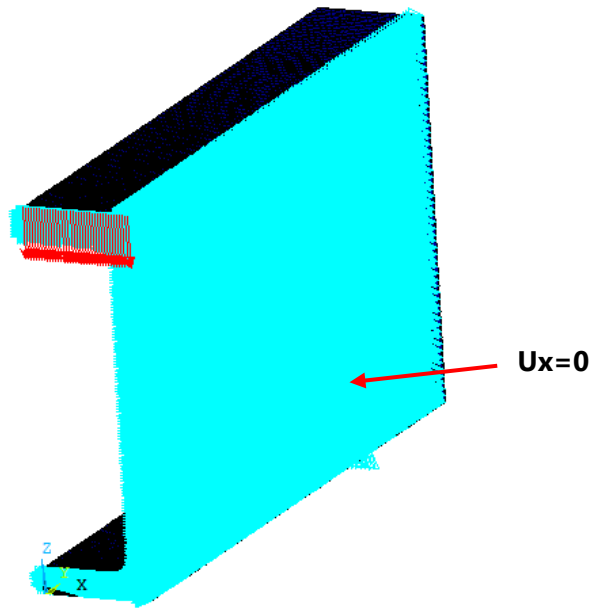
Figure 13: IPE profile boundary conditions

4.3 Material Properties

The material properties of steel used as input for the FEM analysis are following. Steel is defined as a linear isotropic material in ANSYS by means of the Young's Modulus ($E = 210\,GPa$) and the Poisson's ratio ($v = 0.3$).

In the analysis of the I-profile the behaviour of steel is compared with other materials with Young's Modulus $E = 20, 74, 1\,GPa$ and Poisson's ratio $v = 0.2, 0.34, 1$ for concrete, aluminium and clay, respectively.

Table 1: Linear Elastic Properties of steel, see

Properties of Steel	Young's modulus (E)	Poisson's ratio (v)
	210 GPa	0.3

4.4 Element Type

The element used for the analysis in ANSYS is SOLID186, A 3D 20-node structural solid. The type of element is introduced in the software by means of the command ET. Numerical models are meshed using tetrahedron elements. Figure 14 shows the shape of the element used.
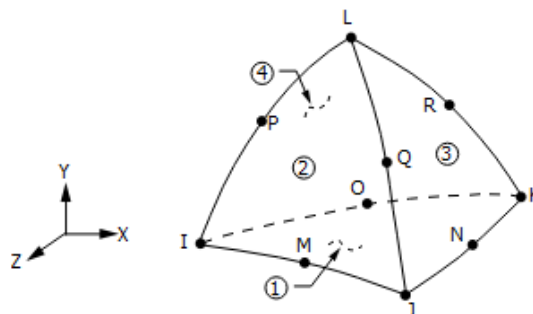
Figure 14: Solid 186 tetrahedron element, retaken from ANSYS library [3]

4.5 Modelling

As previously stated, there are three main models in this thesis. However, these models are very similar between each other as all of them simulate a 3PBT, but for different profiles. In this section, it will be developed how is the procedure of 3D-modelling these profiles step by steps, from keypoints to volume.

4.5.1 Keypoints

The modelling is started by defining the keypoints, theses points are located in the relevant points of the specimen, like corners, starting of finishing points of the crack. The number of keypoints within the three different models varies, however, the procedure is the same. As the models are in 3D, the keypoints are created in the cartesian coordinate system (x, y and z). In ANSYS the command used to define them in the macro is K, followed by the dimensions in the x, y and z coordinates. For example, for the origin of coordinates the point is defined as: K,0,0,0. Figure 15 represents the keypoints in ANSYS for the IPE profile.
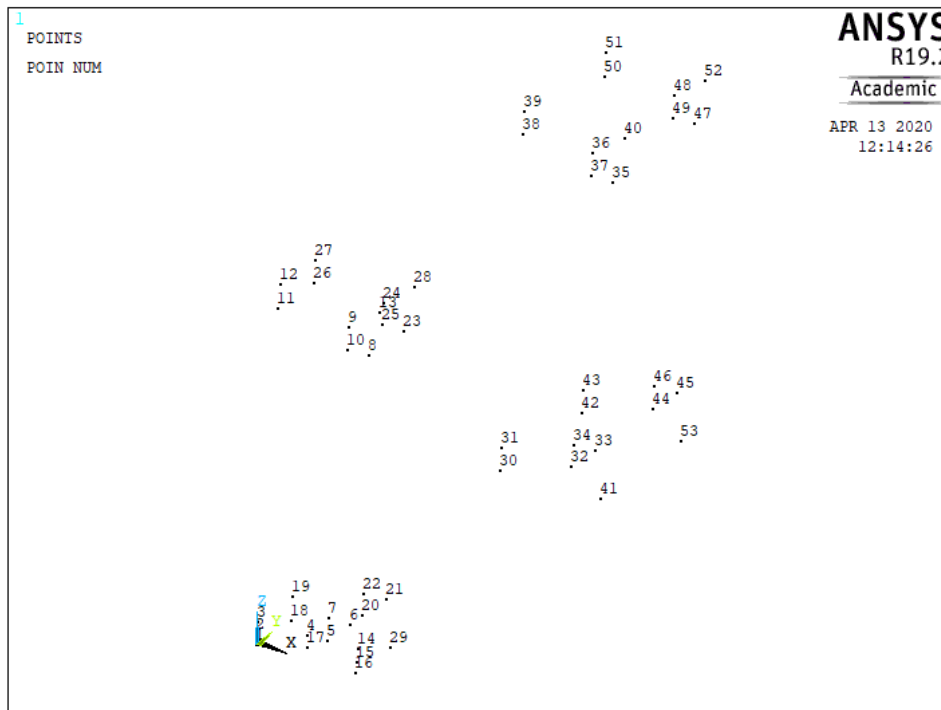
Figure 15: Keypoints in IPE profile modelling

4.5.2 Lines

The lines in ANSYS connect the keypoints. They are used to represent the geometry, the cracks, the line where the load is applied or the line where the support is located order to be able to apply the boundary conditions in the software. The number of lines varies within the 3 models.

Lines are created in ANSYS by the command L or the command arc (in case of a circumference or circular part in the model, as some corners in the IPE and UPE profiles). To create a line, two keypoints are used so the command L joins both of them by means of a line. For example, L,1,2 creates a line between keypoints 1 and 2. Figure 16 illustrates the lines and arcs in the UPE model.
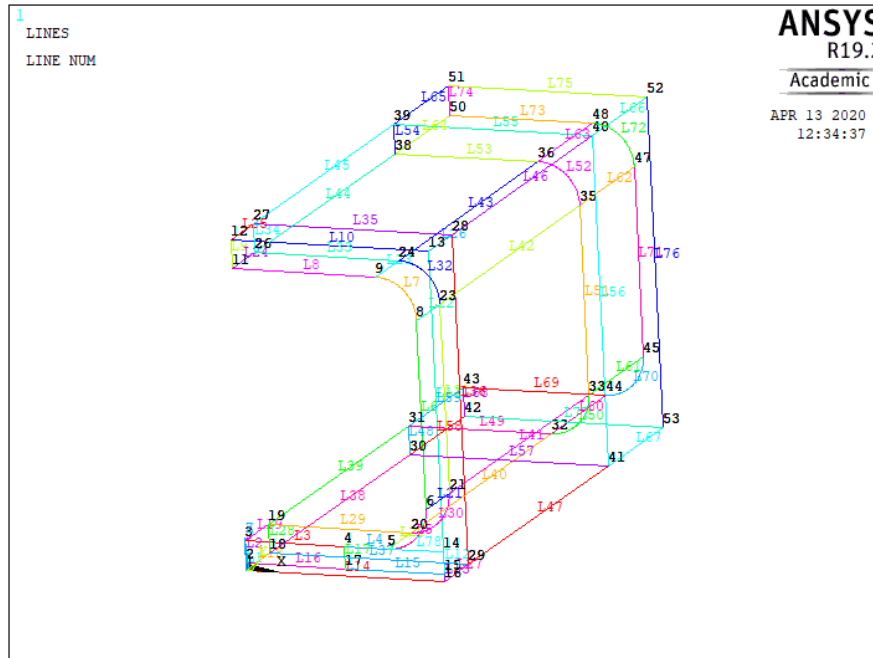
Figure 16: Lines and arcs in the UPE profile model

4.5.3 Areas

After the lines, the areas must be created. They are created by means of the previously defined lines. The command used in ANYS is AL, followed by the lines that delimitate the desired area. For example, AL,1,2,3,4 creates an area in the region enclosed by lines 1,2,3,4. It is important that the software will only create an area in case that the lines form a closed area. Figure 17 represents the areas in the I-profile model.
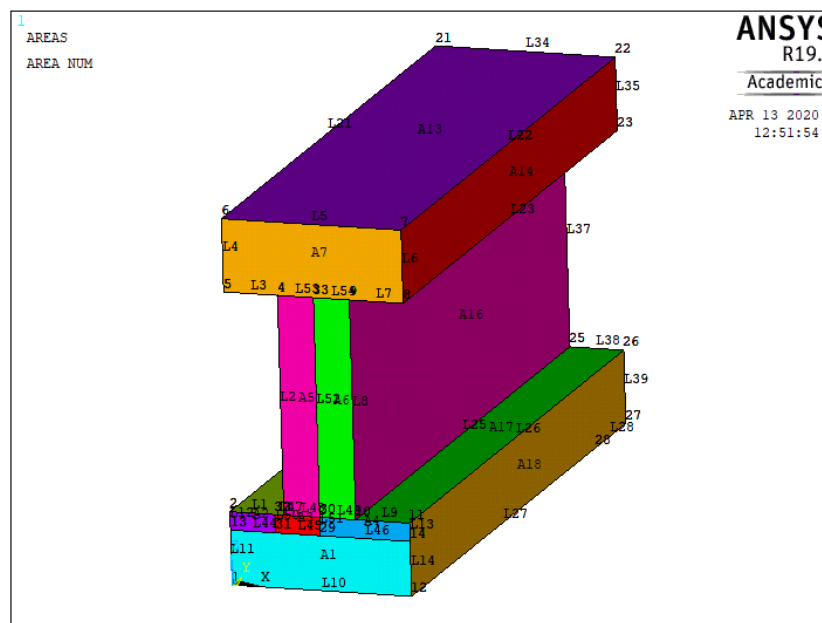
Figure 17: Areas in I profile modelling

4.5.4 Volume and meshing

Once all the areas are defined, the volume must be created. To do so, the areas that conform the volume must be selected with the command ASEL. This command will create a volume from these selected areas, by implementing the command VA. Figure 18 represents the volume of the IPE profile.
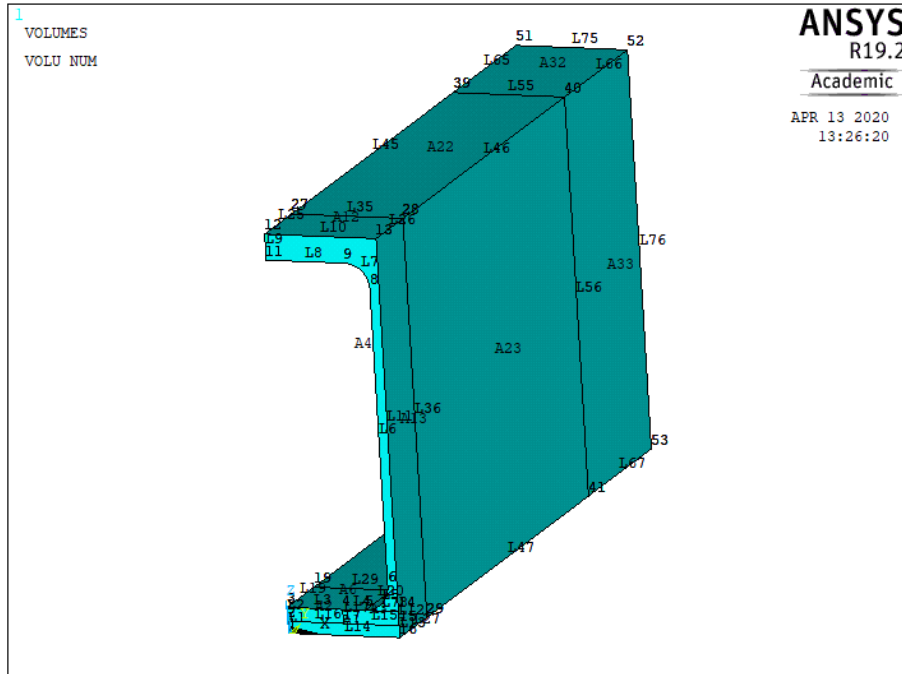
Figure 18: IPE profile volume in ANSYS

The mesh must now be created, dividing the volume in small elements, by means of the command KESIZE it is possible to determine the size of elements close to a keypoint. The command LESIZE determines the size of elements which lay over a given line. Figure 19 represents the mesh in the I-profile, it can be seen that in the region close to the crack tip where the flange and web paths are defined the mesh is finer to ger more accurate values.
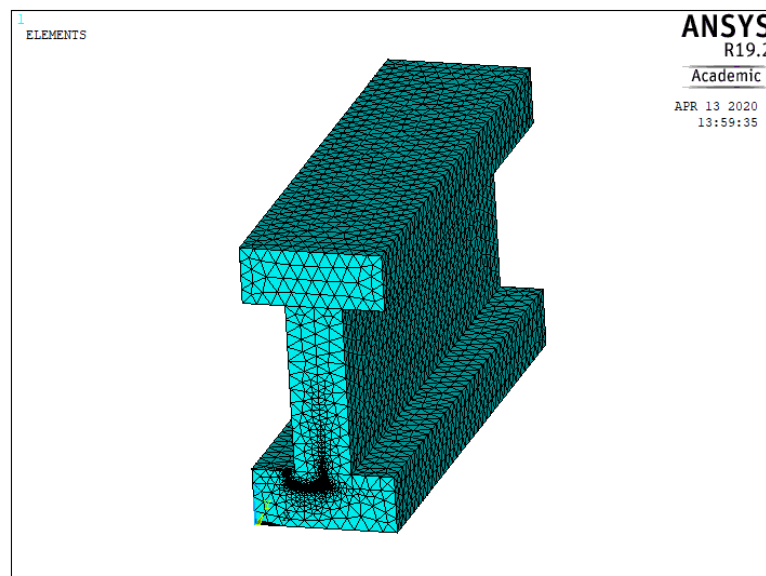
Figure 19: I profile mesh in ANSYS

As the aim of the thesis is to determine the stress fields in the vicinity of the crack tip, the mesh must be very fine in the area close to the crack tip so that accurate results are obtained. Regions far away from the crack can be meshed more coarsely with the objective of reducing computing time. In the models developed for the IPE and the UPE profiles an optimization of the mesh has been developed, having a very fine mesh at the region close to the crack tip but coarse at regions far away from the crack. Moreover, the student version of ANSYS has a limited number of nodes, therefore, this number must not be overpassed, or the software will not work. That is one of the reasons to use bigger size elements at zones far away from the area under study.

Regarding the paths of calculation of the stress in the flange and the web, the mesh here must be the finer in the hole model as the values obtained here for the stresses will be the ones used for further calculations. Figure 20 shows this optimization of the mesh in the IPE profile and Figure 21 the UPE profile optimization.
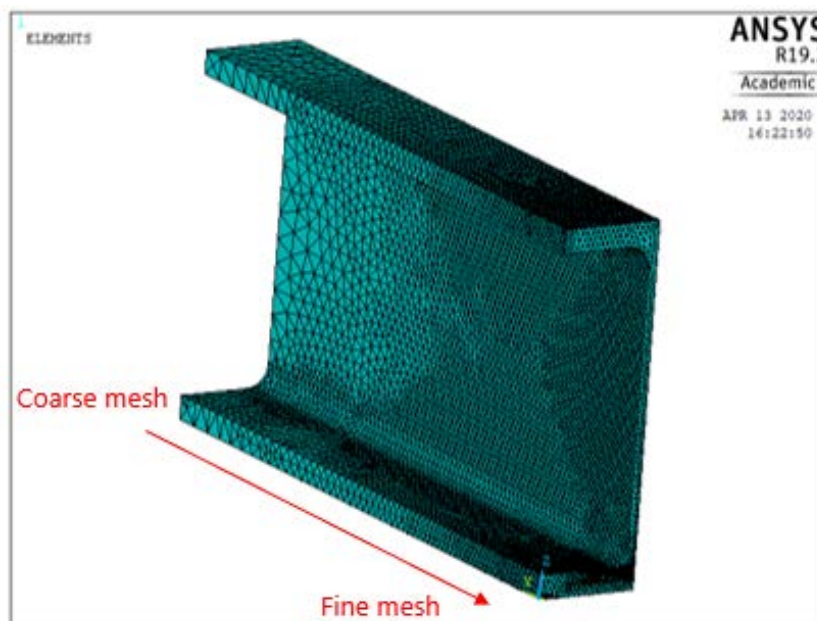
Figure 20: Mesh in the IPE profile
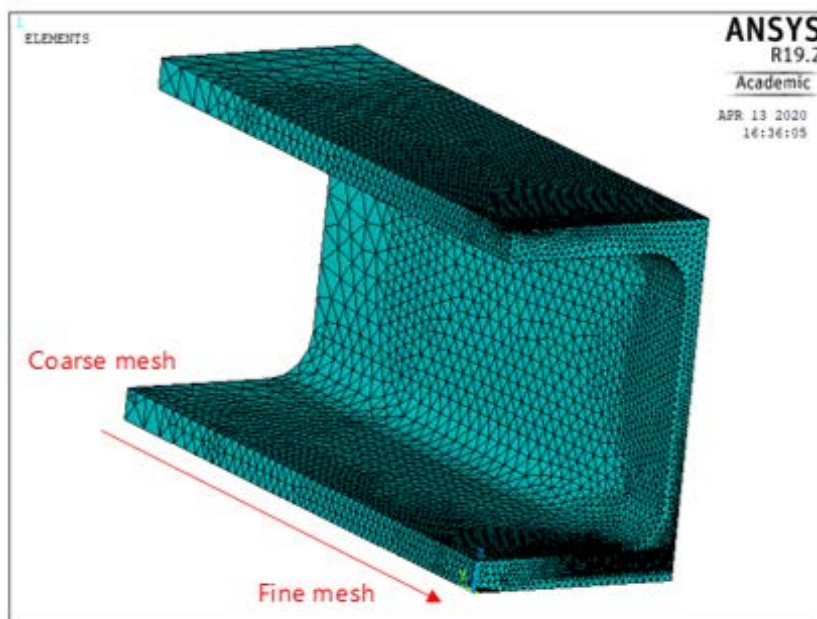
Figure 21: Mesh in the UPE profile

4.5.5 Additional rectangular models

Apart from the models of the I-profile, IPE profile and UPE profile, some rectangular models have been created. The objective is to compare the structural profiles (I, UPE and IPE) with rectangular profiles to observe their differences in behaviour, mainly in their stress fields in front of the crack tip. In these models, also two paths have been considered (flange and web). Figure 22 represents a model for a rectangular profile, light blue designates boundary conditions while red the loading.
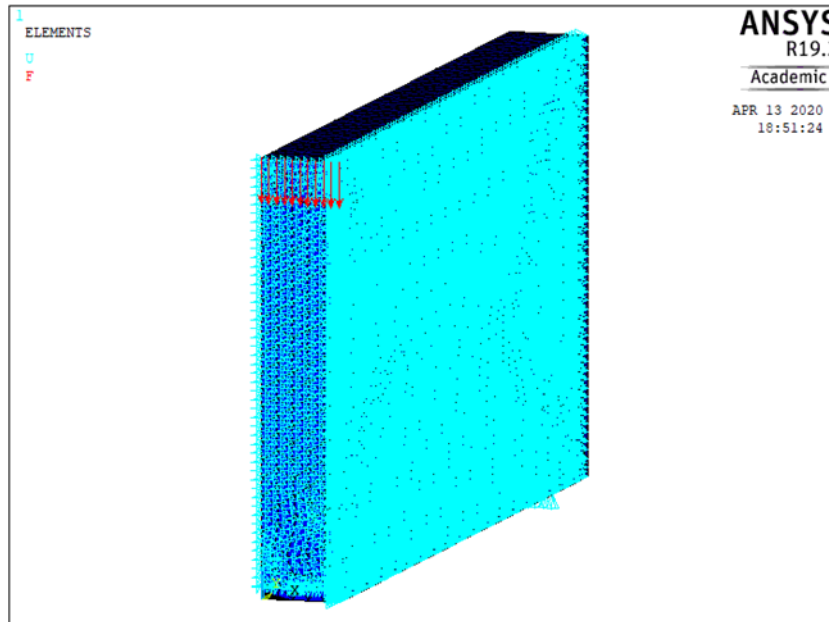
Figure 22: Rectangular FE model with boundary conditions for 3PBT

4.6 Solution in ANSYS

The command SOLVE is the one used to obtain in ANSYS to obtain the solution. Once this command is executed the stiffness matrix which represents a system of linear equations is defined. This system of equations is solved obtaining the values of the displacements and stresses at each node. Basically, the software applies the finite element method to the model and, therefore obtains the solutions.

The main objective of the model is obtaining the stresses (σ_{yy}) in two paths: one in the web and another in the flange. There are two ways of obtaining the stresses in these two paths:

- Using the interface of ANSYS: in the main menu, in the section of general postprocessing, the stresses in the paths can be obtained. However, it is a time-consuming task.

- Implemented code in macro: in this way, which is the one used in the thesis, the macro is the one which automatically obtains the results of the stresses in these two paths and sends the results to a selected folder in the form of two .txt files (one for the web and another for the flange). This code is found at the end of the macro and allows a must faster obtention of data. In addition, this final thesis involved the manipulation of a lot of data between ANSYS and EXCEL, so this method resulted in a considerable reduction of time.

Once the solution has been obtained, the stress distribution for all the profiles can be obtained. Figure 23, Figure 24 and Figure 25 show the stresses in the I profile, IPE profile and UPE profile, respectively.
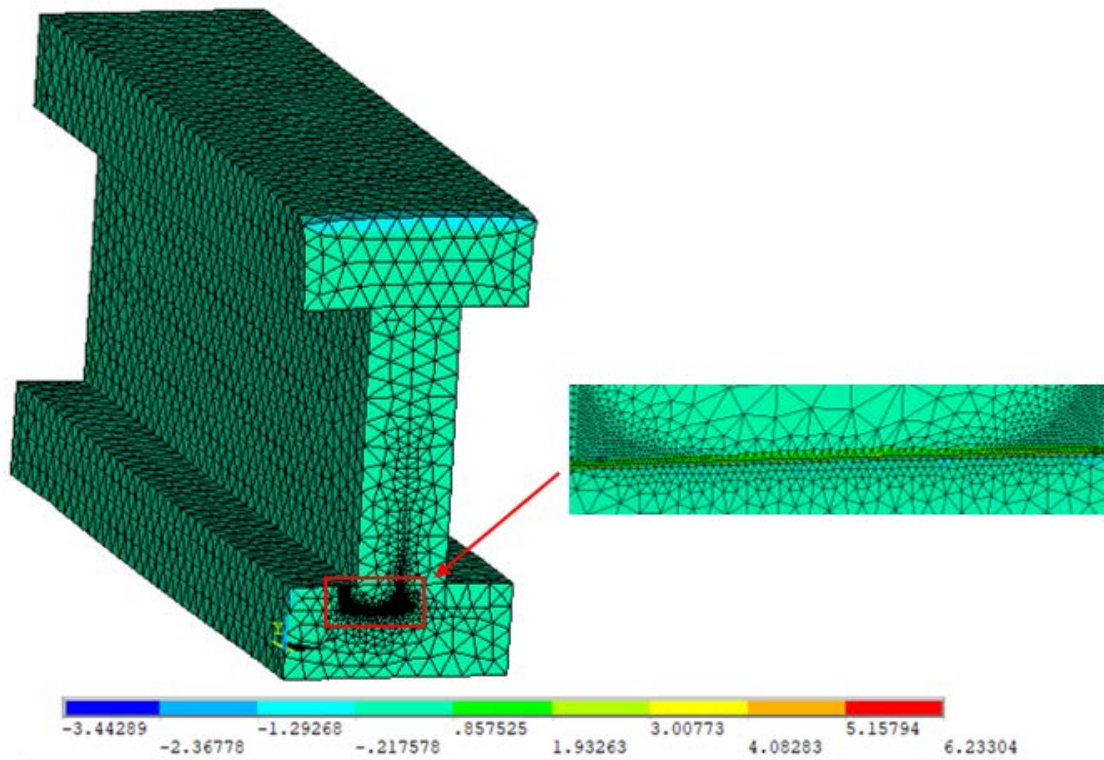
Figure 23: Stress distribution in Y-direction in I profile, with detail in front of crack tip line
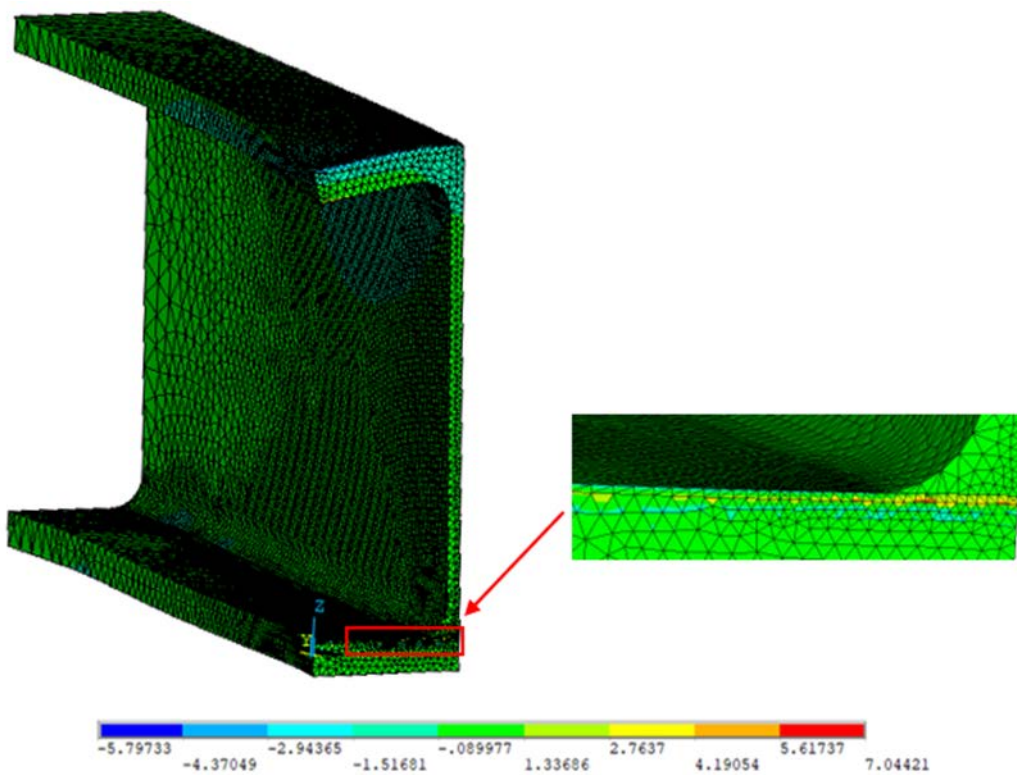
Figure 24: Stress distribution in Y-direction in IPE profile, with detailing of the vicinity of crack tip line
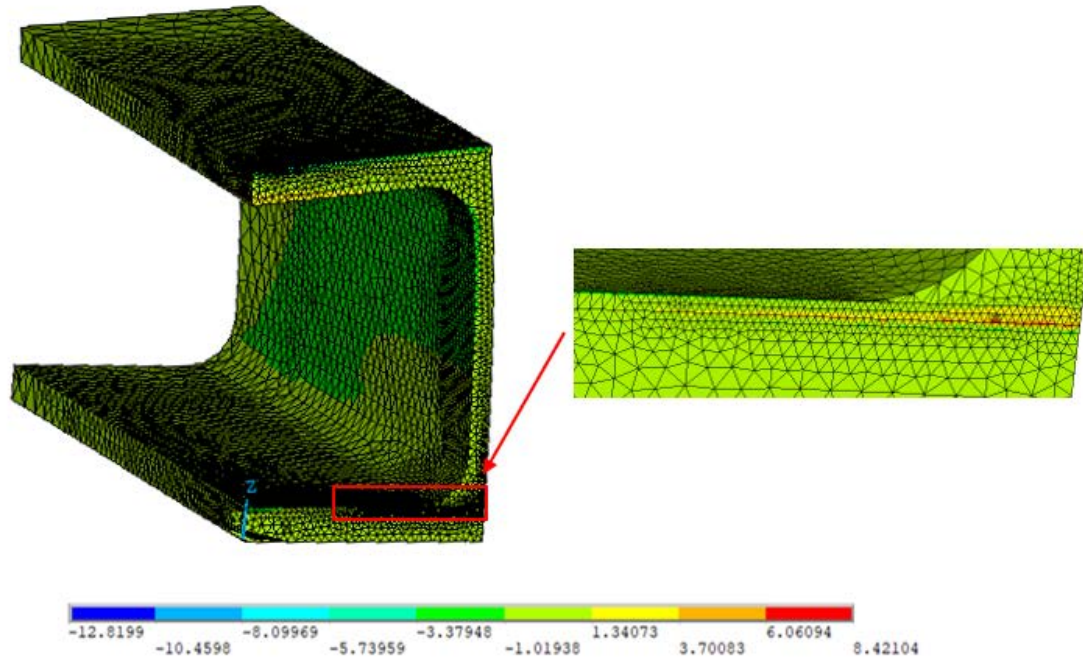
Figure 25: Stress distribution Y-direction in UPE profile, with detailing in front of crack vicinity

4.7 Calculation of the Stress Intensity Factors

The software ANSYS, as described in section 4.6 provides the values of the stresses (σ_{yy}) in function of the distance to the crack tip (r). However, for the analysis developed in this thesis it is required to obtain the stress intensity factor (K). In order to do that the data of the stresses is transferred to an EXCEL file and following equation is applied:

$$K_{\mathrm{I}} = \sigma_{yy} \sqrt{2\pi r} \tag{8}$$

Then, by means of linear regression the relationship between the stress intensity factor (*y*-axis) and the distance to the crack tip (*x*-axis) is approximated [10]. The point where the line of regression cuts the *y*-axis is the stress intensity factor in front of the crack tip which is the desired value to be obtained. It is important to remark that the constants in the regression lines represent the point of cut with the y-axis, and, therefore, the value of the SIF in front of the crack tip. Therefore, this is the important value that must be extracted for the subsequent parametrical study.

This procedure will be repeated for all the parametrical studies which are developed in this thesis, as it allows it to obtain the stress fields in the region of the crack tip.

The following graph, Graph 1, represents with a general case the linear regression relationship between the SIF and the distance to crack tip for the path in the web (blue) and the path in the flange (green) :
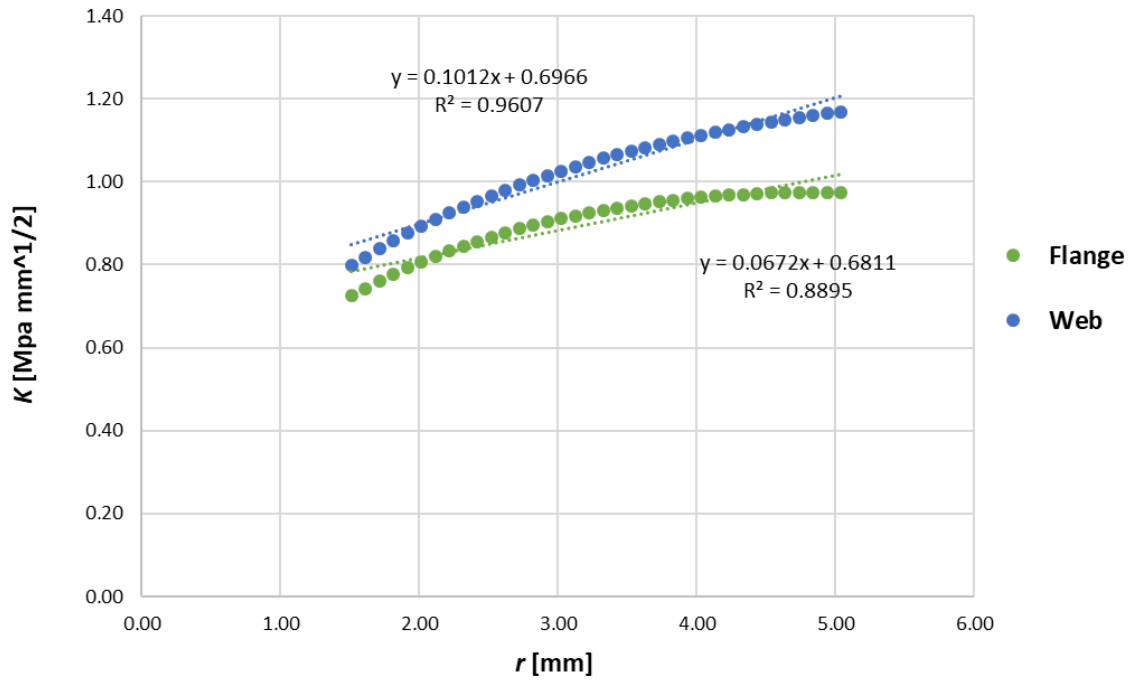
Graph 1: Stress intensity factor versus distance to crack tip and regression lines

5. Numerical Study and Results

In total, 3 different parametrical studies of the 3PBT have been developed for each of the three different profiles. In this sense, the main aim is to obtain the stress intensity factor in the flange and web of each for the three profiles. In the following sections the parametrical studies of each profile will be developed, explained in details and results will be shown.

5.1 I-profile

This is the first analysis; in it a parametrical study of the I profile is carried out, both in the flange and in the web. The variation of the SIF is studied for different geometries of the I profile, crack lengths and values of material properties (Young's modulus and Poisson's ratio). Now the main variables of the study will be defined: a is the crack length, e is the thickness of the web, t is the flange thickness, B is the flange width, W is the height of the profile, S the length of the span and P the applied load. The base or standard dimensions of the profile are the following: B=50 mm, W=100 mm, t=20 mm, e=20 mm, $S = 300$ mm and P=100 N.

Figure 26 represents the basic dimensions of the I profile as well as the description of the path in the flange (green) and in the web (blue). The region with the crack can be seen as a hatched zone in the lower part of the profile.
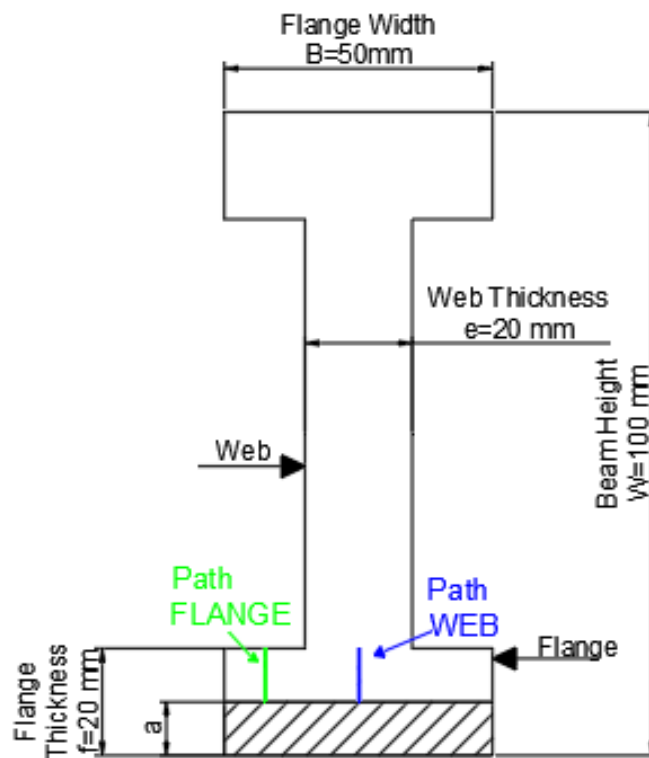
Figure 26: I profile with crack description and paths for analysis of SIF

In the following subchapters, the variation of the SIF will be analysed for different geometries, crack lengths and material properties (so that behaviour of steel is compared with other materials like concrete, aluminium and clay).

5.1.1   Variation of SIF for different geometries and crack lengths

The variation of the SIF is analysed for different geometries by varying the ratio between the thickness of the web (e) and the flange width (B) for a constant value of Poisson's ration ($v = 0.3$). The flange width will stay constant (B=50 mm) and what varies is the thickness of the web (e). The values for this ratio (e/B) are the following: 0.1, 0.2, 0.3, 0.4, 0.5, 0.7, 0.8, 0.9, 1. Thus, the analysis will be performed from a very thin value of the web to a very wide web. It is important to remark that when e/B=1 the profile becomes a rectangular profile.

For each of these e/B ratios different crack lengths will be analysed by varying the ratio between the height of the profile (W) and the crack length (a). The values of the a/W ratios are the following: 0.05, 0.1, 0.15 and 0.19. The following Table 2 summarizes the dimensional ratios used in this parametrical study:

Table 2: Values of ratios for the SIF analysis

Ratio	Values
e/B	0.1, 0.2, 0.3, 0.4, 0.5, 0.7, 0.8, 0.9, 1
a/W	0.05, 0.1, 0.15, 0.19

Figure 27 shows the different geometries or web thicknesses for the values of the ratio, e/B. Figure 28 represents the different crack lengths under analysis for the values of the ratio, a/W.
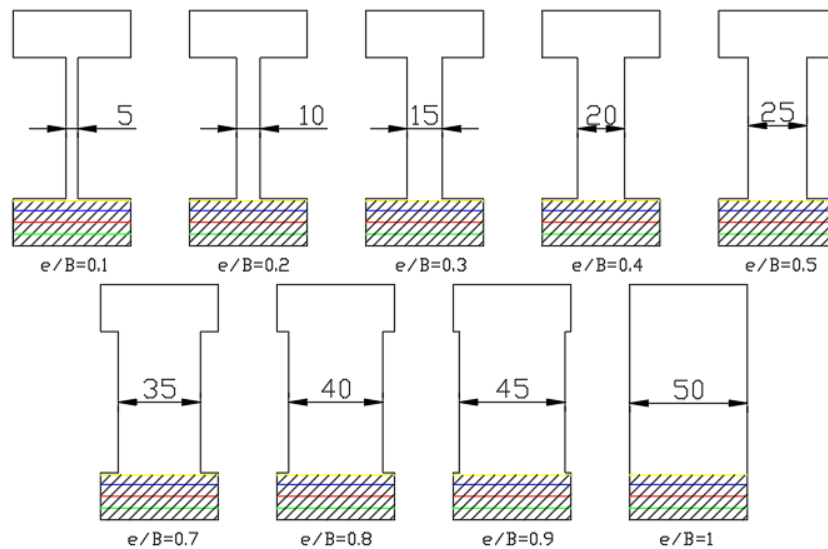
Figure 27: Thicknesses of the I profile for the different *e/W* ratios
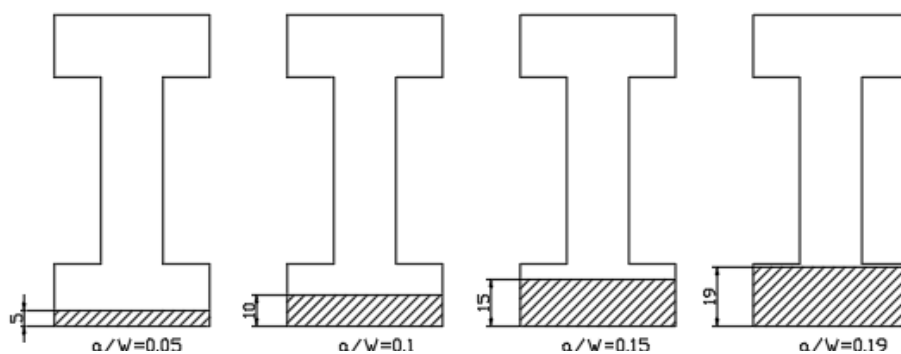
Figure 28: Crack lengths for the different a/W ratios

The simulations in ANSYS are performed for all this combination of ratios, obtaining the values of stresses. Then, these stresses are transformed into SIFs, as explained in section 4.8, in such a way, two graphs are obtained, one for the path in the web and another for the path in the web.

Graph 2 illustrates the SIF for the different web thicknesses versus the crack length, in the web path. In the other hand, Graph 3 illustrates the same but for the path in the flange.
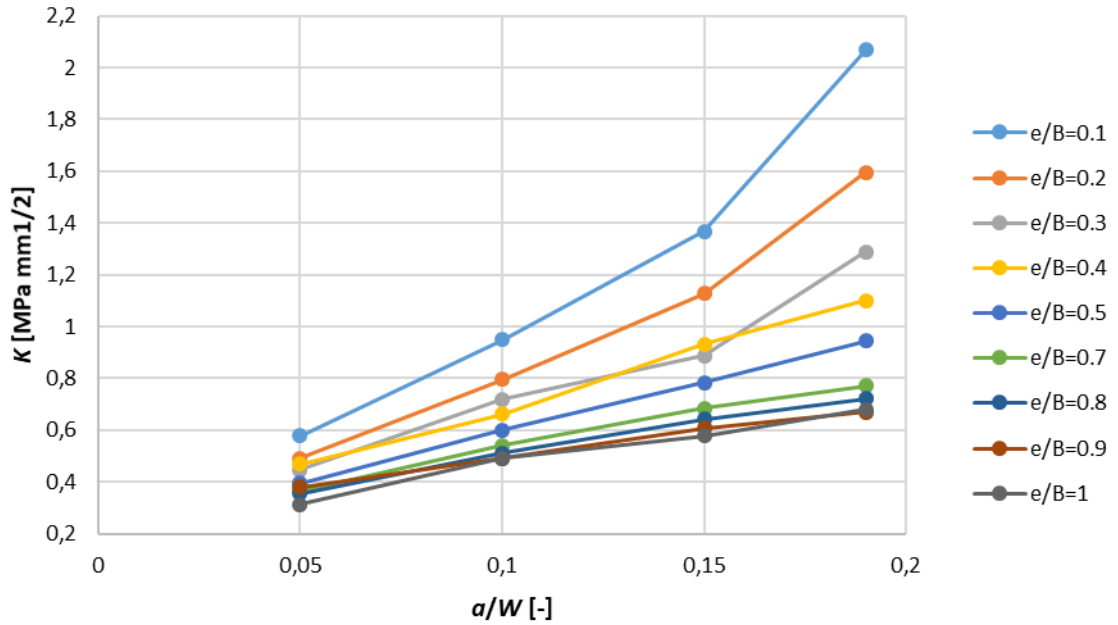
Graph 2: Stress intensity factor versus relative crack length for different web thicknesses for the path in the web
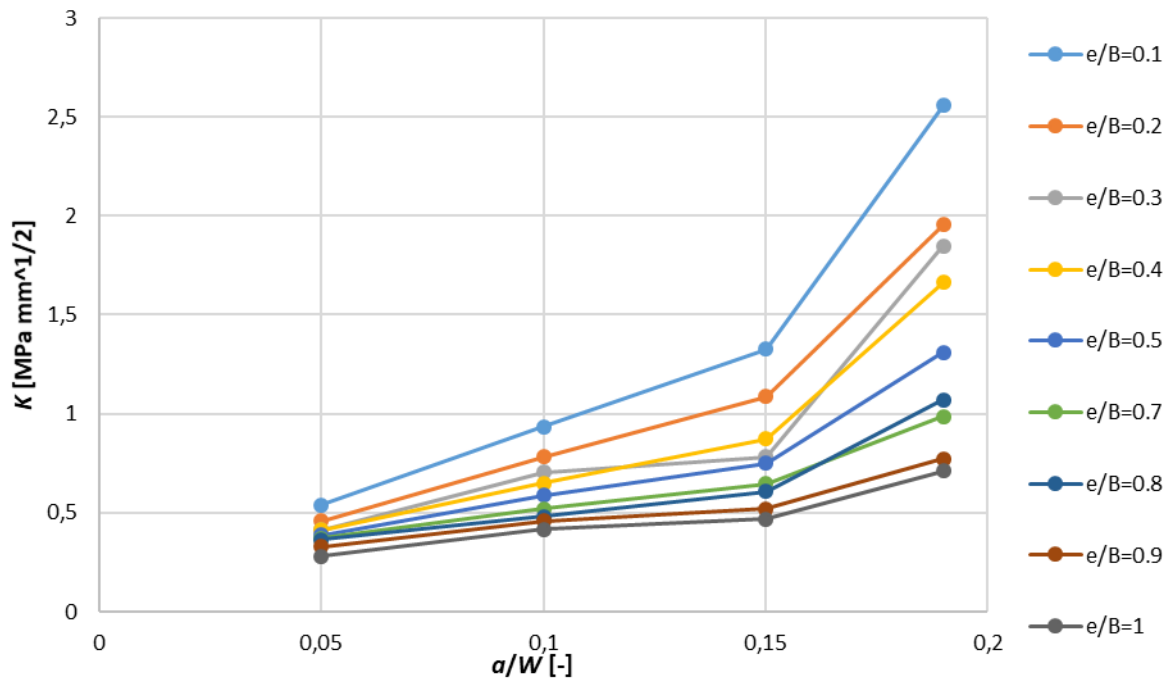
Graph 3: Stress intensity factor versus relative crack length for different web thicknesses for the path in the flange

The following tables (Table 3 for the web path and Table 4 for the flange path) quantify the SIF increase due to the change of web thickness. They show the ratio between the SIF values of a the different web thicknesses over the SIF values of the rectangular profile: $K_{I\,profile}/K_{rectangular}$.

Table 3: Quantification of SIF increase due to change of web thickness and crack length for the web path.

e/B		0.1	0.2	0.3	0.4	0.5	0.7	0.8	0.9	1
$\dfrac{K_{Web}}{K_{rectangular}}$	a/W=0.05	184%	157%	149%	142%	126%	116%	113%	111%	100%
	a/W=0.1	193%	162%	148%	135%	122%	110%	104%	100%	100%
	a/W=0.15	236%	*194%*	153%	161%	135%	118%	111%	105%	100%
	a/W=0.19	304%	234%	189%	162%	139%	113%	106%	103%	100%

Table 4: Quantification of SIF increase due to change of web thickness and crack length for the flange path.

e/B		0.1	0.2	0.3	0.4	0.5	0.7	0.8	0.9	1
$\dfrac{K_{Flange}}{K_{rectangular}}$	a/W=0.05	193%	163%	148%	147%	139%	132%	130%	117%	100%
	a/W=0.1	224%	188%	169%	156%	142%	125%	115%	110%	100%
	a/W=0.15	284%	233%	167%	187%	161%	138%	130%	111%	100%
	a/W=0.2	360%	275%	260%	234%	184%	139%	151%	108%	100%

These tables show that the wider the web the lower the values of the stress intensity factor for every crack length. As expected, when the crack length gets higher the ratio becomes higher.

5.1.2   Variation of material properties

A study has been developed for the I profile with the dimensions of the Figure 26. Therefore, geometrical dimensions remain constant and what varies are the material properties, simulating 4 different materials: concrete, steel, aluminium and clay. The Young's Modulus (E) does not affect the SIF, however, the value of the Poisson´s ratio (v) does so. The values of the Poisson's ratio considered in the study are the following: concrete (v=0.2), steel (v=0.3), aluminium (v=0.34) and clay (v=0.4). The analysis has been performed both for the web path (Graph 4) and the flange path (Graph 5).

It can be appreciated that materials with a lower Poisson's ratio have lower values of SIF than the ones with higher ratio. Nevertheless, as seen in the graph, the difference is really small.
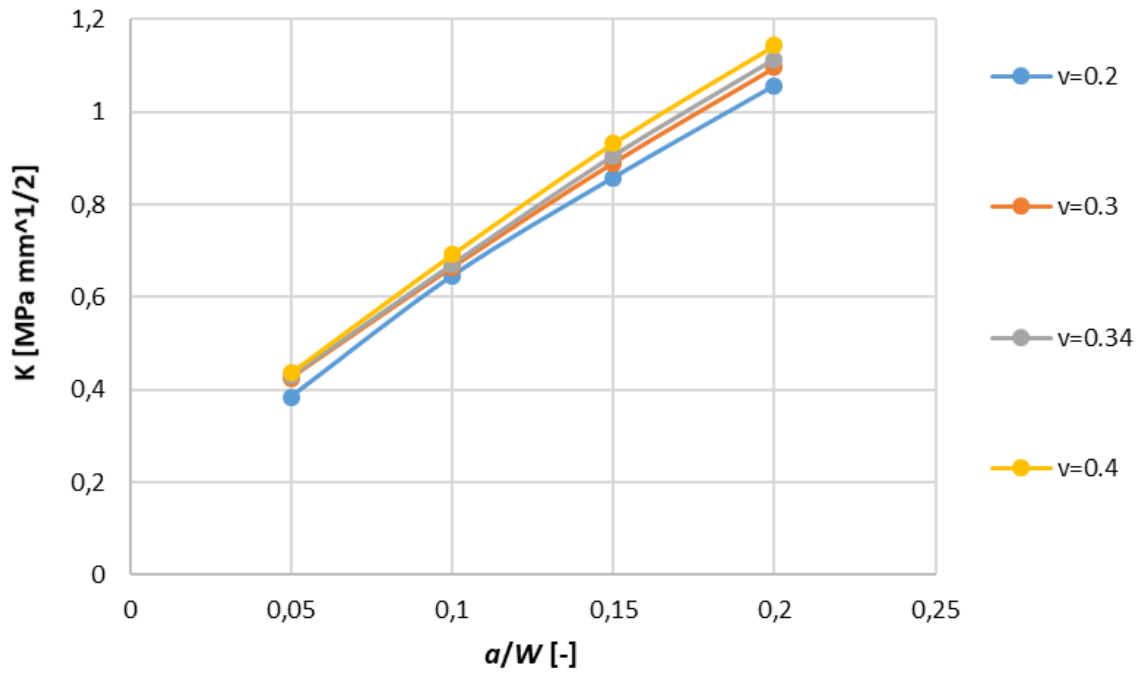
Graph 4: Stress intensity factor versus crack length for different Poisson's ratios in the web path
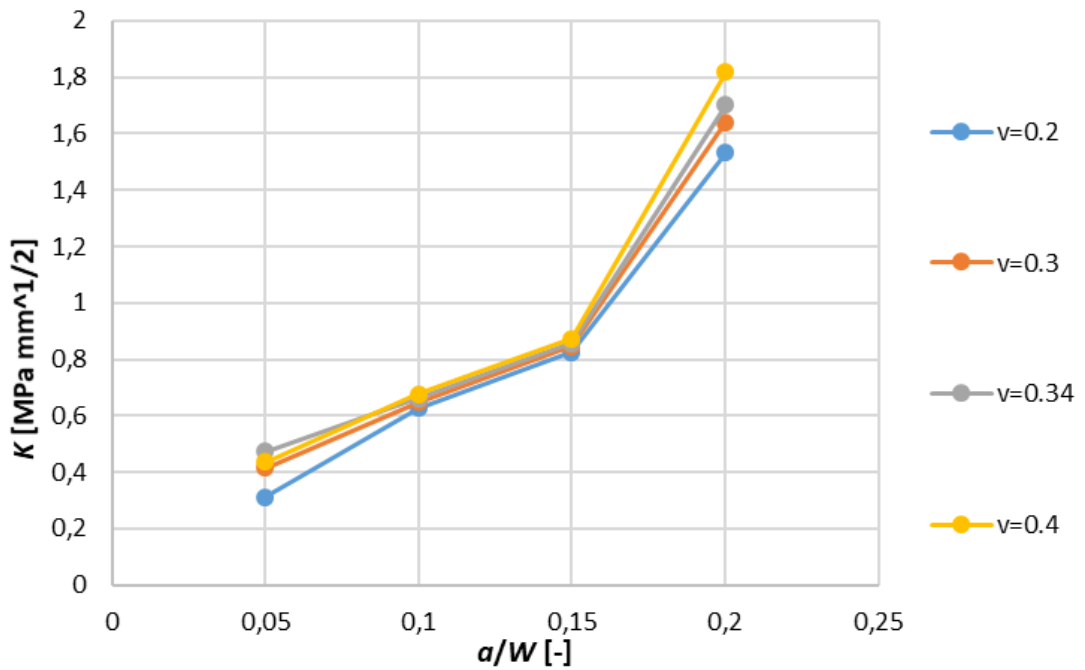
Graph 5: Stress intensity factor versus crack length for different Poisson's ratios in the flange path

5.2 IPE Profile

As previously stated, the IPE profiles are standardized profiles manufactured and used all over the world. There are 18 different types of IPE profiles, they all have the similar shape but different dimensions being IPE 80 the smallest one and IPE 600 the biggest (the number in the profile name refers to the height of the profile). The standards specify the dimensions of all the profiles, as shown in Figure 29.

Identification	Nominal weight 1m	Nominal dimensions					Cross-section	Dimensions for detailing					Surface	
	kg/m			mm			A	h1	d	Ø	pmin	pmax	AL	AG
		b	h	t1	t2	R1	cm2	mm	mm		mm	mm	m2/m	m2/m
IPE 80	6.0	46	80	3.8	5.2	5.0	7.64	69.6	59.6	-	-	-	0.328	54.64
IPE 100	8.1	55	100	4.1	5.7	7.0	10.30	88.6	74.6	-	-	-	0.400	49.33
IPE 120	10.4	64	120	4.4	6.3	7.0	13.20	107.4	93.4	-	-	-	0.475	45.82
IPE 140	12.9	73	140	4.7	6.9	7.0	16.40	126.2	112.2	-	-	-	0.551	42.70
IPE 160	15.8	82	160	5.0	7.4	9.0	20.10	145.2	127.2	-	-	-	0.623	39.47
IPE 180	18.8	91	180	5.3	8.0	9.0	23.90	164.0	146.0	M10	48	48	0.698	37.13
IPE 200	22.4	100	200	5.6	8.5	12.0	28.50	183.0	159.0	M10	54	58	0.768	34.36
IPE 220	26.2	110	220	5.9	9.2	12.0	33.40	201.6	177.6	M12	60	62	0.848	32.36
IPE 240	30.7	120	240	6.2	9.8	15.0	39.10	220.4	190.4	M12	66	68	0.922	30.02
IPE 270	36.1	135	270	6.6	10.2	15.0	45.90	249.6	219.6	M16	72	72	1.041	28.86
IPE 300	42.2	150	300	7.1	10.7	15.0	53.80	278.6	248.6	M16	72	86	1.160	27.46
IPE 330	49.1	160	330	7.5	11.5	18.0	62.60	307.0	271.0	M16	78	96	1.254	25.52
IPE 360	57.1	170	360	8.0	12.7	18.0	72.70	334.6	298.6	M22	88	88	1.353	23.70
IPE 400	66.3	180	400	8.6	13.5	21.0	84.50	373.0	331.0	M22	96	98	1.467	22.12
IPE 450	77.6	190	450	9.4	14.6	21.0	98.82	420.8	378.8	M24	100	102	1.605	20.69
IPE 500	90.7	200	500	10.2	16.0	21.0	115.50	468.0	426.0	M24	102	112	1.744	19.23
IPE 550	106.0	210	550	11.1	17.2	24.0	134.40	515.6	467.6	M24	110	122	1.877	17.78
IPE 600	122.0	220	600	12.0	19.0	24.0	156.00	562.0	514.0	M27	116	118	2.015	16.45

Figure 29: Standard dimensions of IPE profiles, retaken from [9]

The dimensional values that define each IPE profile are described in Figure 30, as well as the two paths involved in the study (the blue one is the path in the web and the green one is the path in the flange).
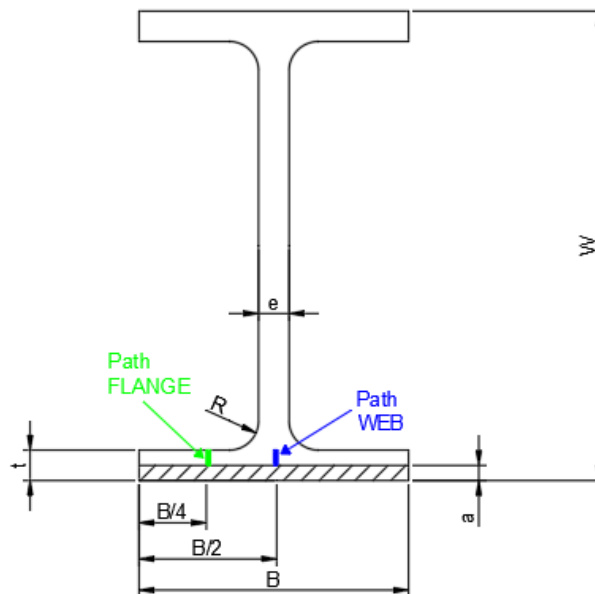
Figure 30: IPE profile description of the paths of study

A parametrical study (3PBT) for all these profiles will be performed in this section. The variation of the SIF will be analysed both in the web and in the flange for different cracks lengths. Please note that P=100 N, $S = 3xW$ mm and the material properties for steel are E=210 GPa v=0.3.

Moreover, the results obtained will be compared with the ones obtained for a rectangular profile. Finally, calibration curves *f(a/w)* will be calculated for the IPE profiles.

5.2.1 Variation of the SIF for different crack lengths

For all the 18 IPE profiles, the stress intensity factor has been calculated for 8 different crack lengths (a), both in the web and flange paths. In this sense, the first value of the ratio a/W is always 0.02, but the rest of values differ from one profile to another due to the geometrical dimensions of the different profiles. There is not a constant of proportionality between all the dimensions of the different profiles.

Graph 6 shows the variation of the SIF versus the crack length for the IPE 180, where the blue line is for the web path and the green line is for the flange path. While Graph 7 is for the IPE 240.
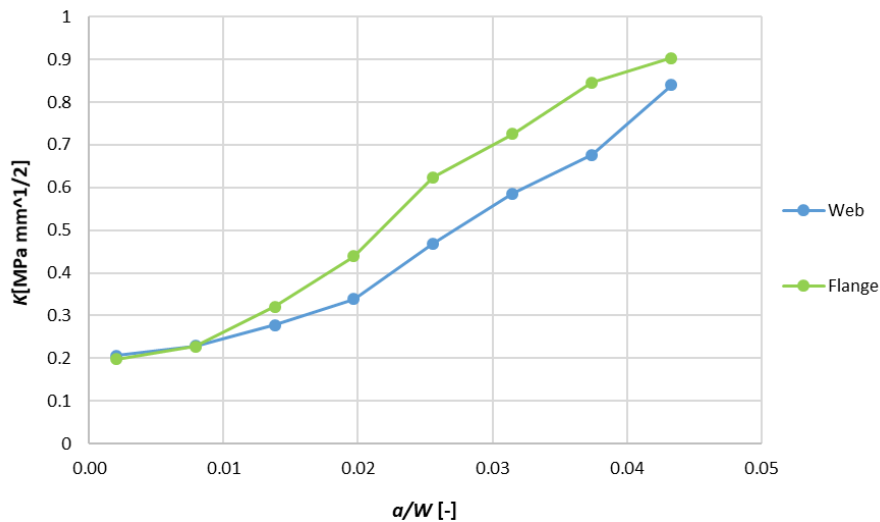
Graph 6: Evolution of SIF versus crack length in an IPE 180 profile
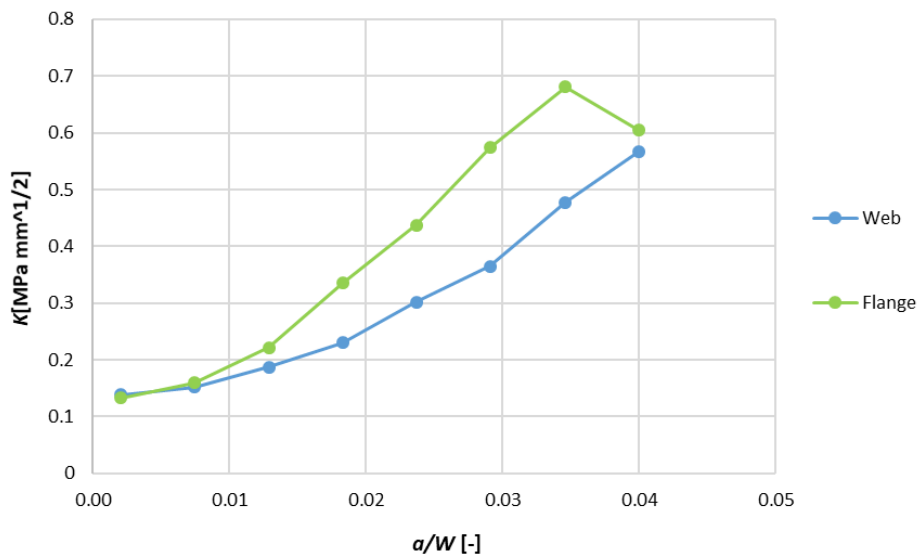
Graph 7: Evolution of SIF versus crack length in an IPE 240 profile

33

It can be appreciated in both graphs that the SIF tends to be higher in the flange than in the web. However, both paths follow the same linear pattern. This analysis was done for all 18 profiles and by plotting the results several graphs have been obtained.

It is important to remark, that the values of a/W (x- axis) are not the same for all the profiles, this is due to the different dimensions that the profiles have. In other words, there is not a constant of proportionality between the thickness of the flange (*t*) and the height of the profile (*W*).

All the profiles have been analysed from the initial ratio *a/W*=0.02 to a final value of *a/W* for which the crack length occupies almost all the flange width. With the aim of plotting the results in a clear way, not all 18 profiles are plotted in the same graph as it could result confusing, but 9 in one and 9 in another. Regarding the web, Graph 8 plots the SIF from IPE 80 to IPE 240 and Graph 9 from IPE 270 to IPE 600. In the same way, but for the flange, Graph 10 represents the SIF from IPE 80 to IPE 240 and Graph 11 from IPE 270 to IPE 600.

Besides, as a general tendency, in both the flange and the web, the bigger profiles (such as IPE 600 or IPE 400) show lower values of SIF than the smaller profiles (such as IPE 80 or IPE 140). This difference may be explained by the difference in area and stiffness of the cross sections.
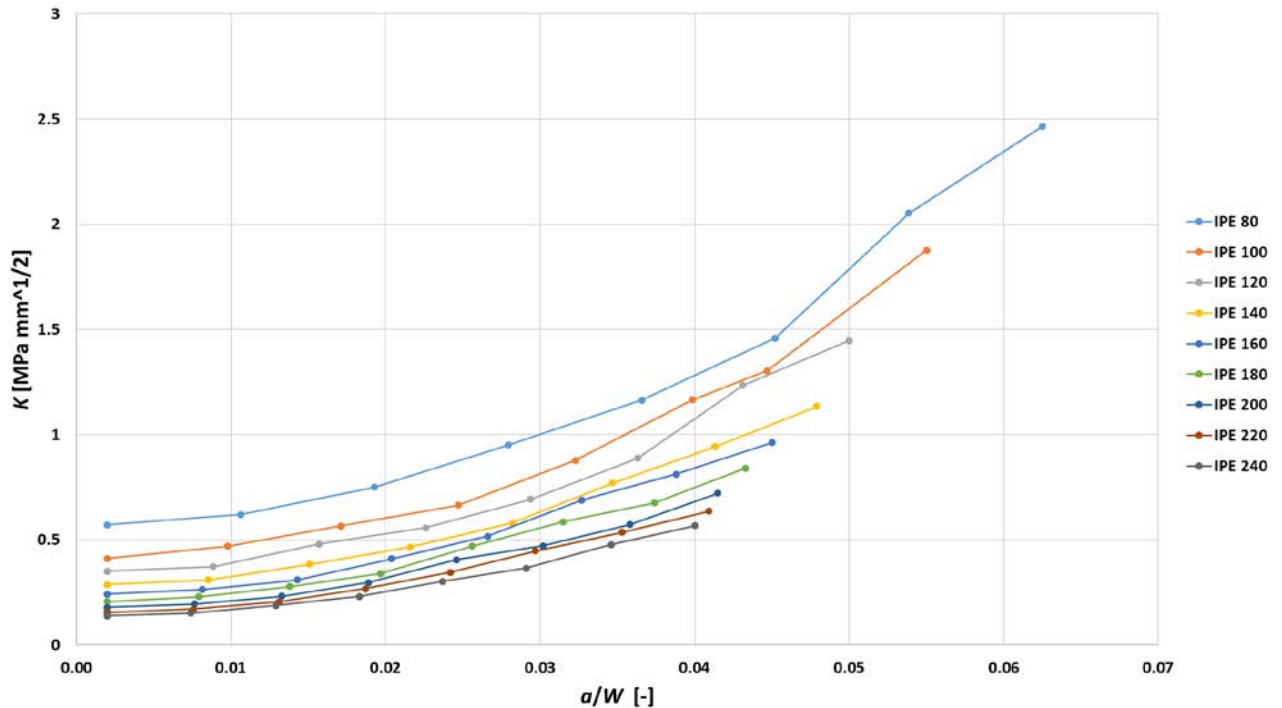
Graph 8: Stress intensity factor in the web versus *a/W* for IPE 80 to IPE 240
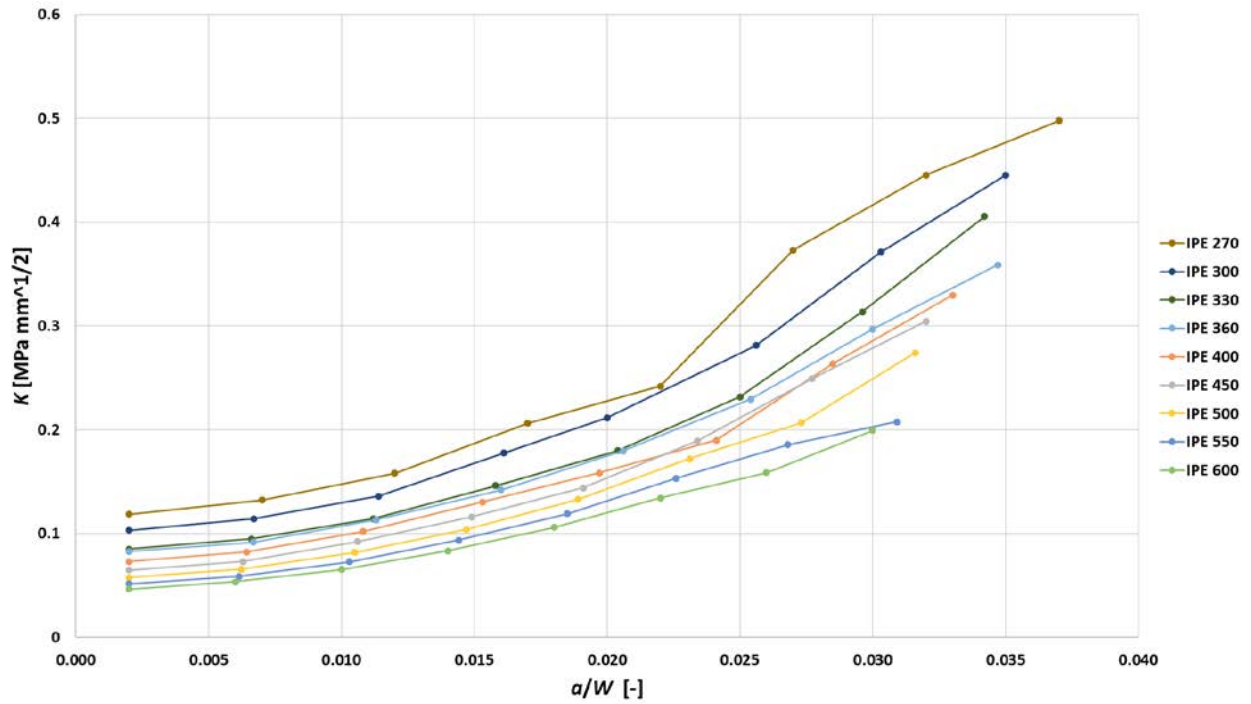
Graph 9: Stress intensity factor in the web versus *a/W* for IPE 270 to IPE 600
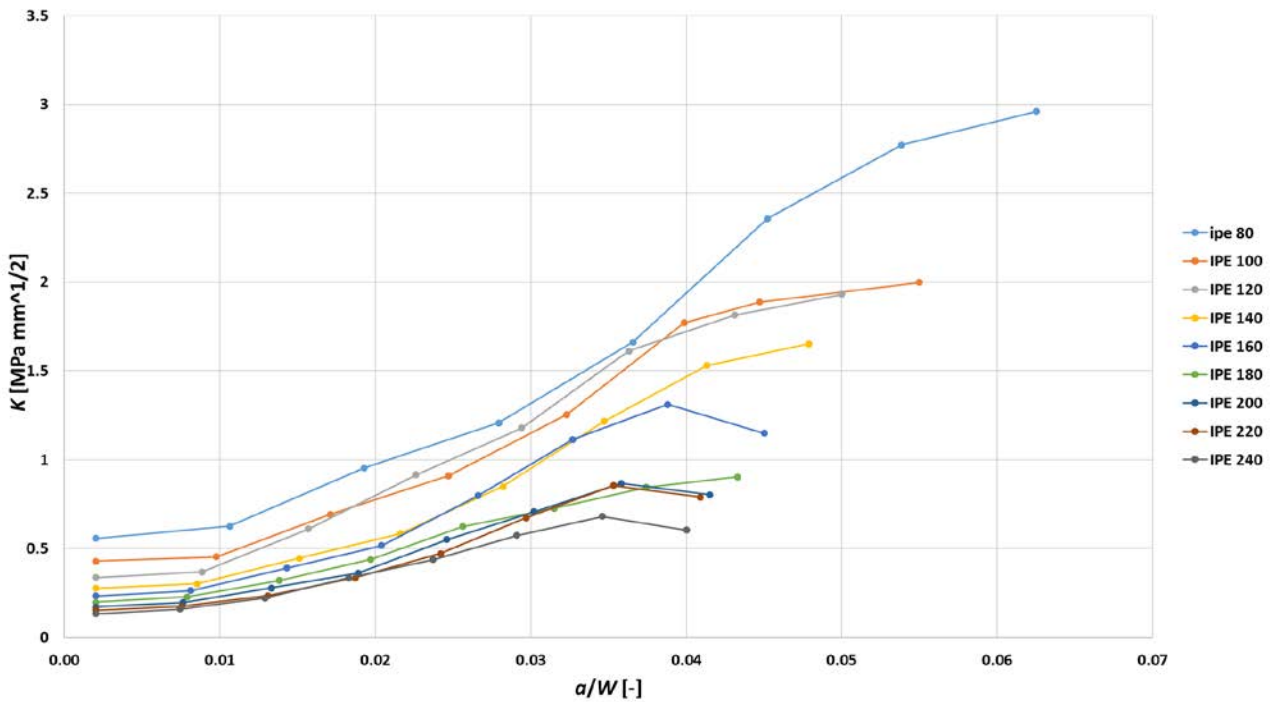
Graph 10: Stress intensity factor in the flange versus *a/W* for IPE 80 to IPE 240
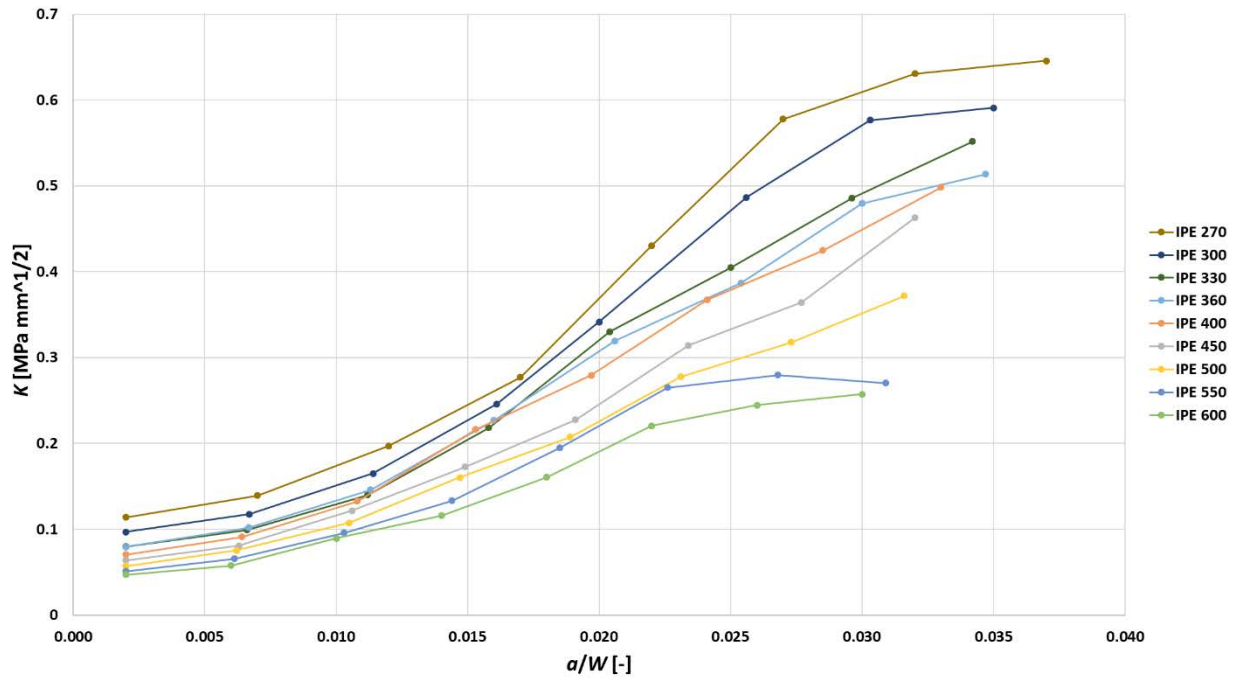
Graph 11: Stress intensity factor in the flange versus *a/W* for IPE 270 to IPE 600

As the ratio *a/W* is not the same for the different IPE profiles, this ratio was transformed into the ratio *a/t* so that the x-values in the graphs are the same in all the profiles and the results can be compared easily. Graph 12 plots the SIF versus the *a/t* ratio for IPE 80 to IPE 240, while Graph 13 does the same for IPE 270 to IPE 600. Regarding the flange, Graph 14 represents the SIF versus *a/t* for IPE 80 to IPE 240 and Graph 15 for IPE 270 to IPE 600.
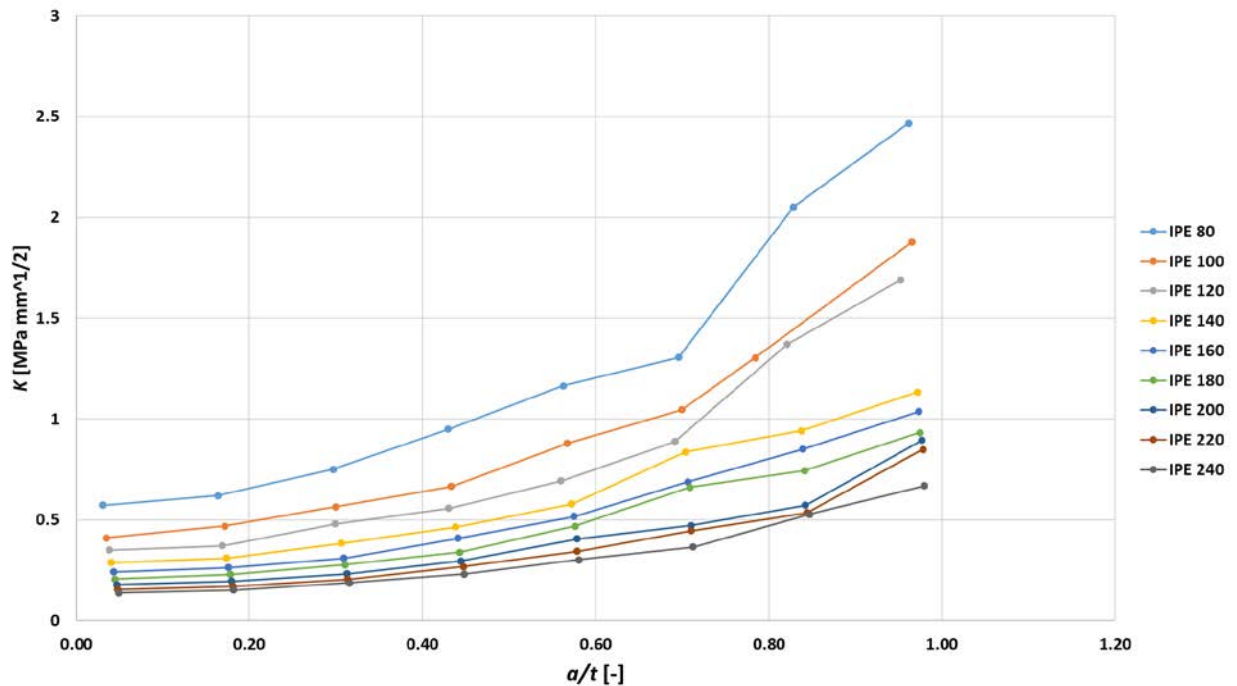
Graph 12: Stress intensity factor in the web versus *a/t* for IPE 80 to IPE 240

36
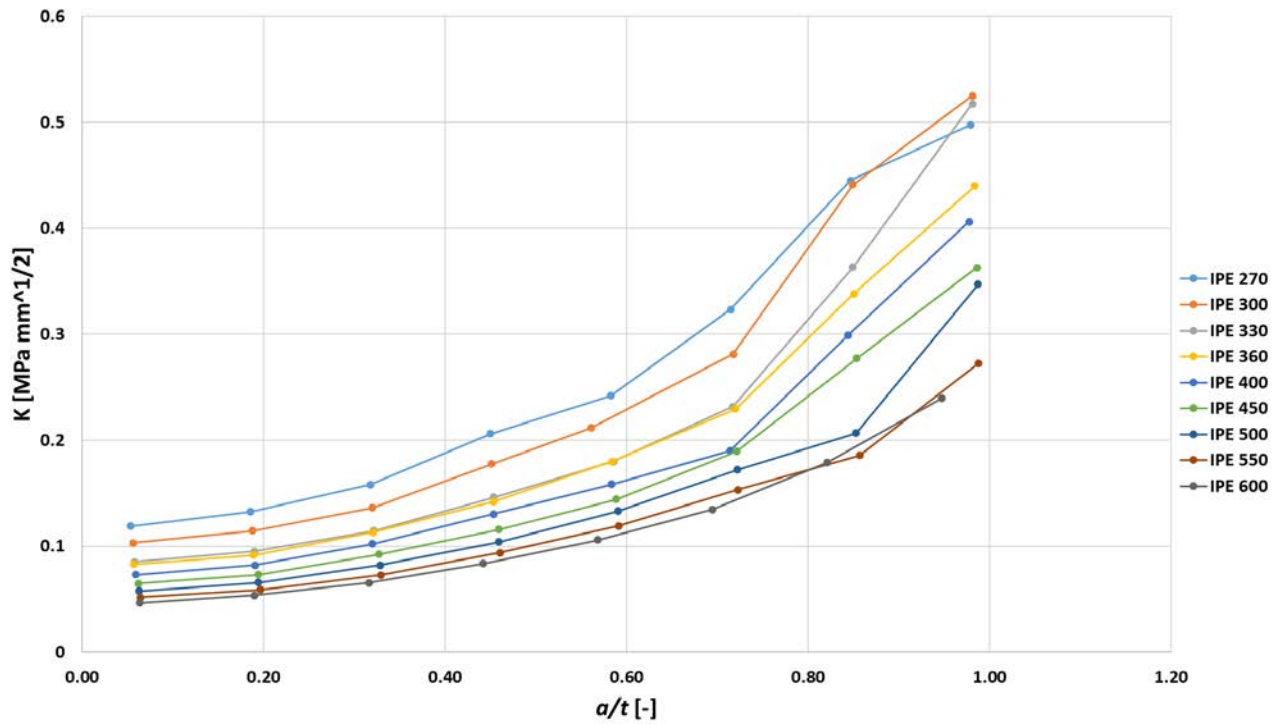
Graph 13: Stress intensity factor in the web versus *a/t* for IPE 270 to IPE 600
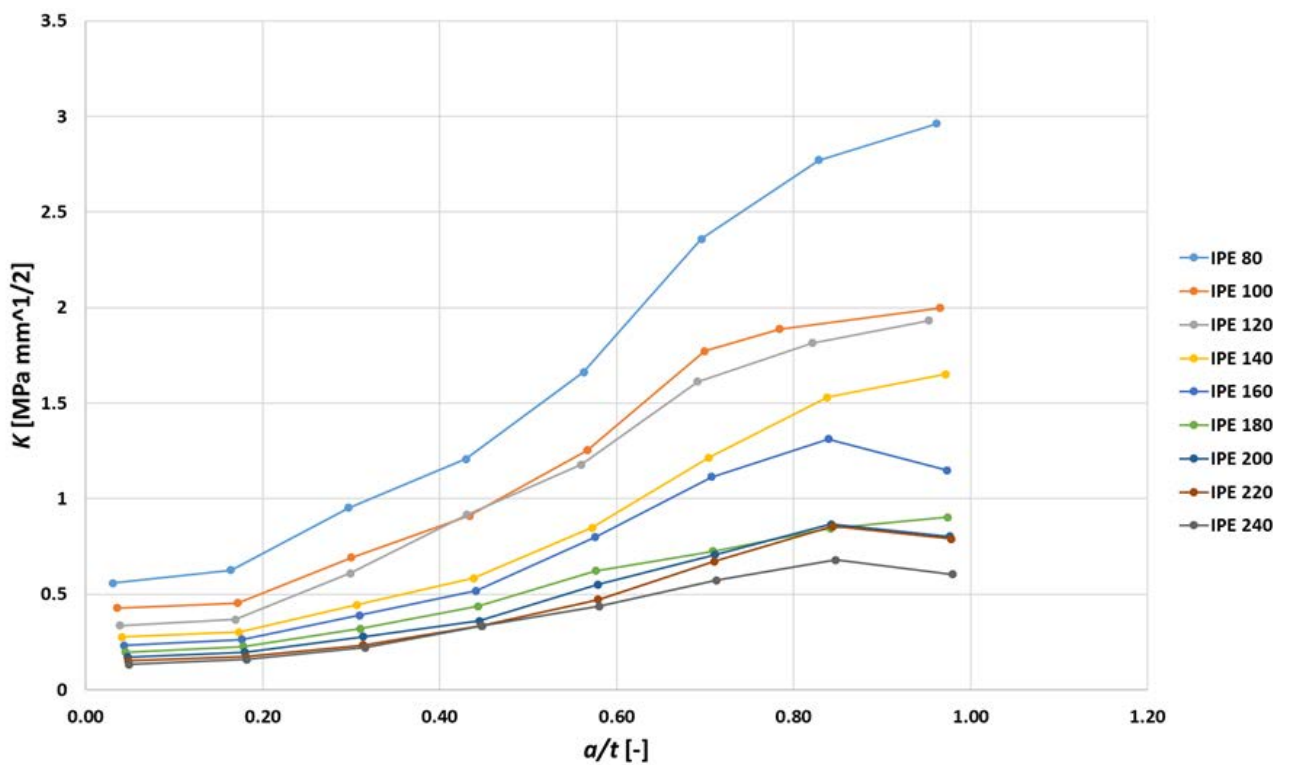
Graph 14: Stress intensity factor in the flange versus *a/t* for IPE 80 to IPE 240
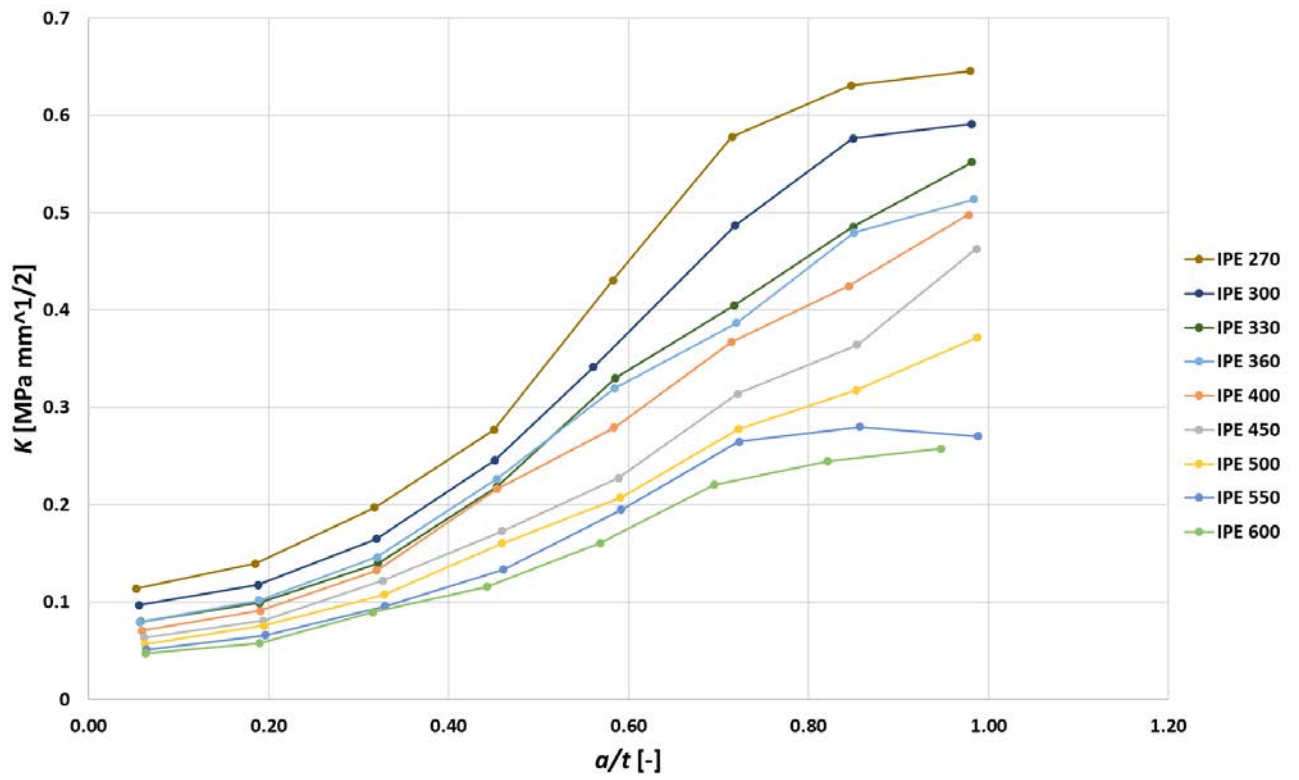
Graph 15: Stress intensity factor in the flange versus *a/t* for IPE 270 to IPE 600

5.2.2 Comparison with a rectangular profile

In this section the values of SIF obtained for the IPE profiles (K_I) will be compared with the ones a rectangular profile (K_{I0}) with the same dimensions of W, B and crack lengths (a) as the IPE under study. For example, for the IPE 100, $W=100$ mm and $B=46$ mm, so the dimensions of the rectangular profile will be the same ones: $W=100$ mm and $B=46$ mm. Figure 31 illustrates both profiles and paths in each of them.
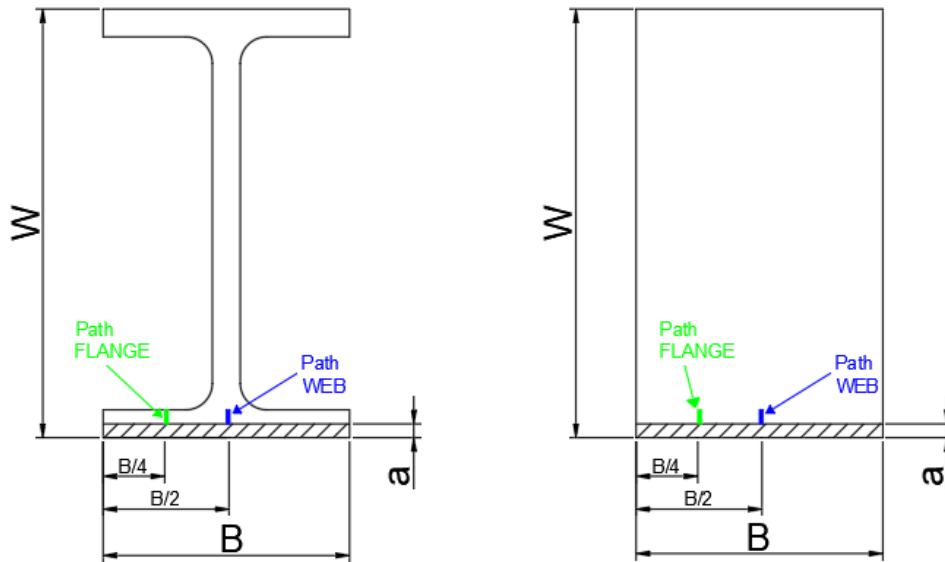
Figure 31: IPE and rectangular profiles

The comparison will be performed by means of the ratio between the SIF in the IPE profile and the SIF in the rectangular profile. The objective is to observe how the removal of material in the centre of the section of an IPE profile affects its SIF and quantify it. Table 5 represents the ratio K_I/K_{I0} for the path in the web and Table 6 for the path in the flange.

These tables show that the SIF is always higher in the IPE than in the rectangular profile, which coincides with what was expected. Moreover, the values of the ratio tend to increase with the crack length. Therefore, the smaller the crack length the smaller the K_I/K_{I0} ratio.

In both tables it can be appreciated that the ratio is higher for the flange than for the web.

Table 5: Ratio K_I/K_{I0} for the path in the web

IPE 80	a/W	0.002	0.011	0.019	0.028	0.037	0.045	0.054	0.063
	K_I/K_{I0}	2.2366	2.2079	3.0178	3.9545	3.6687	4.7354	3.7929	5.9133
IPE 100	a/W	0.002	0.010	0.017	0.025	0.032	0.040	0.045	0.055
	K_I/K_{I0}	3.4985	2.0852	2.8598	4.3266	4.6676	4.1726	4.7796	5.3761
IPE 120	a/W	0.002	0.009	0.016	0.023	0.029	0.036	0.043	0.050
	K_I/K_{I0}	3.8549	3.1610	2.6017	3.0929	4.3104	5.3463	5.3821	5.5798
IPE 140	a/W	0.002	0.009	0.015	0.022	0.028	0.035	0.041	0.048
	K_I/K_{I0}	3.6361	3.1080	3.3445	3.4281	3.7925	3.1957	5.1375	4.9927
IPE 160	a/W	0.002	0.00814	0.0143	0.0204	0.0266	0.0327	0.0388	0.045
	K_I/K_{I0}	3.6635	3.8884	3.4059	3.1840	3.5325	5.6752	6.0419	4.8560
IPE180	a/W	0.002	0.0079	0.0138	0.0197	0.0256	0.0315	0.0374	0.0433
	K_I/K_{I0}	2.8880	3.8125	3.7055	4.1222	7.7913	5.4144	8.3287	8.1769
IPE200	a/W	0.002	0.00764	0.0133	0.0189	0.0246	0.0302	0.0358	0.0415
	K_I/K_{I0}	2.8355	2.8566	4.5038	2.6367	5.2664	5.9637	4.3600	6.6413
IPE 220	a/W	0.002	0.00756	0.0131	0.0187	0.0242	0.0297	0.0353	0.0409
	K_I/K_{I0}	2.2621	3.9216	4.2841	3.2967	3.8838	6.8082	5.9339	8.1669
IPE 240	a/W	0.002	0.00742	0.0129	0.0183	0.0237	0.0291	0.0346	0.04
	K_I/K_{I0}	2.9561	3.1339	4.1449	4.1063	5.2061	6.2870	8.4107	9.6624
IPE 270	a/W	0.002	0.007	0.012	0.017	0.022	0.027	0.032	0.037
	K_I/K_{I0}	2.9955	4.0909	3.6838	5.3175	9.1645	15.4834	7.4305	8.5536
IPE 300	a/W	0.002	0.0067	0.0114	0.0161	0.02	0.0256	0.0303	0.035
	K_I/K_{I0}	5.1879	5.2805	7.7959	7.5342	6.5974	8.4805	8.9211	11.4818
IPE 330	a/W	0.002	0.0066	0.0112	0.0158	0.0204	0.025	0.0296	0.0342
	K_I/K_{I0}	7.2198	10.4211	14.3551	11.8712	13.9828	15.3103	17.9672	23.8803
IPE 360	a/W	0.002	0.00667	0.0113	0.016	0.0206	0.0254	0.03	0.0347
	K_I/K_{I0}	5.7920	6.0199	9.5172	8.3561	9.7129	12.9189	20.9016	29.9318
IPE 400	a/W	0.002	0.00642	0.0108	0.0153	0.0197	0.0241	0.0285	0.033
	K_I/K_{I0}	6.1739	6.1438	10.8835	11.5000	12.7312	14.7600	20.0345	29.0532
IPE 450	a/W	0.002	0.00629	0.0106	0.0149	0.0191	0.0234	0.0277	0.032
	K_I/K_{I0}	5.3958	5.2869	9.7788	10.9780	12.1304	14.8667	17.6105	24.7835
IPE 500	a/W	0.002	0.00622	0.0105	0.0147	0.0189	0.0231	0.0273	0.0316
	K_I/K_{I0}	3.9894	9.8750	9.9500	11.0000	12.9709	19.6026	19.0875	29.2195
IPE 550	a/W	0.002	0.00613	0.0103	0.0144	0.0185	0.0226	0.0268	0.0309
	K_I/K_{I0}	5.9180	10.1154	12.0833	13.3375	12.8876	14.4767	10.4130	17.3600
IPE 600	a/W	0.002	0.006	0.01	0.014	0.018	0.022	0.026	0.03
	K_I/K_{I0}	8.4662	14.0524	11.9848	13.7229	12.8625	14.8310	12.7209	13.4348

Table 6: Ratio K_I/K_{I0} for the path in the flange

IPE 80	*a/W*	0.002	0.011	0.019	0.028	0.037	0.045	0.054	0.063
	K_I/K_{I0}	3.2391	3.6007	2.7383	3.5285	6.1547	3.9041	4.0015	7.8289
IPE 100	*a/W*	0.002	0.010	0.017	0.025	0.032	0.040	0.045	0.055
	K_I/K_{I0}	3.0835	1.1877	3.7988	5.3760	4.7123	4.5510	5.1795	4.8966
IPE 120	*a/W*	0.002	0.009	0.016	0.023	0.029	0.036	0.043	0.050
	K_I/K_{I0}	1.8748	2.6252	2.4633	3.9902	4.0896	3.5530	4.7243	5.0552
IPE 140	*a/W*	0.002	0.009	0.015	0.022	0.028	0.035	0.041	0.048
	K_I/K_{I0}	2.2559	2.1716	3.2111	7.2872	7.7164	6.2035	4.5682	5.1801
IPE 160	*a/W*	0.002	0.00814	0.0143	0.0204	0.0266	0.0327	0.0388	0.045
	K_I/K_{I0}	2.9280	2.6214	2.3780	3.4992	4.1295	8.4787	5.9704	4.6537
IPE180	*a/W*	0.002	0.0079	0.0138	0.0197	0.0256	0.0315	0.0374	0.0433
	K_I/K_{I0}	2.0289	2.7113	2.0808	2.7026	7.9926	5.6039	6.2869	6.8831
IPE200	*a/W*	0.002	0.00764	0.0133	0.0189	0.0246	0.0302	0.0358	0.0415
	K_I/K_{I0}	2.0955	2.6706	3.1401	3.5985	4.8860	3.6104	4.5621	7.2041
IPE 220	*a/W*	0.002	0.00756	0.0131	0.0187	0.0242	0.0297	0.0353	0.0409
	K_I/K_{I0}	3.2541	2.6121	3.4012	3.7906	5.8033	6.5593	6.9674	8.5201
IPE 240	*a/W*	0.002	0.00742	0.0129	0.0183	0.0237	0.0291	0.0346	0.04
	K_I/K_{I0}	3.6533	3.6228	2.9423	6.2727	4.1726	8.2376	7.1179	8.4076
IPE 270	*a/W*	0.002	0.007	0.012	0.017	0.022	0.027	0.032	0.037
	K_I/K_{I0}	1.5681	3.6211	4.0658	8.4329	9.3077	17.6879	11.0605	15.1843
IPE 300	*a/W*	0.002	0.0067	0.0114	0.0161	0.02	0.0256	0.0303	0.035
	K_I/K_{I0}	4.5370	3.7397	3.3861	7.8581	6.3362	12.1870	20.7285	22.3647
IPE 330	*a/W*	0.002	0.0066	0.0112	0.0158	0.0204	0.025	0.0296	0.0342
	K_I/K_{I0}	6.2418	4.6695	4.5789	12.8108	17.2667	18.3500	24.5273	26.7967
IPE 360	*a/W*	0.002	0.00667	0.0113	0.016	0.0206	0.0254	0.03	0.0347
	K_I/K_{I0}	14.8500	11.9239	10.5882	20.1163	24.1548	17.9381	23.2547	43.4198
IPE 400	*a/W*	0.002	0.00642	0.0108	0.0153	0.0197	0.0241	0.0285	0.033
	K_I/K_{I0}	11.8039	10.4222	10.3925	24.0580	17.0469	17.5306	23.6184	36.8590
IPE 450	*a/W*	0.002	0.00629	0.0106	0.0149	0.0191	0.0234	0.0277	0.032
	K_I/K_{I0}	3.6771	6.2353	13.9538	23.2778	22.5098	16.8939	46.4048	34.7581
IPE 500	*a/W*	0.002	0.00622	0.0105	0.0147	0.0189	0.0231	0.0273	0.0316
	K_I/K_{I0}	8.7600	18.0769	12.5155	34.5400	30.1915	20.1045	23.2319	34.2286
IPE 550	*a/W*	0.002	0.00613	0.0103	0.0144	0.0185	0.0226	0.0268	0.0309
	K_I/K_{I0}	4.5106	8.6304	12.6600	24.2885	20.6250	25.2075	19.1549	18.2771
IPE 600	*a/W*	0.002	0.006	0.01	0.014	0.018	0.022	0.026	0.03
	K_I/K_{I0}	8.3061	9.7239	8.3051	18.2391	21.5872	22.9756	17.9216	14.4078

5.2.3 Calibration curves

The calibration curves *f(a/W)* for the IPE profile will be determined in this section. The stress intensity factor in front of the crack tip (*KI*) is defined as:

$$K_I = \Delta\sigma\sqrt{\pi a}\, f\left(\frac{a}{W}\right) \tag{9}$$

where $\Delta\sigma$ is the constant stress range for a 3PBT and *a* is the crack length. In this sense, the calibration curves can be obtained as:

$$f\left(\frac{a}{W}\right) = \frac{K_I}{\Delta\sigma\sqrt{\pi a}} \tag{10}$$

the SIF (*KI*) has already been calculated for all the IPE profiles, *a* is known and the value of the stress for a 3PBT can be obtained as follows:

$$\Delta\sigma = \frac{M}{I}y \tag{10}$$

M is calculated as the maximum moment in the beam, *I* is the moment of inertia and *y* is the distance from the neutral axis to the extremes (where the bending moment is the highest), as shown in Figure 6. The moment of inertia is given as data in the tables of IPE dimensions found in standards. Finally, the bending stress for the IPE profile can be computed as:

$$\Delta\sigma = \frac{M}{I}y = \frac{P \cdot S \cdot W}{8 \cdot I} \tag{10}$$

It is important to remark that this stress varies for each of the profiles as it depends on the characteristics of the section (the height of the section, *W*, the span, *S*, and the moment of inertia, *I*). However, the load is the same for all of them, *P*=100 N.

Graph 16 represents the calibration curves in the web for the IPE 80 to 240 and Graph 17 for the IPE 270 to IPE 600. Regarding the flange, Graph 18 plots calibration curves for IPE 80 to IPE 240, while Graph 19 for IPE 270 to IPE 600. It is important to remark that the value of *f(a/W)* is has no dimensions.
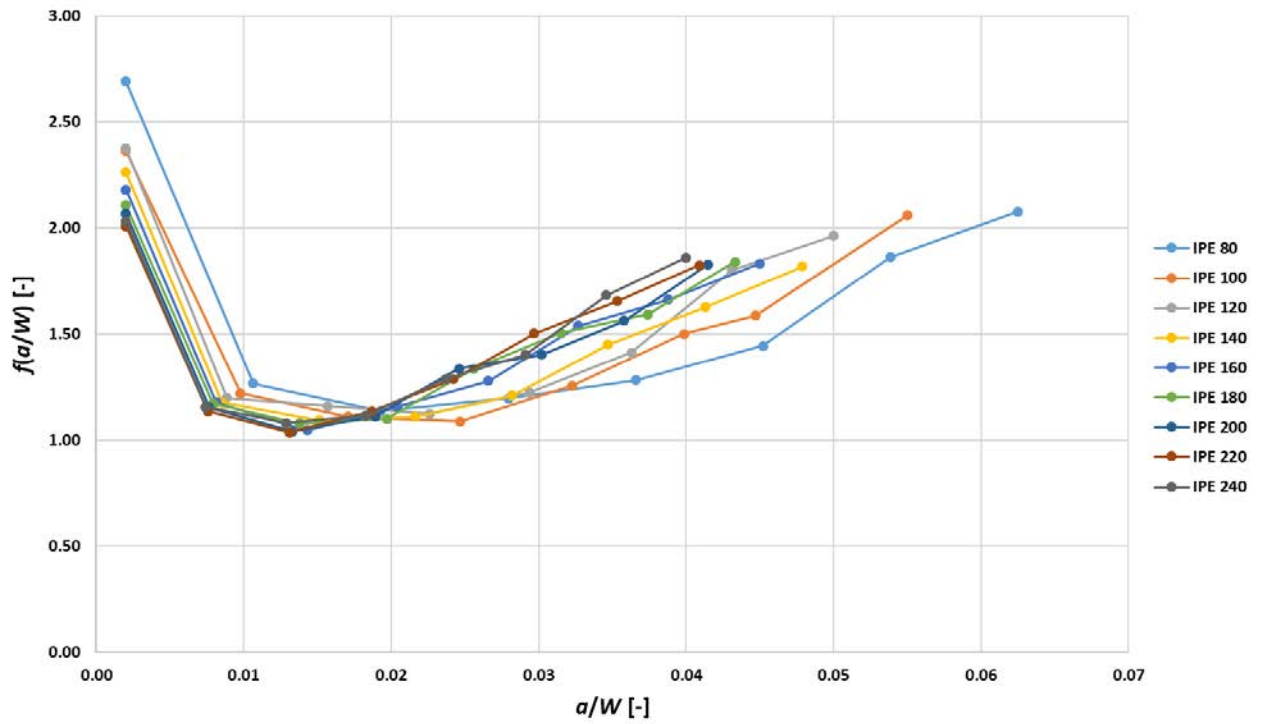
Graph 16: Calibration curves in the web versus *a/W* for the IPE 80 to IPE 240
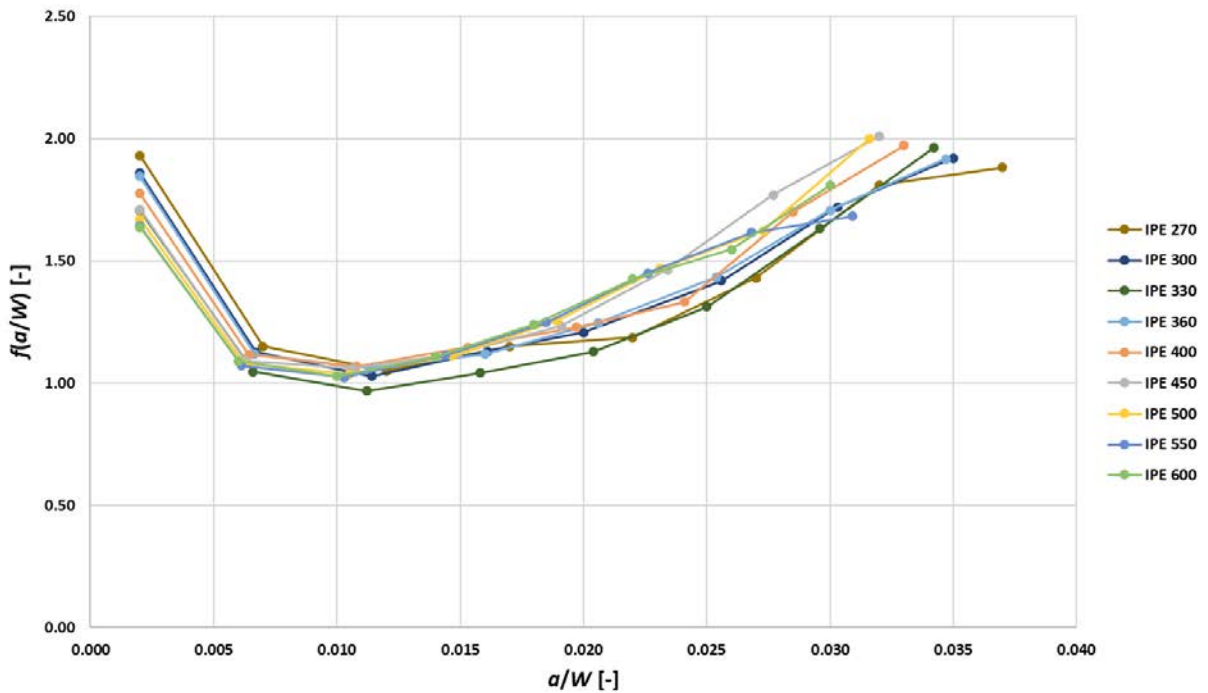
Graph 17: Calibration curves in the web versus *a/W* for the IPE 270 to IPE 600
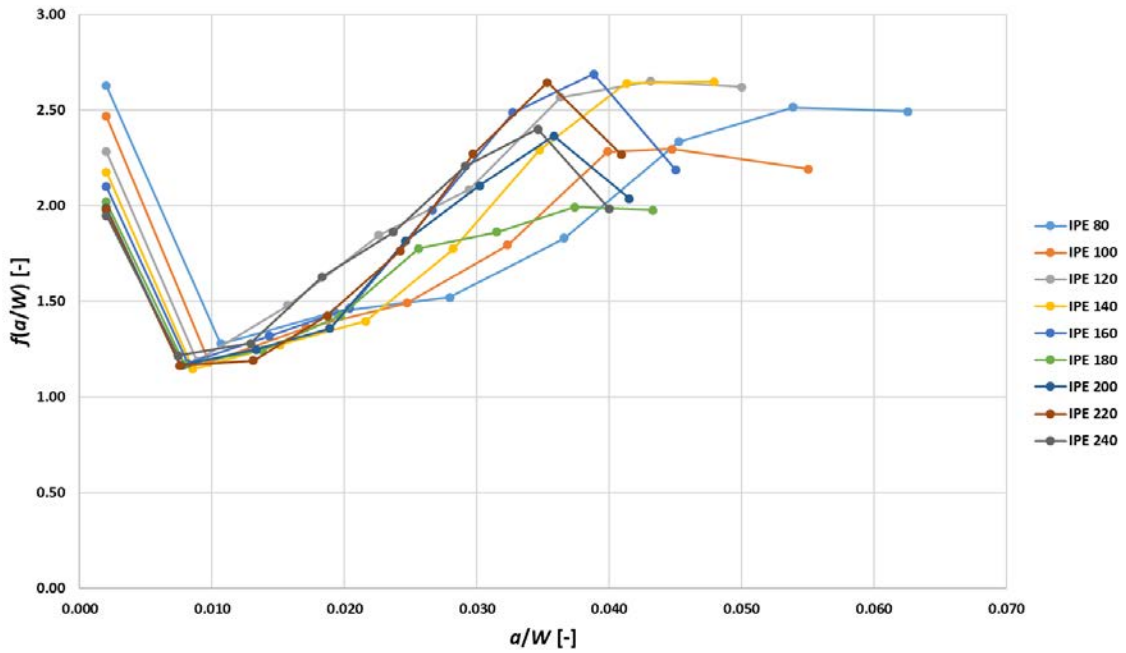
Graph 18: Calibration curves in the flange versus *a/W* for the IPE 80 to IPE 240
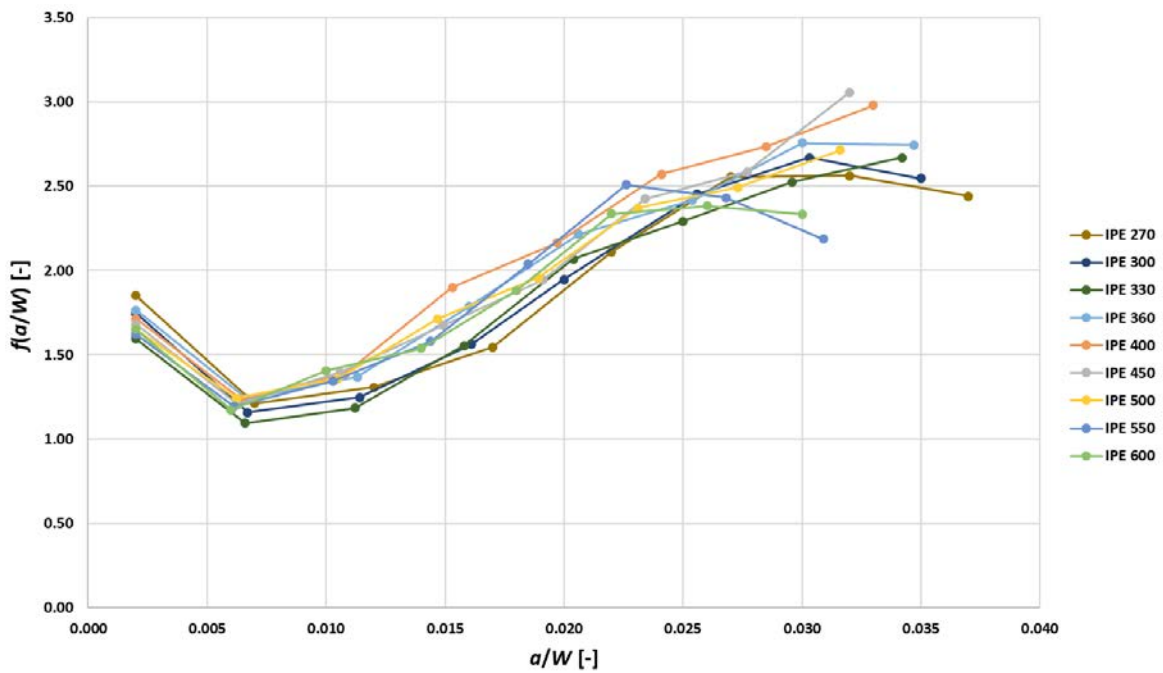
Graph 19: Calibration curves in the flange versus *a/W* for the IPE 270 to IPE 600

As the ratio of a/W varies for all profiles, new calibration curves *f(a/t)* are obtained having *a/t* as the value in the x-axis. In his sense, the results can be better compared. For the web, Graph 20 and Graph 21 represent the calibration curves for IPE 80-IPE 240 and IPE 270-IPE 600, respectively. Graph 22 and Graph 23 represent the calibration curves but in the flange.

Graph 20: Calibration curves in the web versus *a/t* for IPE 80 to IPE 240

Graph 21: Calibration curves in the web versus *a/t* for the IPE 270 to IPE 600

Graph 22: Calibration curves in the flange versus *a/t* for IPE 80 to IPE 240

Graph 23: Calibration curves in the flange versus a/t for IPE 240 to IPE 600
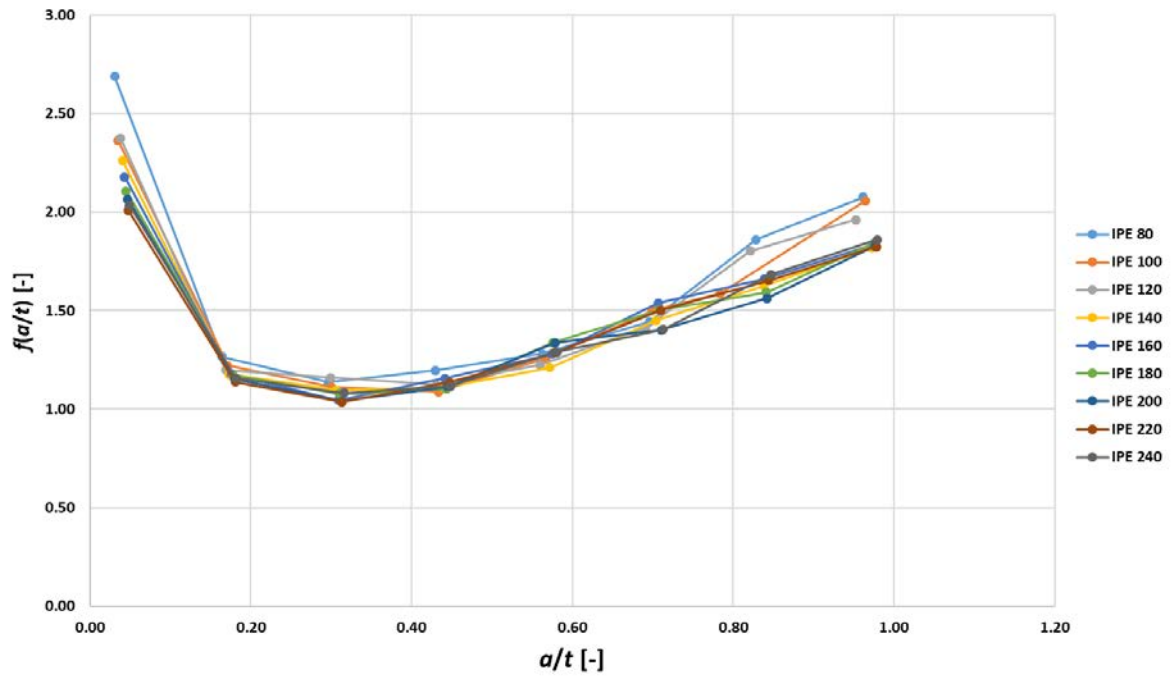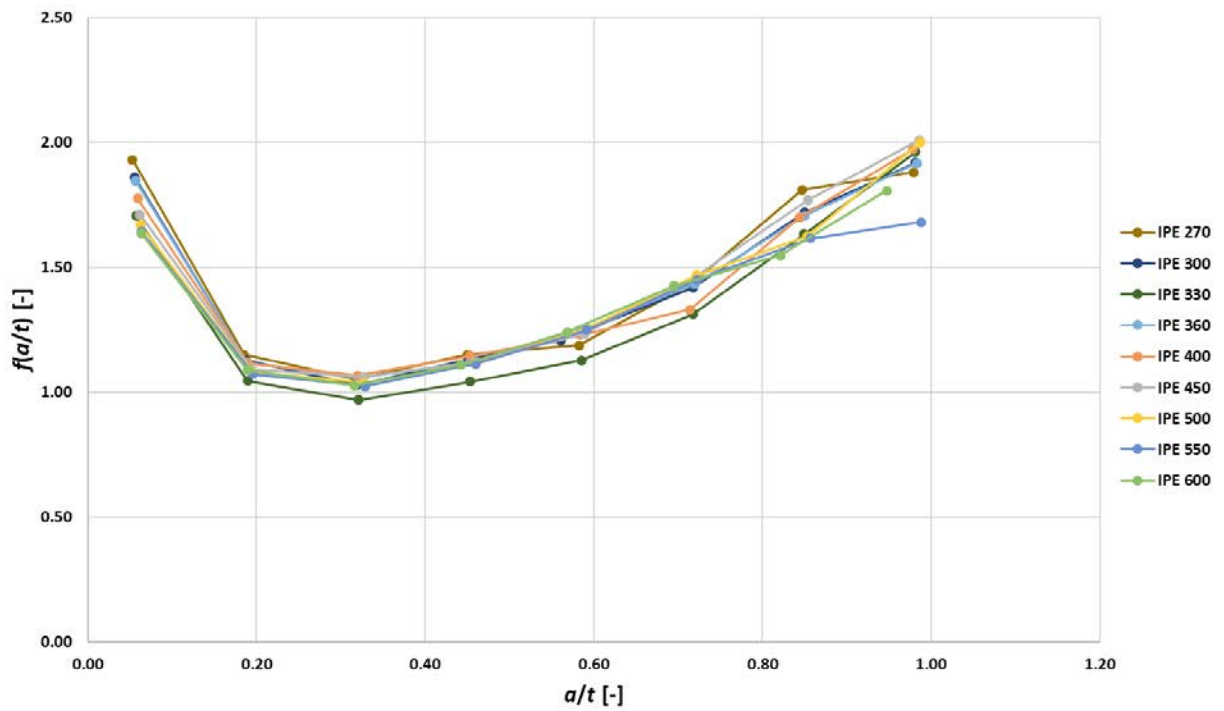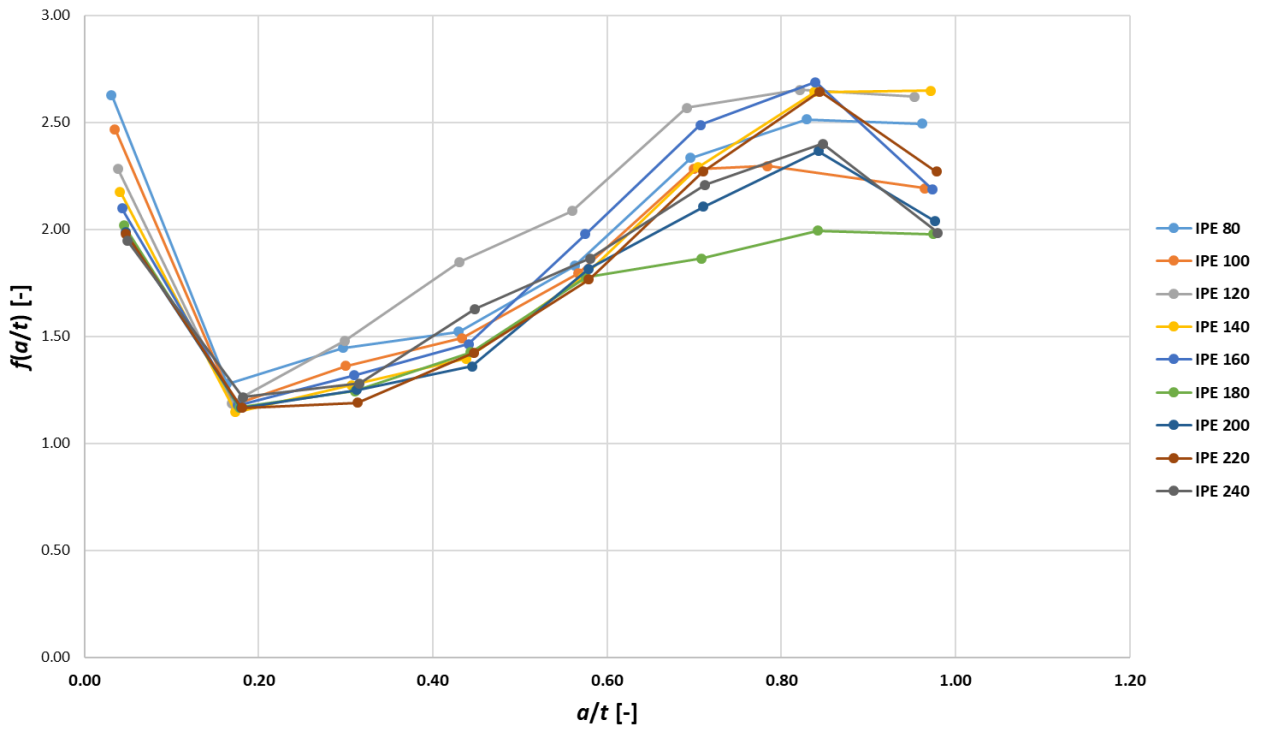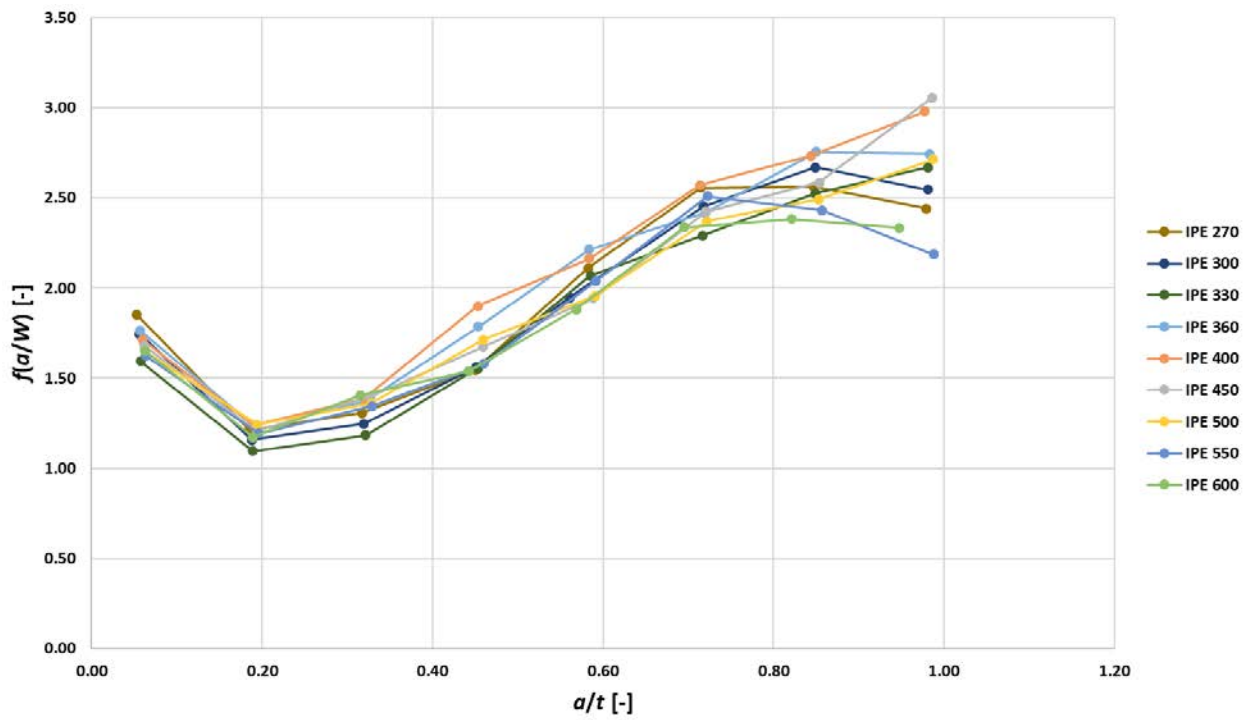
5.3 UPE Profile

UPE profiles are standardised and, therefore, widely used in the construction sector. These profiles are not symmetrical in the longitudinal direction and the web is located in one of the sides, in contrast to IPE profiles where the web is in the middle of the section. There are 14 different UPE profiles depending on its dimensions, ranging from UPE 80 (smallest one) to UPE 400 (biggest one). In standards, the dimensions and properties of the different profiles are given. Figure 32 provides the dimensions for the different profiles.

Identification	Nominal dimensions										Cross-section	Nominal weight 1m	Surface	
	h	b	s	t	R	h1	d	Ø	emin	emax	A	G	AL	AG
	mm	mm	mm	mm	mm	mm	mm		mm	mm	cm2	kg/m	m2/m	m2/m
UPE 80	80	50	4,0	7,0	10	66	46	-	-	-	10,1	7.90	0,343	43,45
UPE 100	100	55	4,5	7,5	10	85	65	M12	35	36	12,5	9,82	0,402	41,00
UPE 120	120	60	5,0	8,0	12	104	80	M12	35	41	15,4	12,1	0,460	37,98
UPE 140	140	65	5,0	9,0	12	122	98	M16	35	38	18,4	14,5	0,520	35,95
UPE 160	160	70	5,5	9,5	12	141	117	M16	36	43	21,7	17,0	0,579	34,01
UPE 180	180	75	5,5	10,5	12	159	135	M16	36	48	25,1	19,7	0,639	32,40
UPE 200	200	80	6,0	11,0	13	178	152	M20	46	47	29,0	22,8	0,697	30,60
UPE 220	220	85	6,5	12,0	13	196	170	M22	47	49	33,9	26,6	0,756	28,43
UPE 240	240	90	7,0	12,5	15	215	185	M24	47	51	38,5	30,2	0,813	26,89
UPE 270	270	95	7,5	13,5	15	243	213	M27	48	50	44,8	35,2	0,892	25,34
UPE 300	300	100	9,5	15,0	15	270	240	M27	50	55	56,6	44,4	0,968	21,78
UPE 330	330	105	11,0	16,0	18	298	262	M27	54	60	67,8	53,2	1,043	19,60
UPE 360	360	110	12,0	17,0	18	326	290	M27	55	65	77,9	61,2	1,121	18,32
UPE 400	400	115	13,5	18,0	18	364	328	M27	57	70	91,9	72,2	1,218	16,87

Figure 32: Standard dimensions of UPE profiles [9]

In this section a numerical study simulating a 3PBT is developed in order to study the variation of the SIF in both the web and the flange of the all the UPE profiles for different crack lengths, by varying the ratio a/W. Please note that P=100 N, $S = 3xW$ mm, v=0.3 (steel). The characteristic dimensions of each UPE profile as well as the paths of study of the SIF in the flange (green) and in the web (blue) are illustrated in Figure 33.
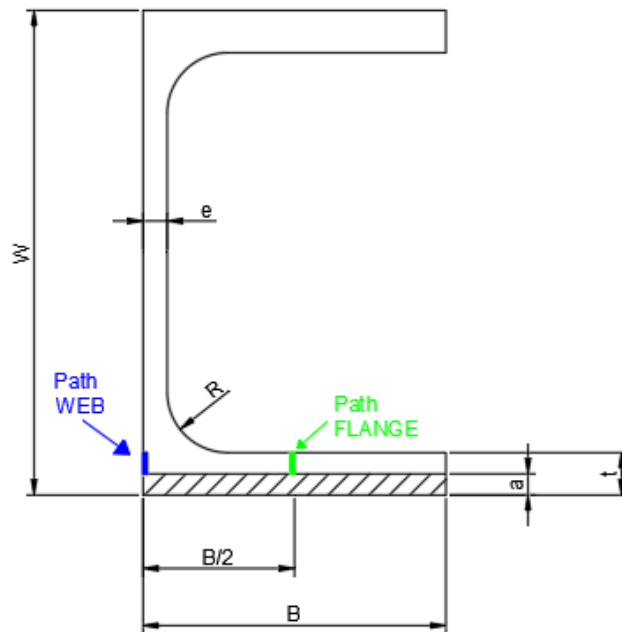
Figure 33: UPE dimensions and paths for calculation of SIF

Moreover, the results obtained will be compared with a rectangular profile, with same dimensions of height (*W*) and width (*B*) as the UPE profiles under study. Finally, the calibration curves will be calculated for all the 14 UPE profiles.

5.3.1 Variation of the SIF for different crack lengths

The SIF variation in an UPE profile is calculated for 8 different crack lengths, a, by varying the ratio *a/W*, the initial value for this ratio is always 0.002 but the last value depends on the UPE profile under study, as the flange width (*t*) and the height (*W*) of the profile different from one profile to another. In other words, the ratio *t/W* is different for each profile.

By means of the simulation of ANSYS, SIF is calculated in all profiles both in the web and in the flange. Graph 24 represents the SIF variation with the crack length for UPE 160 and Graph 25 for UPE 240.
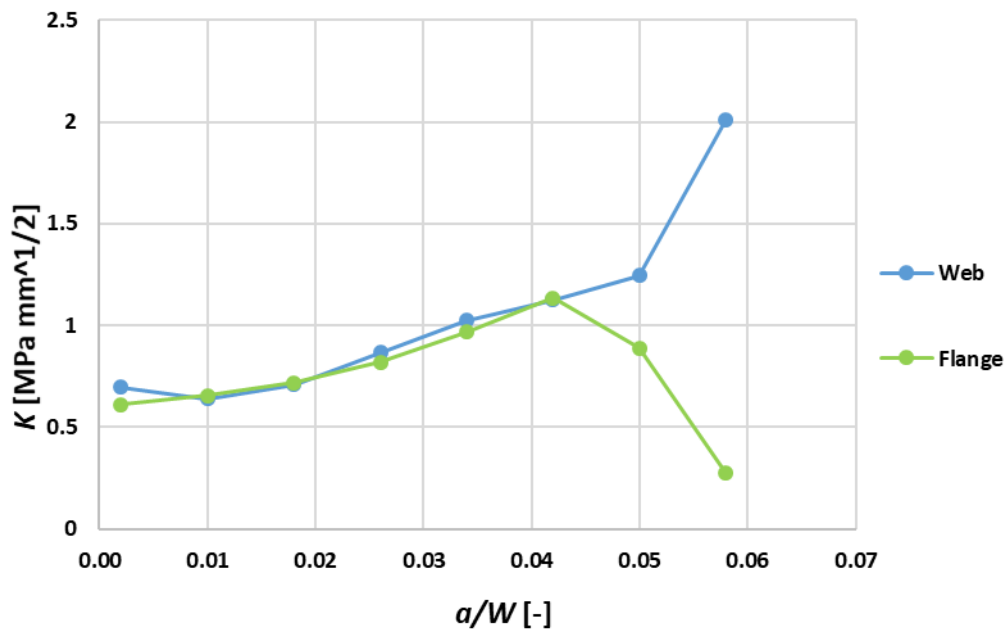
Graph 25: Evolution of SIF versus crack length in an UPE 160 profile
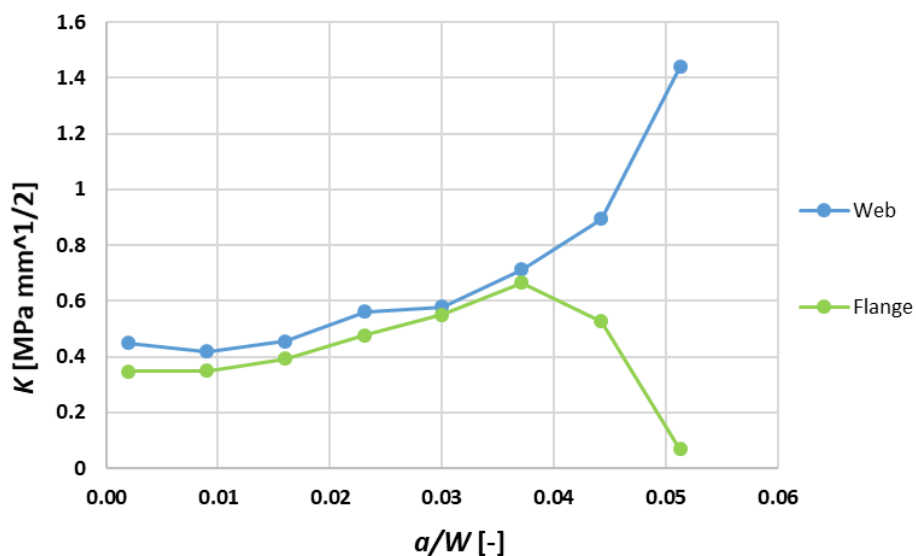
Graph 24: Evolution of SIF versus crack length in an UPE 240 profile

It can be appreciated that the SIF in the web tends to increase in an almost linear way while in the flange it firstly increases but then it decreases. As it can be appreciated, values of the SIF in the web are higher than in flange.

By calculating the SIF in all the profiles in the same way as for UPE 160 and UPE 240, several graphs have been obtained. The evolution of SIF versus ratio *a/W* in the web is represented by Graph 26 for profiles UPE 80 to UPE 200 and by Graph 27 for profiles UPE 200 to UPE 400. Regarding the flange, Graph 28 plots the SIF from the UPE 80 to UPE 200, while Graph 29 does so for UPE 220 to UPE 400.
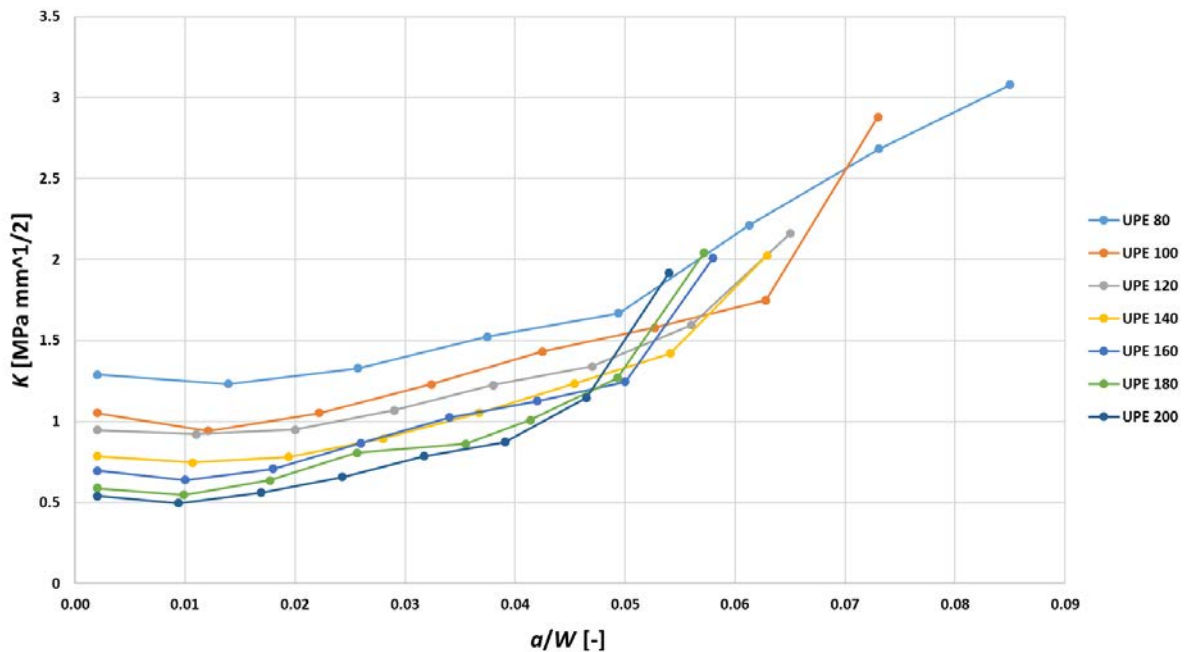
Graph 27: Stress intensity factor in the web versus *a/W* for UPE 80 to UPE 200
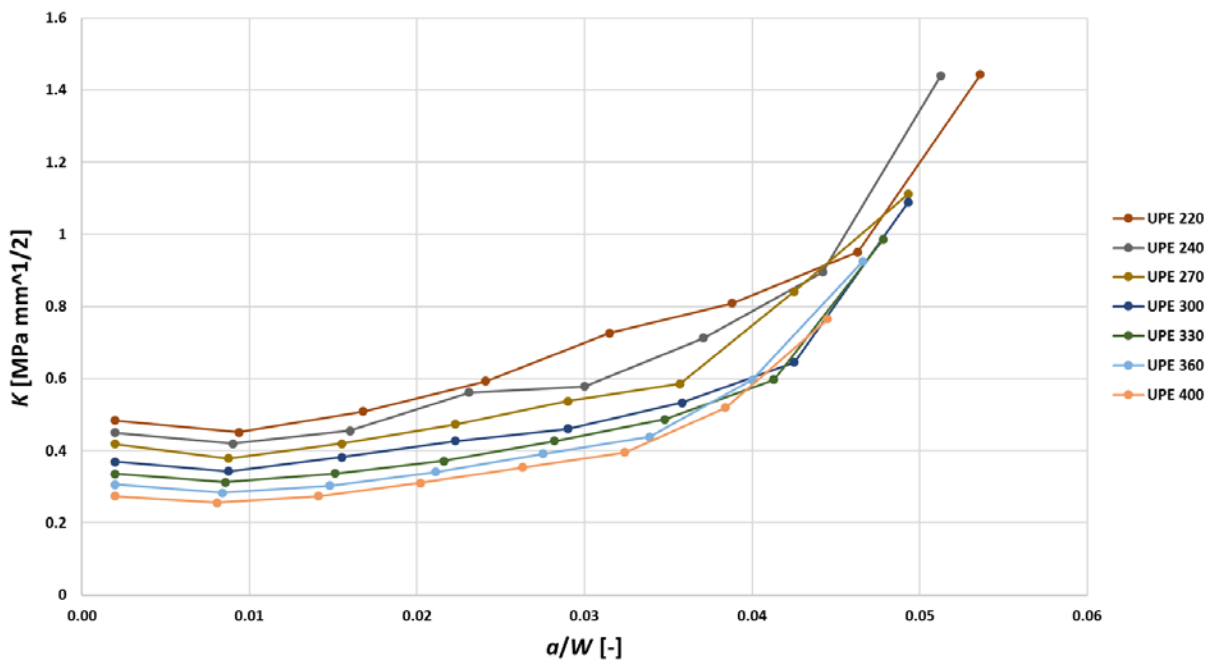
Graph 26: Stress intensity factor in the web versus *a/W* for UPE 220 to UPE 400
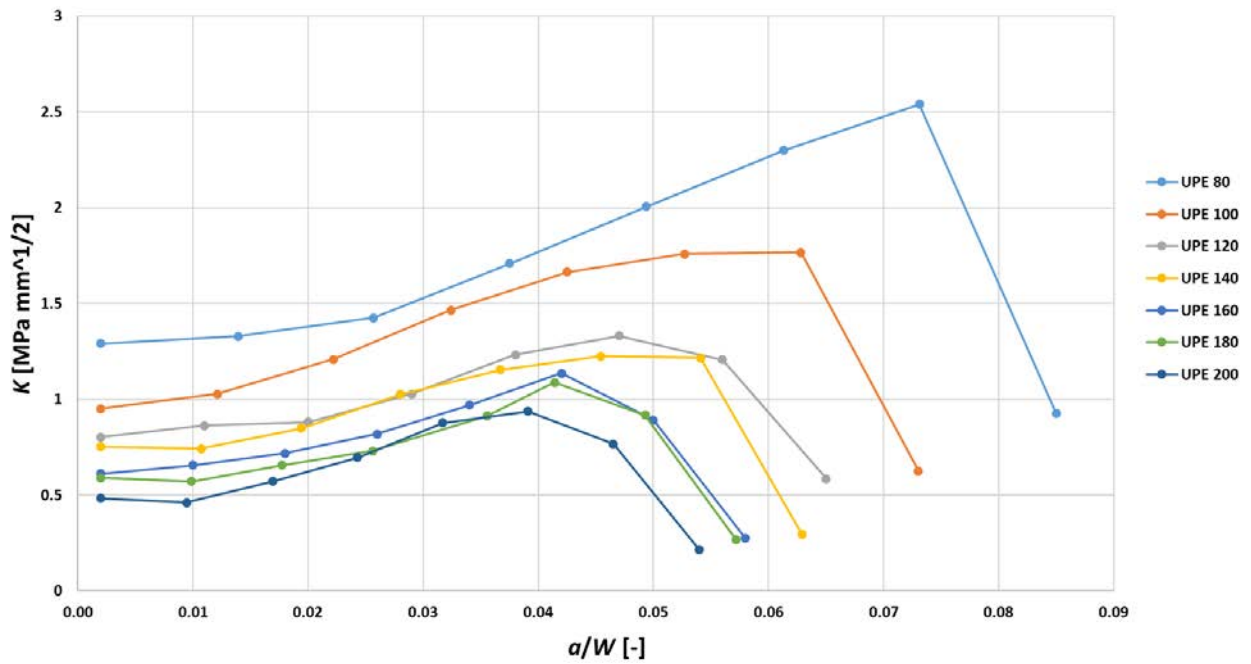
Graph 28: Stress intensity factor in the flange versus *a/W* for UPE 80 to UPE 200
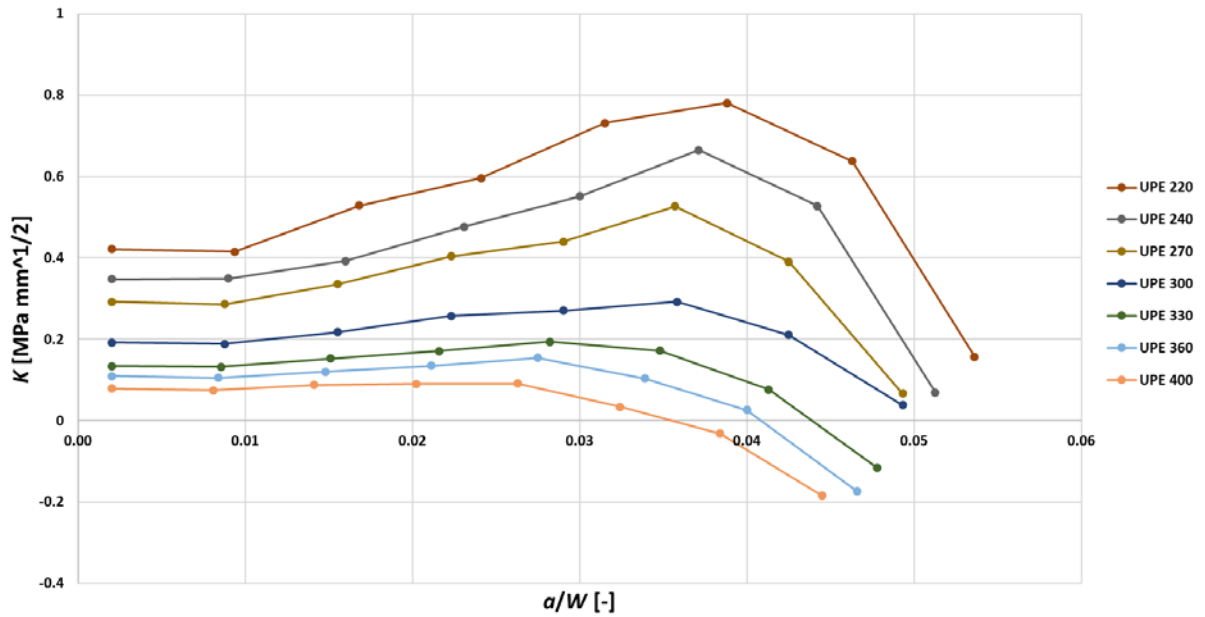
Graph 29: Stress intensity factor in the flange versus *a/W* for UPE 200 to UPE 400

In adittion, more graphs are obtained by plotting the SIF versus *a/t* so that the results can be more clear for analyzing. Graph 30 plots the SIF versus the *a/t* ratio for UPE 80 to UPE 200, while Graph 31 does the same for UPE 220 to UPE 400. Regarding the flange, Graph 32 represents the SIF versus *a/t* for UPE 80 to UPE 200 and Graph 33 for UPE 220 to UPE 400.
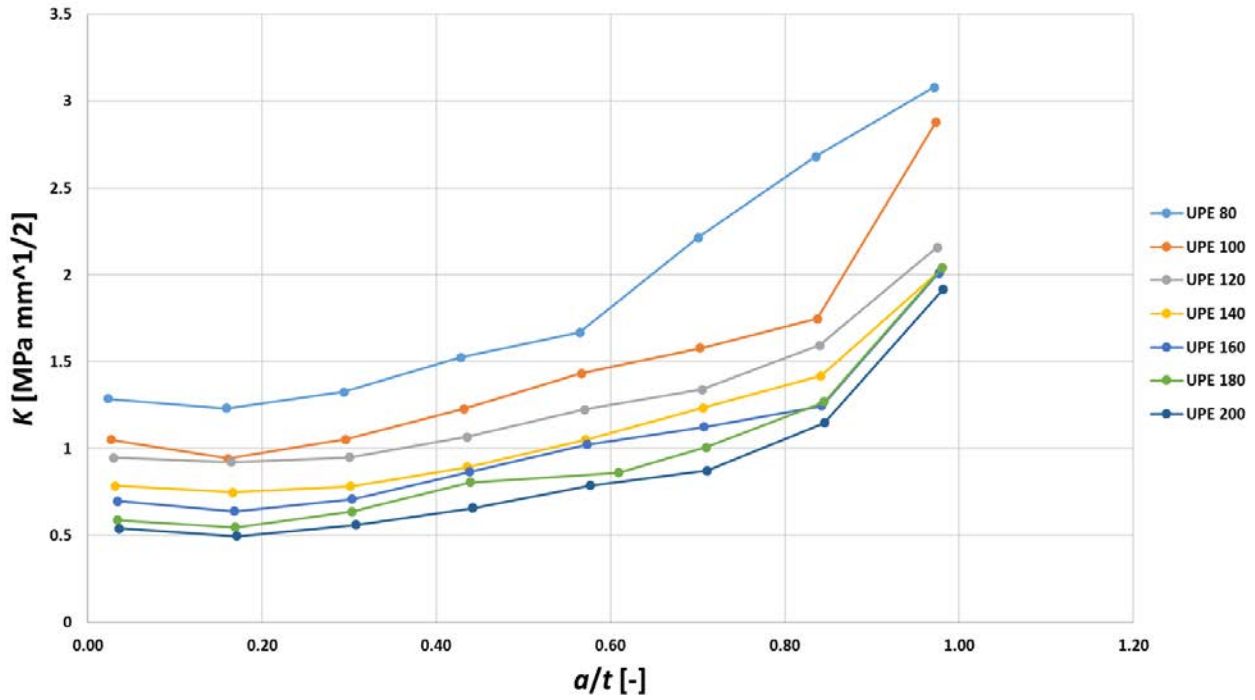
Graph 30: Stress intensity factor in the web versus *a/t* for UPE 80 to UPE 200
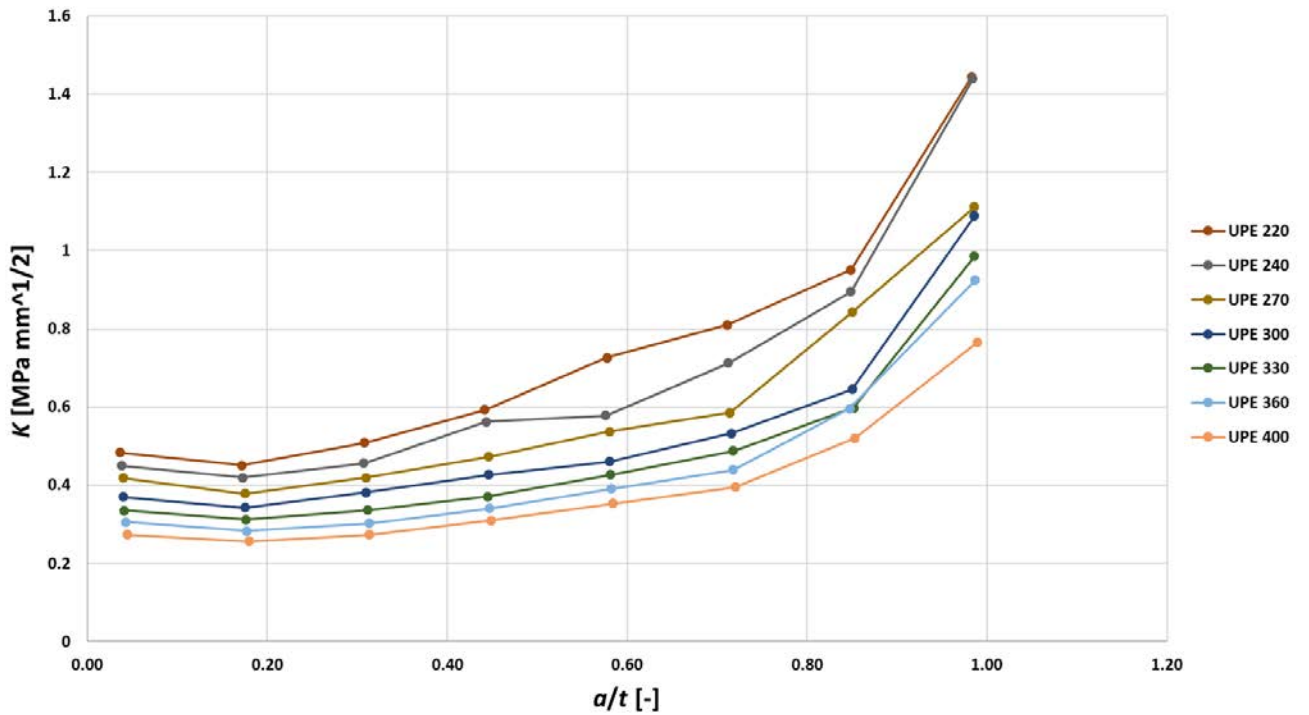
Graph 31: Stress intensity factor in the web versus *a/t* for UPE 220 to UPE 400
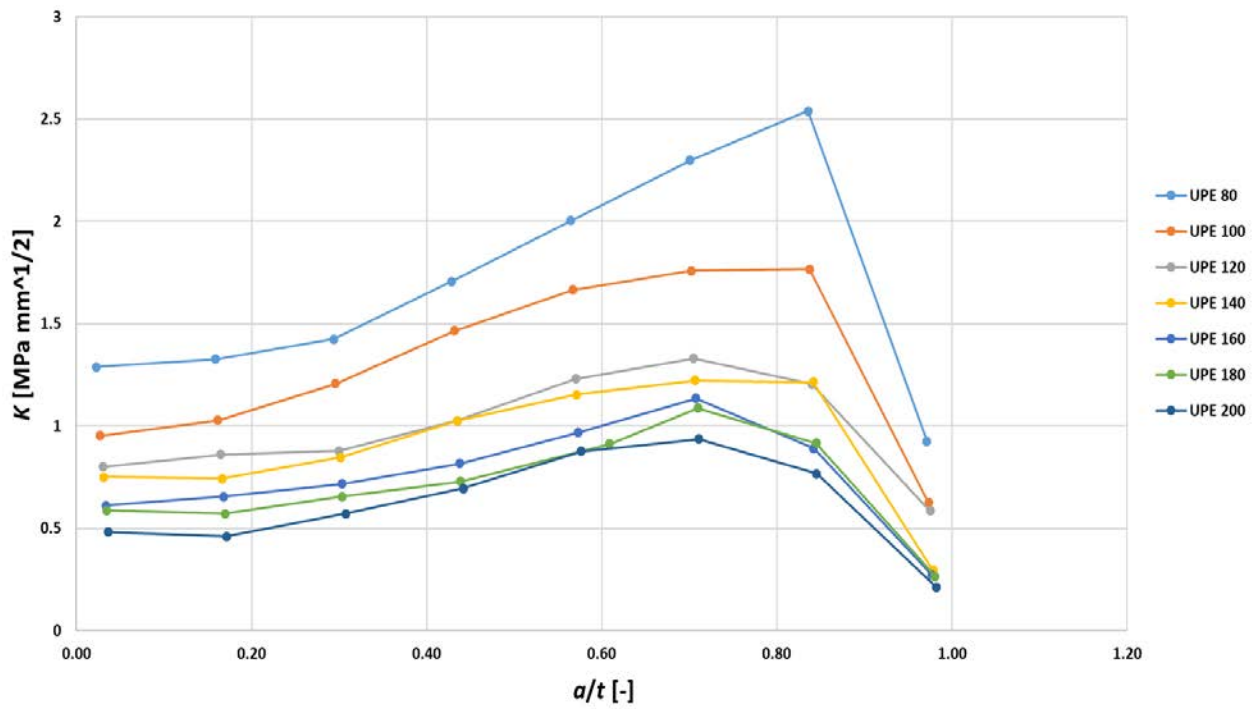
Graph 32: Stress intensity factor in the flange versus *a/t* for UPE 80 to UPE 200
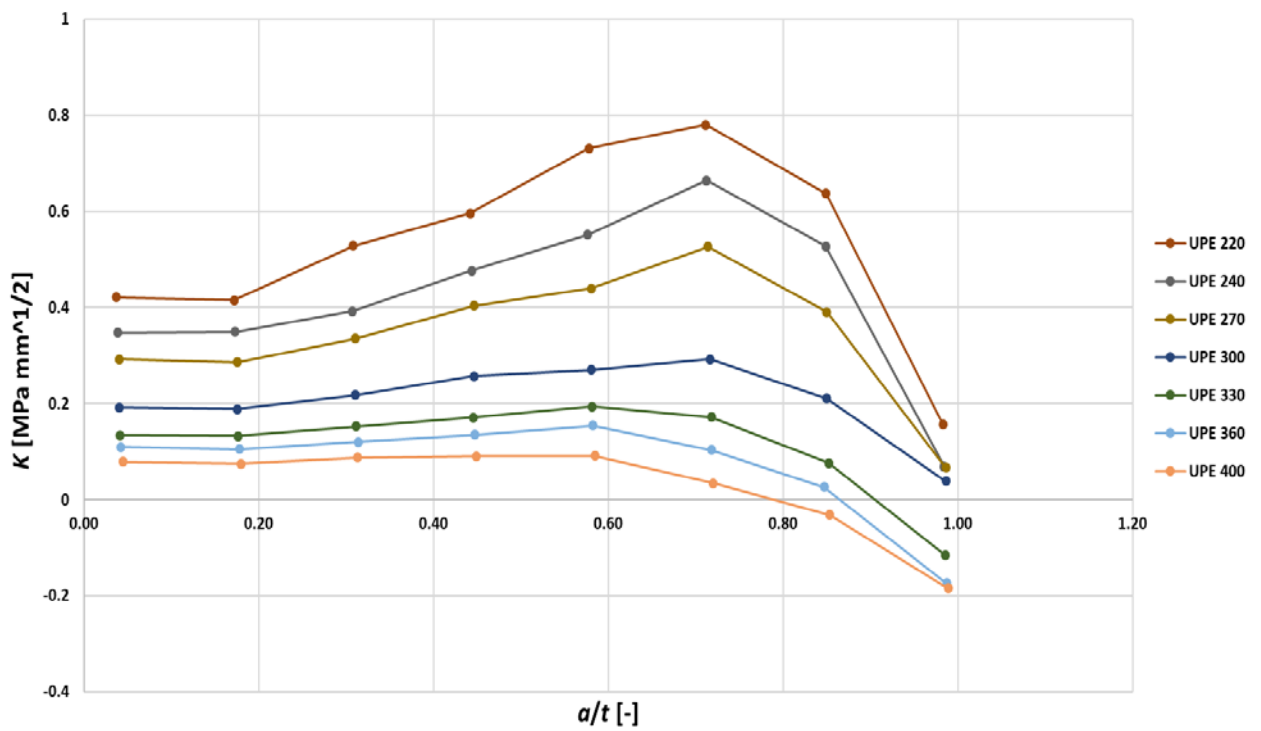
Graph 33: Stress intensity factor in the flange versus *a/t* for UPE 220 to UPE 400

5.3.2 Comparison with a rectangular profile

In this section the values of the SIF in the UPE profiles (KI) are compared with the ones obtained in rectangular cross-section profiles ($K0$). In case, of an UPE 100 with a height, W=100 mm, and a width, B=55 mm; the dimensions of the rectangular profile would be W=100 mm and B=55 mm. In Figure 34, both UPE and rectangular profile can be observed as well as their calculation paths.
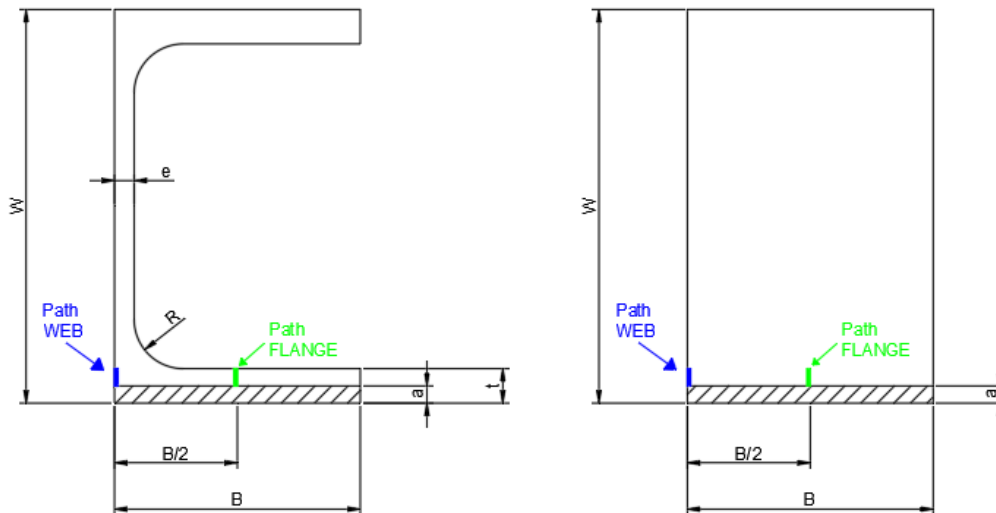
Figure 34: UPE and rectangular profile dimensions and paths for calculation of SIF

The way of comparing both profiles is means of the ratio K_I/K_{I0}, as explained in page 39 for the IPE profile. The aim is to observe how the reduced amount of material in the UPE profile affects its performance.

Table 7 represents the values of the ratio for all the given UPE profiles in the web and Table 8 does so for the flange.

For the web it can be appreciated that the ratio tends to increase with the crack length and with the size of the profile. However, for the flange it can be seen that the values of the ratio are much smaller than in the case of the web. In addition, the ratios in the flange tend to increase with the crack length, then reach a maximum value for an intermediate value of the crack length, and, finally, the values of the ratio decrease (for some profile even reaching a negative ratio).

Table 7: Ratio K_I/K_{I0} for the path in the web

UPE 80	a/W	0.0020	0.0106	0.0193	0.0279	0.0366	0.0452	0.0539	0.0625
	K_I/K_{I0}	7.0487	6.7365	5.3231	7.5170	10.8741	13.7597	11.5259	15.3655
UPE 100	a/W	0.0020	0.0098	0.0171	0.0247	0.0323	0.0399	0.0447	0.0550
	K_I/K_{I0}	8.3953	11.2853	12.0860	13.8090	16.441	21.4337	22.0699	18.2845
UPE 120	a/W	0.0020	0.0089	0.0157	0.0226	0.0294	0.0363	0.0431	0.0500
	K_I/K_{I0}	8.9412	22.2998	18.6769	20.2416	13.9559	21.6914	19.0328	18.2409
UPE 140	a/W	0.0020	0.0086	0.0151	0.0216	0.0282	0.0347	0.0413	0.0479
	K_I/K_{I0}	10.0635	14.0217	17.1180	21.1585	20.9890	21.7923	25.1214	23.4303
UPE 160	a/W	0.0020	0.0081	0.0143	0.0204	0.0266	0.0327	0.0388	0.0450
	K_I/K_{I0}	11.8618	18.6213	25.2270	24.0379	31.3966	24.6682	26.5940	26.4933
UPE 180	a/W	0.0020	0.0079	0.0138	0.0197	0.0256	0.0315	0.0374	0.0433
	K_I/K_{I0}	13.7546	17.9938	24.8952	28.7723	23.4591	31.5749	19.1695	22.6874
UPE 200	a/W	0.0020	0.0076	0.0133	0.0189	0.0246	0.0302	0.0358	0.0415
	K_I/K_{I0}	12.4414	20.9962	33.5664	23.7574	31.6549	22.7879	37.1496	37.6409
UPE 220	a/W	0.0020	0.0076	0.0131	0.0187	0.0242	0.0297	0.0353	0.0409
	K_I/K_{I0}	15.5801	21.1745	32.0566	27.7222	27.4206	31.6680	41.2338	27.0283
UPE 240	a/W	0.0020	0.0074	0.0129	0.0183	0.0237	0.0291	0.0346	0.0400
	K_I/K_{I0}	13.0233	22.2844	43.1609	26.9279	47.7452	30.1900	54.4469	30.6891
UPE 270	a/W	0.0020	0.0070	0.0120	0.0170	0.0220	0.0270	0.0320	0.0370
	K_I/K_{I0}	19.2469	23.9326	37.9452	32.6104	36.4672	57.1095	29.3364	33.1915
UPE 300	a/W	0.0020	0.0067	0.0114	0.0161	0.0200	0.0256	0.0303	0.0350
	K_I/K_{I0}	18.4722	28.6957	27.3224	36.9420	51.4839	36.0506	50.8360	33.8642
UPE 330	a/W	0.0020	0.0066	0.0112	0.0158	0.0204	0.0250	0.0296	0.0342
	K_I/K_{I0}	20.2209	20.3191	30.5225	50.6240	37.0709	32.3893	47.7778	45.6774
UPE 360	a/W	0.0020	0.0067	0.0113	0.0160	0.0206	0.0254	0.0300	0.0347
	K_I/K_{I0}	18.1749	29.0306	30.0733	46.3209	45.6068	40.1760	34.6000	49.6327
UPE 400	a/W	0.0020	0.0064	0.0108	0.0153	0.0197	0.0241	0.0285	0.0330
	K_I/K_{I0}	18.8584	22.6145	34.4906	39.7723	37.5439	36.5714	25.5603	49.8571

Table 8: Ratio K_I/K_{I0} for the path in the flange

UPE 80	a/W	0.0020	0.0106	0.0193	0.0279	0.0366	0.0452	0.0539	0.0625
	K_I/K_{I0}	4.0055	4.9368	6.1968	8.0509	3.9495	6.1494	3.5389	1.8645
UPE 100	a/W	0.0020	0.0098	0.0171	0.0247	0.0323	0.0399	0.0447	0.0550
	K_I/K_{I0}	4.5455	4.9074	9.4701	12.0610	14.1600	9.2980	6.9077	2.6289
UPE 120	a/W	0.0020	0.0089	0.0157	0.0226	0.0294	0.0363	0.0431	0.0500
	K_I/K_{I0}	3.9813	5.0085	9.3382	11.0346	8.6797	7.3202	4.6055	5.0578
UPE 140	a/W	0.0020	0.0086	0.0151	0.0216	0.0282	0.0347	0.0413	0.0479
	K_I/K_{I0}	5.0655	9.8845	12.2424	13.7561	10.9312	7.1756	5.3524	2.8864
UPE 160	a/W	0.0020	0.0081	0.0143	0.0204	0.0266	0.0327	0.0388	0.0450
	K_I/K_{I0}	2.5753	4.5163	8.7730	12.0308	9.6490	8.4940	6.8083	2.5036
UPE 180	a/W	0.0020	0.0079	0.0138	0.0197	0.0256	0.0315	0.0374	0.0433
	K_I/K_{I0}	5.0105	7.5916	7.7908	16.7384	14.3434	7.8227	9.6477	3.4175
UPE 200	a/W	0.0020	0.0076	0.0133	0.0189	0.0246	0.0302	0.0358	0.0415
	K_I/K_{I0}	4.1116	10.2741	8.1790	14.5188	10.9963	5.5186	9.7090	3.2092
UPE 220	a/W	0.0020	0.0076	0.0131	0.0187	0.0242	0.0297	0.0353	0.0409
	K_I/K_{I0}	9.7447	5.2683	11.0355	14.6779	24.0000	9.1004	7.0470	2.2788
UPE 240	a/W	0.0020	0.0074	0.0129	0.0183	0.0237	0.0291	0.0346	0.0400
	K_I/K_{I0}	8.0229	8.5764	14.4516	15.5020	20.8649	7.5952	6.1885	1.5758
UPE 270	a/W	0.0020	0.0070	0.0120	0.0170	0.0220	0.0270	0.0320	0.0370
	K_I/K_{I0}	7.2840	6.8630	8.6878	13.4973	12.2186	10.1320	4.4588	1.4851
UPE 300	a/W	0.0020	0.0067	0.0114	0.0161	0.0200	0.0256	0.0303	0.0350
	K_I/K_{I0}	5.0000	4.4970	9.6104	13.3091	7.2747	5.7030	2.7985	1.1103
UPE 330	a/W	0.0020	0.0066	0.0112	0.0158	0.0204	0.0250	0.0296	0.0342
	K_I/K_{I0}	4.4643	6.8394	8.6578	9.9745	11.1692	3.9755	1.5217	-3.2511
UPE 360	a/W	0.0020	0.0067	0.0113	0.0160	0.0206	0.0254	0.0300	0.0347
	K_I/K_{I0}	3.1168	4.0770	6.5939	4.1270	8.8548	2.4533	0.6053	-7.2135
UPE 400	a/W	0.0020	0.0064	0.0108	0.0153	0.0197	0.0241	0.0285	0.0330
	K_I/K_{I0}	2.2931	2.8450	4.9296	3.4028	5.8462	1.2885	0.8757	-8.5333

5.3.3 Calibration curves

The calibration curves are calculated as in section 5.2.3, page 42. Therefore, the bending stress caused by the load applied at the middle of the span in the 3PBT must be calculated. The SIF has been obtained in the former sections.

In this sense, calibration curves can be calculated. Graph 34 and Graph 35, represent the calibration curves versus *a/W* ratio in the web, from profile UPE 80 and UPE 200, and from profile UPE 220 to UPE 400, respectively. In the flange, Graph 36 plots the calibration curves from UPE 80 to UPE 200 and Graph 37 from UPE 220 to UPE 400.
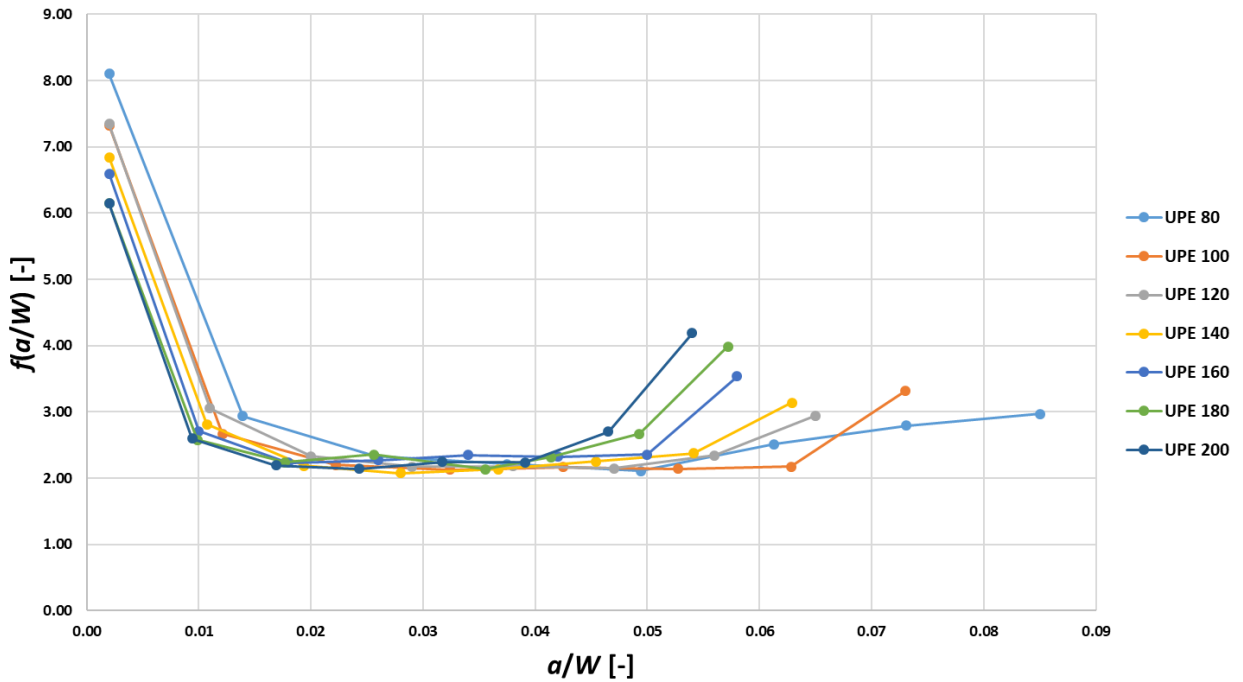
Graph 35: Calibration curves in the web versus *a/W* for the UPE 80 to UPE 200
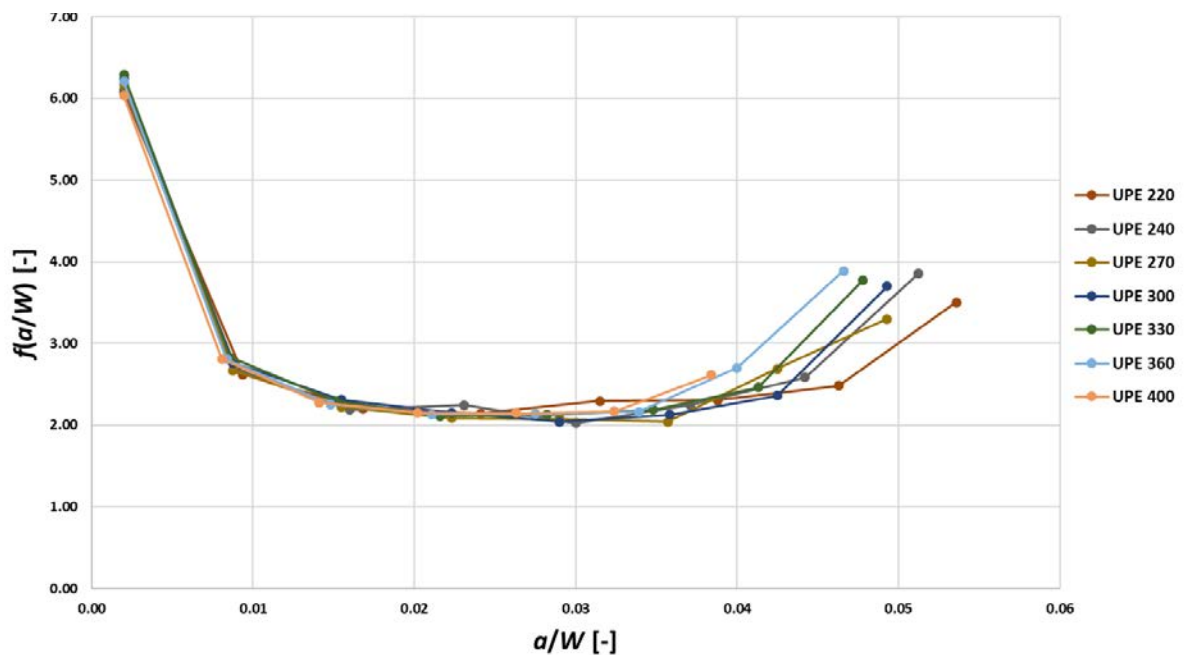
Graph 34: Calibration curves in the web versus *a/W* for the UPE 220 to UPE 400
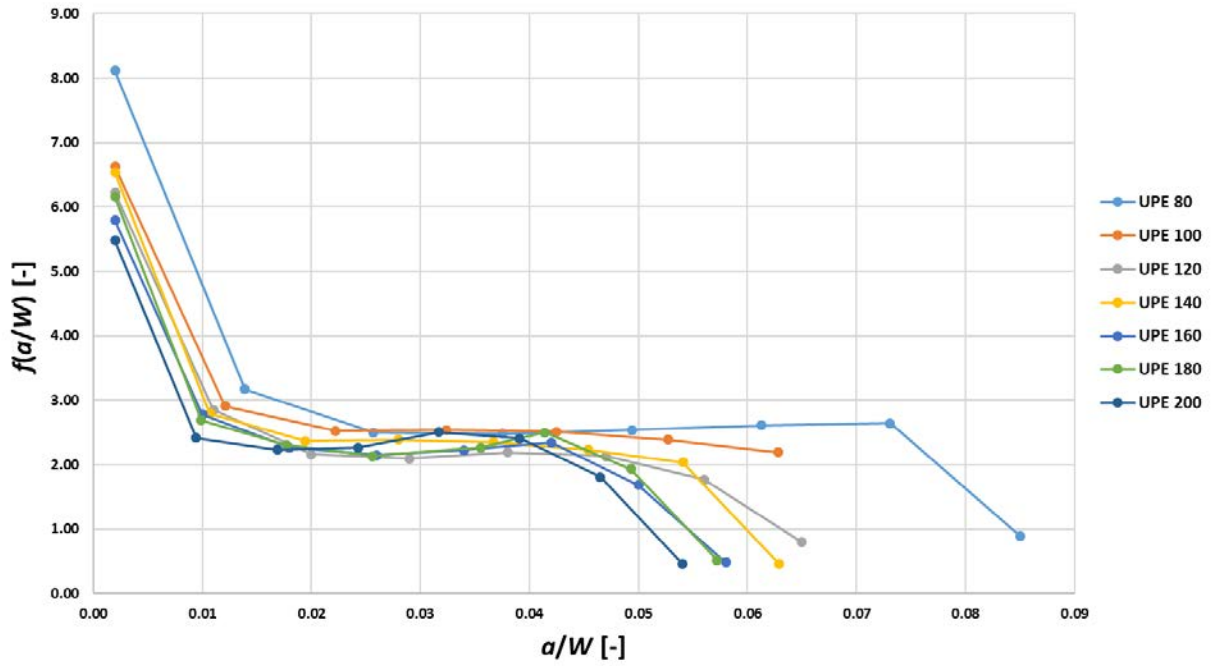
Graph 36: Calibration curves in the flange versus *a/W* for the UPE 80 to UPE 200
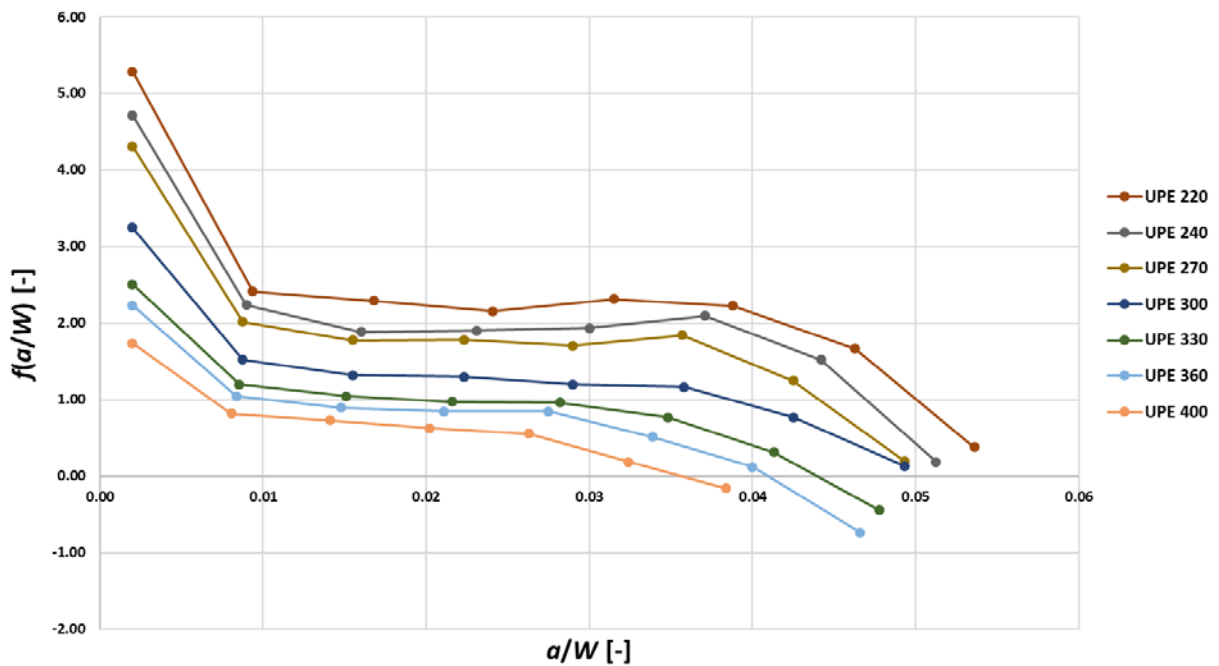
Graph 37: Calibration curves in the flange versus *a/W* for the UPE 220 to UPE 400

More calibration curves are obtained by changing the ratio a/W to the ratio a/t. For the web, Graph 38 and Graph 39 represent the calibration curves for UPE 80-UPE 200 and UPE 220-UPE 400, respectively. Graph 40 and Graph 41 represent the calibration curves but in the flange.

Graph 38: Calibration curves in the web versus *a/t* for the UPE 80 to UPE 200

Graph 39: Calibration curves in the web versus *a/t* for the UPE 220 to UPE 400

Graph 40: Calibration curves in the flange versus *a/t* for the UPE 80 to UPE 200

Graph 41: Calibration curves in the flange versus *a/t* for the UPE 220 to UPE 400

6. Conclusion

In this thesis, the stress fields in a three-point bending test are studied for three different profiles: I profile, IPE prof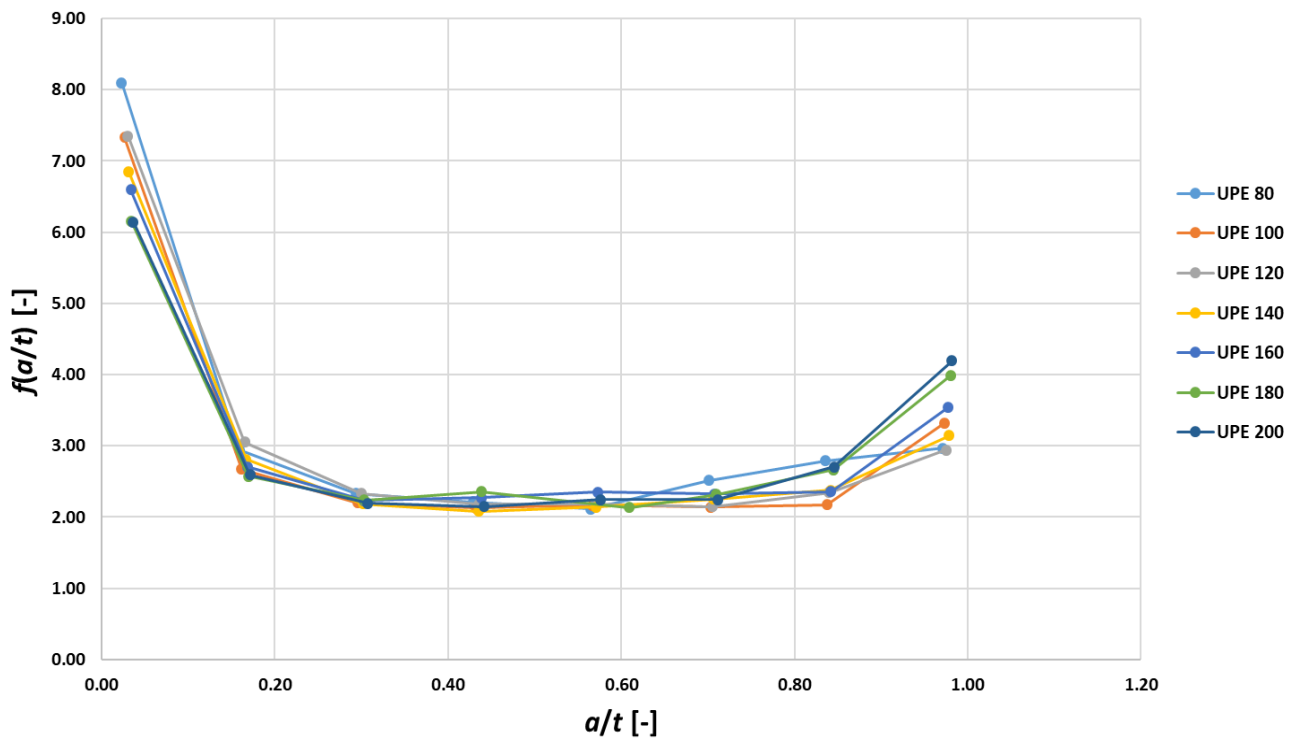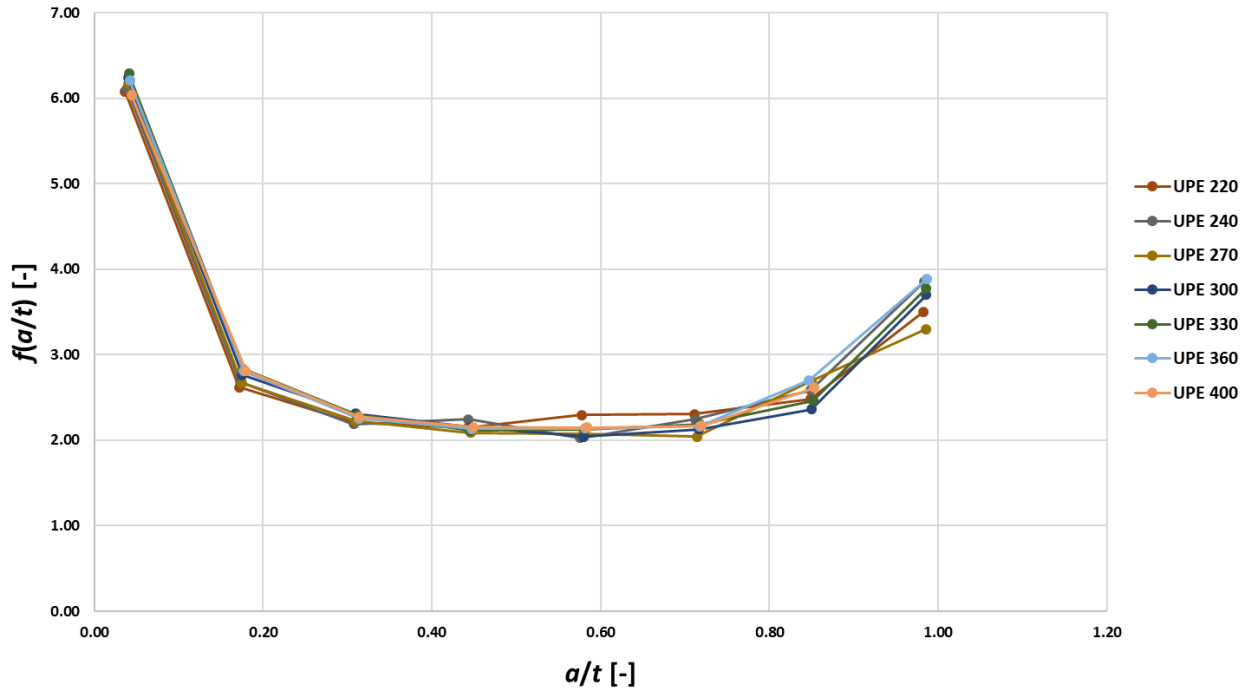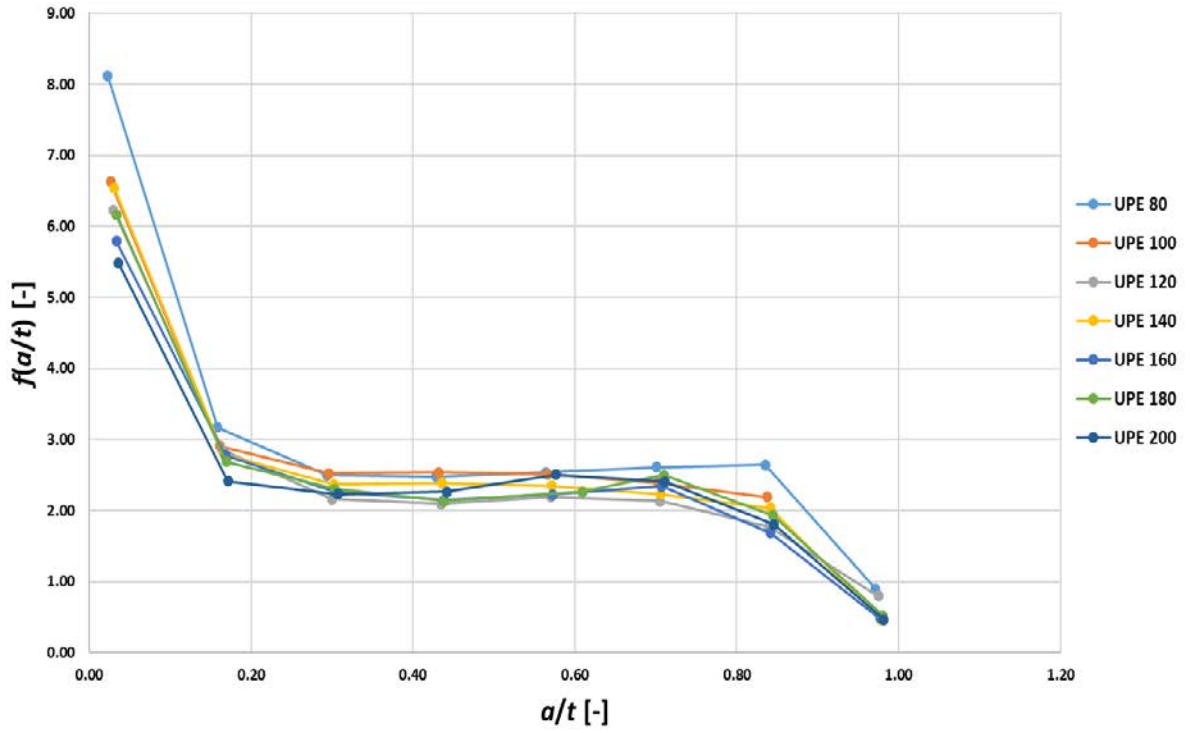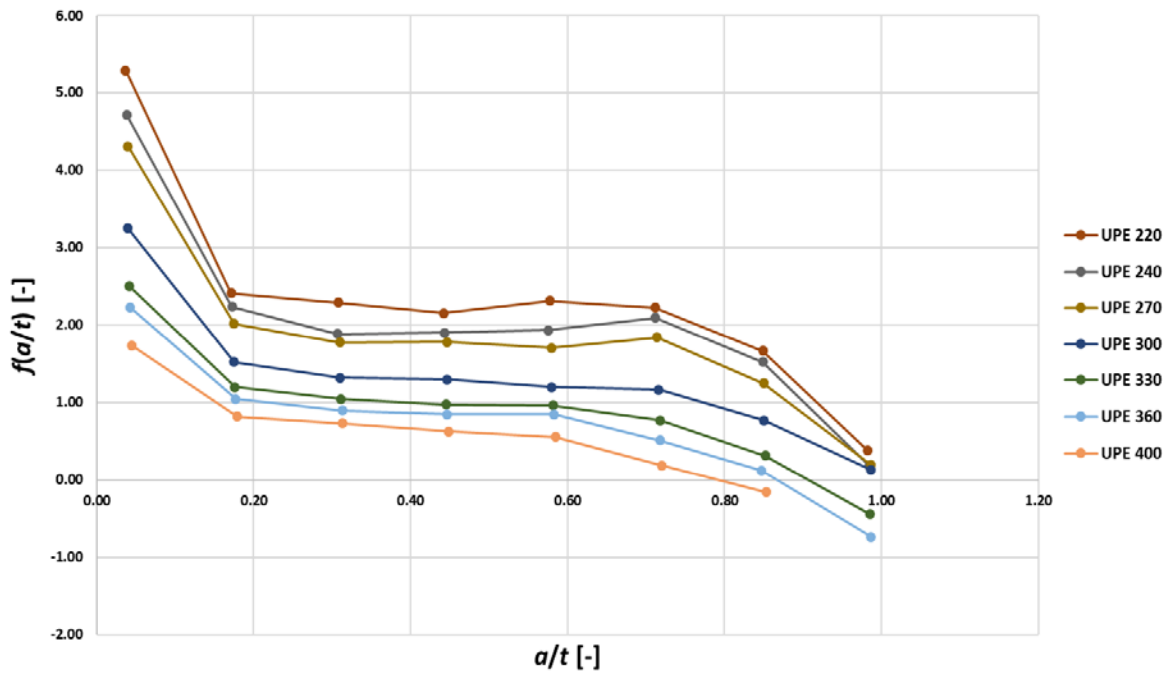ile and UPE profile. The results of this parametrical study are obtained by means of ANSYS, a Finite Element Software. Afterwards, the results obtained are plotted so that the evolution of the SIF with the crack length and the calibration curves for the different profiles can be observed.

Initially the I-profile is analysed for different crack lengths, thicknesses of the web and material properties. From the results the following conclusions can be drawn:

- The stress distribution is strongly related to the length of the existing crack. As expected, the wider the crack the higher the value of the SIF. Both the web and the flange paths show a linear relationship between the SIF and the crack length.

- The difference with a rectangular profile gets smaller when the crack length is smaller (around 80%), however, for longer cracks the difference increases (about 200%).

- Regarding the influence of the material, the Young's modulus does not affect the value of the SIF. The Poisson's ratio slightly influences the stress fields, for materials with a small ratio (concrete; v=0.2) the SIF is smaller than for materials with a higher ratio (aluminium; v=0.34). However, this difference is not very significant and can be appreciated both in the web and the flange.

The study in IPE profiles is performed for different crack lengths, observing the stress fields for these profiles and calculating the calibration curves. Moreover, the SIF in the IPE profiles is compared with rectangular profiles. The results show the following:

- The values of the SIF are higher in the flange than in the web of the different IPE profiles. In both paths, the SIF has a linear relationship and increases with the size of the crack.

- By comparing the IPE profiles with rectangular profiles, it can be appreciated that the larger the crack the higher the ratio (K_I/K_{I0}) between the SIF in the IPE profiles (K_I) and the SIF in the rectangular profile (K_{I0}). Moreover, the values of the ratio are higher than ones obtained for the I profile. This may be explained by the lower area and, therefore, stiffness in the IPE profiles.

- Different calibration curves are obtained as there is no the same constant of proportionality between the flange thickness (*t*) and the height (*W*) of the profiles, so the ratio *t/W* is different for each profile. That is the reason why the calibration curves of all IPE profiles do not lie in the same line. However, for all the IPE profiles they follow the same trend.

- In case of the web, the tendency for all the calibration curves in all profiles is similar to a U-shaped valley; it starts with a negative slope but at the middle it starts increasing its value. Regarding the flange, the calibration curves tend more to have a S-shape.

- For some profiles, the last value of the calibration curve (when the crack occupies almost all the flange thickness) in the flange shows a drop in the value, which may be caused by a highly reduction of the stiffness in this part of the beam.

Regarding the UPE profiles, they are studied for different crack lengths and compared with rectangular profiles. In addition, calibration curves are calculated for them. The main conclusions of this study are the following:

- The SIF in the web tends to increase with crack length in a linear way. In case of the flange, it increases with crack length but when the last two values it starts to decrease.

- Comparing the UPE profiles with a rectangular profile by means of the ratio K_I/K_0 it can be observed that this ratio is much higher in the web than in the flange.

- As happened with the IPE profiles, there is no proportionality between the flange thickness and the height of the profile (t/W ratio different for each profile). This is the reason why a calibration curve is obtained for each UPE profile. However, the calibration curves follow a pattern both in the web and in the flange.

- The calibration curves in the web show a big drop at the beginning, then the value keeps constant and finally it starts to increase. While in the flange, calibration curves start with a decrease, then the values remain constant and finally they decrease again.

This thesis has mainly focused on the parametrical study of profiles for different crack lengths. The results obtained should be compared with values obtained in test performed in the laboratory. As future research, it could be analysed how the span could affect the stress fields in the vicinity of the crack tip. Moreover, other standard profiles could be also analysed.

References

[1] Aisc (2006) *Construction Steel Construction Manual, American Institute of Steel Construction*; 13th edition.

[2] Anderson, T. L., *Fracture Mechanics: fundamentals and applications*. CRC press, 2017.

[3] ANSYS, Academic research, Crack analysis guide Mechanical APDL Documentation guide, Release 17.2,2016.

[4] ASTM E399-90, Standard Test Method for Plane-Strain Fracture Toughness of Metallic Materials. AnnualBook of ASTM Standards. Philadelphia, PA: American Society for Testing and Materials.

[5] ASTM E647-15. (2015) Standard Test Method for Measurement of Fatigue Crack Growth Rates. West Conshohocken, PA: American Society for Testing and Materials.

[6] Belzunce, J., Tecnología de Materiales: Comportamiento en servicio de materiales, Escuela Politécnica de Ingeniería de Gijón, Gijón, 2012, p.48.

[7] Gonzalez.M.A.Y and H.K.D.H.Bhadeshia. 2008. Cast Iron, University of Cambridge.(Online).http://blog.360.yahoo.com/blog_Qsn_5Uwdq.eOs6t_ht15gjs?p=11(22 February 2009).

[8] Guinea, G. V., Pastor, J., Planas, Elices, M (1998), Stress intensity factor, compliance and CMOD for a general three-point-bend beam, International Journal of Fracture 89, pp. 103-116.

[9] IPE Beams (2009). EUROPEAN STANDARD UNIVERSAL I BEAMS (I SECTION) WITH PARALLEL FLANGES. DIMENSIONS, SPECIFICATIONS, ACCORDANCE WITH FORMER STANDARD EU pp. 19-57.

[10] Irwin, G.R. (1957) Analysis of Stresses and Strains Near the End of a Crack Traversing a Plate, *Journal of Applied Mechanics*, 24, pp. 361-364.

[11] Kai Lu, Toshiyuki Meshii (2014) Three- dimensional T-stresses for three-point-bend specimens with large thickness variation. Engineering Fracture Mechanics 116, pp. 197-203.

[12] Kala, Z. (2019a) Estimating probability of fatigue failure of steel structures. *Acta et Commentationes Universitatis Tartuensis de Mathematica*, 23(2), pp. 245-254.

[13] Kala, Z. (2019b) *Global sensitivity analysis of reliability of structural bridge system. Engineering Structures*, 194, pp. 36-45.

[14] Klesnil, M. Lukáš P. (1992) *Fatigue of Metallic Materials*, Volume 71 2nd Edition, Elsevier Science.

[15] Lehner, P., Krejsa, M., Pařenica, P., Křivý, V. Brožovský, J. (2019) Fatigue damage analysis of a riveted steel overhead crane support truss. International Journal of Fatigue, 128, 1-9, article number 105190

[16] Murakami, Y (1986) *Stress Intensity Factors Handbook*, Pergamon, New York.

[17] Paris, P.C. Erdogan, F. (1963) A Critical Analysis of Crack Propagation Laws, *Journal Basic Engineering*, 85, 4, pp. 528-533

[18] Schijve, J (2009) *Fatigue of Structures and Materials*, Springer Netherlands

[19] Seitl, S, Viszlay, V., Cifuentes, H., Veselý, V., Two parameter fracture mechanics: evaluation of T-stress for a general three-point-bend specimen, *Anales de la Mecánica de Fractura* (Vol. 32), pp. 310-315.

[20] Seitl, S., Miarka, P., Kala, Z. (2018) Geometry functions for edge cracks in steel bridge under three- and four- point bending with various span, *Transactions of VSB-Technical University of Ostrava, Civil engineering series*, 18, 2, pp. 44-49.

[21] Seitl, S., Miarka, P., Malíková, L., Krejsa, M. (2017) Comparison of Calibration Functions for Short Edge Cracks under Selected Loads, *Key Engineering Materials*, Vol. 754, pp.353-356.

[22] Tada, H. Paris, P.C., Irwin, G.R. (2000) The stress analysis of Cracks Handbook, New York, 2000.

[23] Zerbst, U., Vormwald, M., Pippan, R., Gänser, H.-P., Sarrazin-Baudoux, C., Madia, M. (2016) About the Fatigue Crack Propagation Threshold of Metals as a Design Criterion – A Review, *Engineering Fracture Mechanics*, 153, pp. 190–243.

List of Abbreviations

LEFM   Linear elastic fracture mechanics
EPFM   Elastic-plastic fracture mechanics
3PBT   Three-point bending test
FEM   Finite element method
NA   Neutral axis
SIF   Stress intensity factor
IPE   I-Profile Européennes
UPE   U-Profile with parallel flanges

List of Symbols

a	Crack length
r	Distance to crack tip
K	Stress intensity factor
K_I	Stress intensity factor mode I
K_{II}	Stress intensity factor mode II
K_{III}	Stress intensity factor mode III
K_{IC}	Fracture toughness / critical value of SIF for mode I
C	Specimen's geometry constant
E	Young's modulus
v	Poisson's ratio
B	Width of profile
W	Height of profile
t	Thickness of flange
e	Thickness of web
R	Radius
P	Applied load / force
σ	Applied bending stress
M	Applied bending moment
I	Moment of inertia of the section
y	Distance from neutral axis to point of calculation of bending stress
e/B	Web thickness-width of profile ratio
a/W	Crack length-height of profile ratio
K_I/K_{I0}	Ratio between stress intensity factor of IPE/UPE profile and stress intensity factor of rectangular profile

List of Figures

List of Graphs

List of Tables

Curriculum Vitae

Jorge Álvarez Morán

Personal Information

- Date of birth: May 5th, 1998
- Place of birth: Gijón (Asturias), Spain
- ID: 53775268A
- Address: San Bernardo 16 2ºB, 33201 Gijón, Asturias, Spain
- Phone Number: +34 628468498
- E-mail: **jorgealvmoran@outlook.com**

Studies

- Student of last year Mechanical Engineering (2016-2020) bachelor in the Gijón Polytechnic School of Engineering, University of Oviedo. Mean mark: 8.838, obtaining distinction in six subjects. Studying in the bilingual program of the Bachelor´s degree, in which most of the subjects are taught in English.
- Erasmus + mobility (2019-2020) in Faculty Civil Engineering, Brno University of Technology, Brno, Czech Republic. Realization of the Final Bachelor Thesis.

Languages

- **Spanish:** Native
- **English:** Advanced level both written and spoken. Obtained certificates:
    - Certificate in Advanced English (C1), December 2018.
    - First Certificate in English (B2), June 2014.
    - Trinity Exams: Grade 7 (June 2012) and Grade 5 (June 2011).
- **German:** Basic level. Studied during high school.

Skills and Aptitudes

- **Software Skills:**
    - Microsoft Office: Excel, Word, Powerpoint.
    - Autodesk (CAD): Inventor, Autocad, PowerMill.
    - ANSYS.
    - Matlab.
- **Skills:**
    - Dedication.
    - Work-in-team capability.
    - Willingness to learn.
    - Leadership capability.
    - Decision making.
    - Problem-solving.

Additional Information

- "José Riera Award" received in 2019, given to the student with the best academic record in the Mechanical Engineering Bachelor in the Gijón Polytechnic School of Engineering.

- Social works for one year (2014-2015), helping people with mental disabilities.

- Summer Course (2014) received in the Barcelona Polytechnic School of Engineering: "The electric vehicle: a new technological challenge in automotive industry".

- Internship in Prodintec (2016), a company in Gijón focused on research and development in the engineering industry.

- European driving license.

Annex

Annex I: APDL Macro for the 3PBT for the I-Profile

```
! Macro for 3D calculation of stresses in a 3PBT for an I-profile
/clear
/PREP7
/PNUM,KP,1
/PNUM,LINE,1
/PNUM,AREA,1
/PNUM,VOLU,1
/PBC,ALL,,1
W=100             ! height of the I profile
S_W=3            ! S/W ratio
e=20              ! dimension of the web
t=20              ! thickness of the flange
B=50              ! width of the I profile
a_W=0.15          ! a/W
a = a_W*W         ! crack length
S = S_W*W/2       ! 1/2 of span
P = 100/2         ! 1/2 of load
!-------------------------
! Characteristics of the material
!-------------------------
UIMP,1,EX, , ,30e3,       ! Young modulus
UIMP,1,NUXY, , ,0.3,      ! Poisson's ratio
!-------------------------
! Element type
!-------------------------
ET,1,SOLID186
KEYOPT,1,2,0
KEYOPT,1,3,0
KEYOPT,1,6,0
KEYOPT,1,8,0
!-------------------------
! Keypoints
!-------------------------
K,1,0,0,0
K,2,0,0,t
K,3,(B-e)/2,0,t
K,4,(B-e)/2,0,W-t
```

K,5,0,0,W-t

K,6,0,0,W

K,7,B,0,W

K,8,B,0,W-t

K,9,(B-e)/2+e,0,W-t

K,10,(B-e)/2+e,0,t

K,11,B,0,t

K,12,B,0,0

K,13,0,0,a

K,14,B,0,a

K,15,0,S,0

K,16,0,S+1/6*S,0

K,17,0,S+1/6*S,t

K,18,(B-e)/2,S+1/6*S,t

K,19,(B-e)/2,S+1/6*S,W-t

K,20,0,S+1/6*S,W-t

K,21,0,S+1/6*S,W

K,22,B,S+1/6*S,W

K,23,B,S+1/6*S,W-t

K,24,(B-e)/2+e,S+1/6*S,W-t

K,25,(B-e)/2+e,S+1/6*S,t

K,26,B,S+1/6*S,t

K,27,B,S+1/6*S,0

K,28,B,S,0

K,29,B/2,0,a

K,30,B/2,0,t

K,31,B/4,0,a

K,32,B/4,0,t

K,33,B/2,0,W-t

!--------------------------

! Lines

!--------------------------

L,2,32   !L1

L,3,4   !L2

L,4,5   !L3

L,5,6   !L4

L,6,7   !L5

L,7,8   !L6

L,8,9   !L7

L,9,10   !L8

L,10,11	!L9
L,12,1	!L10
L,13,1	!L11
L,13,2	!L12
L,11,14	!L13
L,14,12	!L14
L,1,15	!L15
L,15,16	!L16
L,2,17	!L17
L,3,18	!L18
L,4,19	!L19
L,5,20	!L20
L,6,21	!L21
L,7,22	!L22
L,8,23	!L23
L,9,24	!L24
L,10,25	!L25
L,11,26	!L26
L,12,28	!L27
L,28,27	!L28
L,16,17	!L29
L,17,18	!L30
L,18,19	!L31
L,19,20	!L32
L,20,21	!L33
L,21,22	!L34
L,22,23	!L35
L,23,24	!L36
L,24,25	!L37
L,25,26	!L38
L,26,27	!L39
L,27,16	!L40
L,15,28	!L41
L,4,9	!L42
L,19,24	!L43
L,13,31	!L44
L,31,29	!L45
L,29,14	!L46
L,32,3	!L47
L,3,30	!L48

```
L,30,10                         !L49
L,31,32                         !L50
L,29,30                         !L51
L,30,33                         !L52
L,4,33                          !L53
L,33,9                          !L54
!--------------------------
! Areas
!--------------------------
AL,11,44,45,46,14,10            ! A1
AL,12,1,50,44                   ! A2
AL,50,47,48,51,45               ! A3
AL,51,49,9,13,46                ! A4
AL,48,2,53,52                   ! A5
AL,52,54,8,49                   ! A6
AL,3,4,5,6,7,54,53              ! A7
AL,11,12,17,29,16,15            ! A8
AL,1,47,18,30,17                ! A9
AL,2,19,31,18                   ! A10
AL,3,20,19,32                   ! A11
AL,4,21,33,20                   ! A12
AL,5,21,22,34                   ! A13
AL,22,35,23,6                   ! A14
AL,23,36,24,7                   ! A15
AL,24,37,25,8                   ! A16
AL,25,38,26,9                   ! A17
AL,13,14,26,39,28,27            ! A18
AL,10,15,41,27                  ! A19
AL,41,28,40,16                  ! A20
AL,40,38,37,39,43,31,30,29      ! A21
AL,36,35,34,33,32,43            ! A22
!--------------------------
! Volumes
!--------------------------
ASEL,S,AREA,,1
ASEL,A,AREA,,2
ASEL,A,AREA,,3
ASEL,A,AREA,,4
ASEL,A,AREA,,5
ASEL,A,AREA,,6
```

```
ASEL,A,AREA,,7
ASEL,A,AREA,,8
ASEL,A,AREA,,9
ASEL,A,AREA,,10
ASEL,A,AREA,,11
ASEL,A,AREA,,12
ASEL,A,AREA,,13
ASEL,A,AREA,,14
ASEL,A,AREA,,15
ASEL,A,AREA,,16
ASEL,A,AREA,,17
ASEL,A,AREA,,18
ASEL,A,AREA,,19
ASEL,A,AREA,,20
ASEL,A,AREA,,21
ASEL,A,AREA,,22
VA,ALL
!---------------------------
! Meshing
!---------------------------
I=5
Q=0.1
Kesize,1,I
Kesize,2,I
Kesize,3,I
Kesize,4,I
Kesize,5,I
Kesize,6,I
Kesize,7,I
Kesize,8,I
Kesize,9,I
Kesize,10,I
Kesize,11,I
Kesize,12,I
Kesize,13,I
Kesize,14,I
Kesize,15,I
Kesize,16,I
Kesize,17,I
Kesize,18,I
```

```
Kesize,19,I
Kesize,20,I
Kesize,21,I
Kesize,22,I
Kesize,23,I
Kesize,24,I
Kesize,25,I
Kesize,26,I
Kesize,27,I
Kesize,28,I
Kesize,29,Q
Kesize,30,Q
Kesize,31,Q
Kesize,32,Q
Kesize,33,I
LESIZE,10,5
!--------------------------
! Mesh settings
!--------------------------
MSHAPE,1,3D
MSHKEY,0
!*
CM,_Y,VOLU
VSEL, , , ,        1
CM,_Y1,VOLU
CHKMSH,'VOLU'
CMSEL,S,_Y
!*
VMESH,_Y1
!*
CMDELE,_Y
CMDELE,_Y1
CMDELE,_Y2
!--------------------------
! Boundary conditions
!--------------------------
! Symmetry conditions
ASEL,S,AREA,,2
ASEL,A,AREA,,3
ASEL,A,AREA,,4
```

```
ASEL,A,AREA,,5
ASEL,A,AREA,,6
ASEL,A,AREA,,7
NSLA,S,1
D,ALL,UY,0                ! displacement on selected nodes in direction Y  is equal 0
! Boundary condition instead of support
Lsel,s,line,,41
Nsll,s,1
D,ALL,UZ,0               ! displacement on selected nodes in direction Z  is equal 0
D,ALL,UX,0
! Loading
Lsel,s,line,,5
Nsll,s,1
*GET,POCET,NODE,0,COUNT
F,ALL,FZ,-P/POCET
allsel,all
/solu
solve
EPLOT
FINISH
/POST1
Lsel,s,line,,50          ! selecting lines where the nodes are attached for stress syy
Nsll,s,1
nplot
Lsel,a,line,,51          ! selecting lines where !the nodes are attached for stress syy
Nsll,s,1
nplot
! Results to file
FILENAME1='PATH_MIDDLE_%a%_%PP%'
FILENAME2='PATH_FLANGE_%a%_%PP%'
! Central Line
FLST,2,2,1
FITEM,2,node(B/2,0,a)              ! nodes coordinates x,y,z
FITEM,2,node(B/2,0,t)
PATH,cesta,2,50,50,               ! cesta is the name of the path
PPATH,P51X,1
PDEF,sy,S,Y,AVG !stress SY
PAGET,bbb,TABLE                   ! the values are inserted in the table
PAGET,lll,LABELS
/nopr
```

```
/outp,temp,inp
/com, *cfopen,C:\Users\Jorge\Desktop\Jorge-TFG\Results\%FILENAME1%,txt   !filename
/com, *vwrite
/com, (5x,'LENGHT',10x,'SY')          ! label on the top
/com, *vwrite,bbb(1,4),bbb(1,5)       ! position in the table
/com, (3E15.6)                        ! numerical format
/com, *cfclos
/outp
/inp,temp,inp
/gopr
! Lateral line
FLST,2,2,1
FITEM,2,node(B/4,0,a)                 ! nodes coordinates x,y,z
FITEM,2,node(B/4,0,t)
PATH,cesta1,2,50,50,                  ! cesta is the name of the path
PPATH,P51X,1
PDEF,sy,S,Y,AVG !stress SY
PAGET,ccc,TABLE                       ! the values are inserted in the table
PAGET,kkk,LABELS
/nopr
/outp,temp,inp
/com, *cfopen,C:\Users\Jorge\Desktop\Jorge-TFG\Results\%FILENAME2%,txt
/com, *vwrite
/com, (5x,'delka',10x,'SY')           ! label on top
/com, *vwrite,ccc(1,4),ccc(1,5)       ! position in the table
/com, (3E15.6)                        ! numerical format
/com, *cfclos
/outp
/inp,temp,inp
/gopr
```

Annex II: APDL Macro for the 3PBT in the IPE profile

```
! Macro for 3D calculation of stresses in Standard IPE beam in a 3PBT
/clear
/PREP7
/PNUM,KP,1
/PNUM,LINE,1
/PNUM,AREA,1
/PNUM,VOLU,1
/PBC,ALL,,1
! Only one quarter of the specimen will be modelled by using symmetry
W=80            ! height of the specimen
S_W=3          ! S/W ratio
B=46/2          ! length of the flange
e=3.8/2         ! 1/2 thickness of the web
t=5.2           ! thickness of the flange
r=5             ! radius of the flange to web
a_W= 0.03       ! a/W Ratio
a= a_W*W        ! crack length
S=S_W*W/2       ! 1/2 of the span
P=100/4         ! 1/4 of the load
!--------------------------
! Characteristics of the material
!--------------------------
UIMP,1,EX, , ,210e3,      ! Young's modulus
UIMP,1,NUXY, , ,0.3,      ! Poisson's ratio
!--------------------------
! Element type
!--------------------------
ET,1,SOLID186
KEYOPT,1,2,0
KEYOPT,1,3,0
KEYOPT,1,6,0
KEYOPT,1,8,0
!--------------------------
! Keypoints
!--------------------------
! Cross section in the crack
K,1,0,0,0
K,2,0,0,a
```

K,3,0,0,t

K,4,B/2,0,t

K,5,B-e-r,0,t

K,6,B-e,0,t+r

K,7,B-e-r,0,t+r

K,8,B-e,0,W-t-r

K,9,B-e-r,0,W-t

k,10,B-e-r,0,W-t-r

K,11,0,0,W-t

K,12,0,0,W

K,13,B,0,W

K,14,B,0,t

K,15,B,0,a

K,16,B,0,0

K,17,B/2,0,a

! Cross section located at S/8 from the crack

K,18,0,S/8,0

K,19,0,S/8,t

K,20,B-e-r,S/8,t

K,21,B-e,S/8,t+r

K,22,B-e-r,S/8,t+r

K,23,B-e,S/8,W-t-r

K,24,B-e-r,S/8,W-t

k,25,B-e-r,S/8,W-t-r

K,26,0,S/8,W-t

K,27,0,S/8,W

K,28,B,S/8,W

K,29,B,S/8,0

! Cross section located at 7S/8 from the crack; in the support

K,30,0,7*S/8,0

K,31,0,7*S/8,t

K,32,B-e-r,7*S/8,t

K,33,B-e,7*S/8,t+r

K,34,B-e-r,7*S/8,t+r

K,35,B-e,7*S/8,W-t-r

K,36,B-e-r,7*S/8,W-t

k,37,B-e-r,7*S/8,W-t-r

K,38,0,7*S/8,W-t

K,39,0,7*S/8,W

K,40,B,7*S/8,W

K,41,B,7*S/8,0

! Cross section at the end of the beam

K,42,0,S+1/6*S,0

K,43,0,S+1/6*S,t

K,44,B-e-r,S+1/6*S,t

K,45,B-e,S+1/6*S,t+r

K,46,B-e-r,S+1/6*S,t+r

K,47,B-e,S+1/6*S,W-t-r

K,48,B-e-r,S+1/6*S,W-t

k,49,B-e-r,S+1/6*S,W-t-r

K,50,0,S+1/6*S,W-t

K,51,0,S+1/6*S,W

K,52,B,S+1/6*S,W

K,53,B,S+1/6*S,0

!---------------------------

! Lines

!---------------------------

L,1,2	! L1
L,2,3	! L2
L,3,4	! L3
L,4,5	! L4
ARC,5,6,7,r	! L5
L,6,8	! L6
ARC,8,9,10,r	! L7
L,9,11	! L8
L,11,12	! L9
L,12,13	! L10
L,13,14	! L11
L,14,15	! L12
L,15,16	! L13
L,16,1	! L14
L,15,17	! L15
L,2,17	! L16
L,4,17	! L17
L,1,18	! L18
L,3,19	! L19
L,5,20	! L20
L,6,21	! L21
L,8,23	! L22
L,9,24	! L23

L,11,26	! L24
L,12,27	! L25
L,13,28	! L26
L,16,29	! L27
L,18,19	! L28
L,19,20	! L29
ARC,20,21,22,r	! L30
L,21,23	! L31
ARC,23,24,25,r	! L32
L,24,26	! L33
L,26,27	! L34
L,27,28	! L35
L,28,29	! L36
L,29,18	! L37
L,18,30	! L38
L,19,31	! L39
L,20,32	! L40
L,21,33	! L41
L,23,35	! L42
L,24,36	! L43
L,26,38	! L44
L,27,39	! L45
L,28,40	! L46
L,29,41	! L47
L,30,31	! L48
L,31,32	! L49
ARC,32,33,34,r	! L50
L,33,35	! L51
ARC,35,36,37,r	! L52
L,36,38	! L53
L,38,39	! L54
L,39,40	! L55
L,40,41	! L56
L,41,30	! L57
L,30,42	! L58
L,43,31	! L59
L,44,32	! L60
L,45,33	! L61
L,47,35	! L62
L,48,36	! L63

L,50,38	! L64
L,51,39	! L65
L,52,40	! L66
L,53,41	! L67
L,42,43	! L68
L,43,44	! L69
ARC,44,45,46,r	! L70
L,45,47	! L71
ARC,47,48,49,r	! L72
L,48,50	! L73
L,50,51	! L74
L,51,52	! L75
L,52,53	! L76
L,53,42	! L77
L,5,14	! L78

!---------------------------

!Areas

!---------------------------

AL,1,16,15,13,14	! A1
AL,2,3,17,16	! A2
AL,17,15,12,78,4	! A3
AL,78,11,10,9,8,7,6,5	! A4
AL,1,2,19,28,18	! A5
AL,19,29,20,3,4	! A6
AL,20,30,21,5	! A7
AL,21,6,22,31	! A8
AL,22,7,23,32	! A9
AL,23,33,24,8	! A10
AL,24,9,25,34	! A11
AL,25,10,26,35	! A12
AL,26,36,27,11,13,12	! A13
AL,37,18,14,27	! A14
AL,28,39,48,38	! A15
AL,39,29,40,49	! A16
AL,30,41,50,40	! A17
AL,41,31,42,51	! A18
AL,42,43,32,52	! A19
AL,43,33,44,53	! A20
AL,44,34,45,54	! A21
AL,45,35,46,55	! A22

```
AL,46,36,47,56                        ! A23
AL,38,37,47,57                        ! A24
AL,58,48,59,68                        ! A25
AL,59,49,60,69                        ! A26
AL,60,50,61,70                        ! A27
AL,61,51,62,71                        ! A28
AL,62,52,63,72                        ! A29
AL,63,53,64,73                        ! A30
AL,64,54,65,74                        ! A31
AL,65,55,66,75                        ! A32
AL,66,76,67,56                        ! A33
AL,58,57,67,77                        ! A34
AL,68,69,70,71,72,73,74,75,76,77      ! A35
!---------------------------
!VOLUMES
!---------------------------
ASEL,S,AREA,,1
ASEL,A,AREA,,2
ASEL,A,AREA,,3
ASEL,A,AREA,,4
ASEL,A,AREA,,5
ASEL,A,AREA,,6
ASEL,A,AREA,,7
ASEL,A,AREA,,8
ASEL,A,AREA,,9
ASEL,A,AREA,,10
ASEL,A,AREA,,11
ASEL,A,AREA,,12
ASEL,A,AREA,,13
ASEL,A,AREA,,14
ASEL,A,AREA,,15
ASEL,A,AREA,,16
ASEL,A,AREA,,17
ASEL,A,AREA,,18
ASEL,A,AREA,,19
ASEL,A,AREA,,20
ASEL,A,AREA,,21
ASEL,A,AREA,,22
ASEL,A,AREA,,23
ASEL,A,AREA,,24
```

```
ASEL,A,AREA,,25
ASEL,A,AREA,,26
ASEL,A,AREA,,27
ASEL,A,AREA,,28
ASEL,A,AREA,,29
ASEL,A,AREA,,30
ASEL,A,AREA,,31
ASEL,A,AREA,,32
ASEL,A,AREA,,33
ASEL,A,AREA,,34
ASEL,A,AREA,,35
VA,ALL
!---------------------------
! Meshing
!---------------------------
I=W/15      ! coarse meshing
Q=W/25      ! intermediate meshing
L=W/50      ! fine-intermediate meshing
G=W/65      ! fine meshing
Y=0.5       ! finest mesh
Kesize,1,G
Kesize,2,G
Kesize,3,G
Kesize,4,Y
Kesize,5,Y
Kesize,6,G
Kesize,7,G
Kesize,8,G
Kesize,9,G
Kesize,10,G
Kesize,11,G
Kesize,12,G
Kesize,13,G
Kesize,14,Y
Kesize,15,Y
Kesize,16,G
Kesize,17,Y
Kesize,18,G
Kesize,19,G
Kesize,20,G
```

Kesize,21,G

Kesize,22,G

Kesize,23,G

Kesize,24,G

Kesize,25,G

Kesize,26,G

Kesize,27,G

Kesize,28,G

Kesize,29,G

Kesize,30,Q

Kesize,31,Q

Kesize,32,Q

Kesize,33,Q

Kesize,34,Q

Kesize,35,Q

Kesize,36,Q

Kesize,38,Q

Kesize,39,Q

Kesize,40,Q

Kesize,41,Q

Kesize,42,I

Kesize,44,I

Kesize,45,I

Kesize,46,I

Kesize,47,I

Kesize,48,I

Kesize,49,I

Kesize,50,I

Kesize,51,I

Kesize,52,I

Kesize,53,I

LESIZE,5,G

LESIZE,9,G

LESIZE,50,L

LESIZE,70,L

LESIZE,40,L

LESIZE,41,L

LESIZE,60,L

LESIZE,61,L

LESIZE,52,L

```
LESIZE,72,L
LESIZE,42,L
LESIZE,43,L
LESIZE,62,L
LESIZE,63,L
!---------------------------
! Mesh settings
!---------------------------
MSHAPE,1,3D
MSHKEY,0
!*
CM,_Y,VOLU
VSEL, , , ,       1
CM,_Y1,VOLU
CHKMSH,'VOLU'
CMSEL,S,_Y
!*
VMESH,_Y1
!*
CMDELE,_Y
CMDELE,_Y1
CMDELE,_Y2
!---------------------------
! Boundary conditions
!---------------------------
! Boundary conditions for symmetry
ASEL,S,AREA,,2
ASEL,A,AREA,,3
ASEL,A,AREA,,4
NSLA,S,1
D,ALL,UY,0    ! displacement on selected nodes in direction Y  is equal 0
ASEL,S,AREA,,13
ASEL,A,AREA,,23
ASEL,A,AREA,,33
NSLA,S,1
NPLOT
D,ALL,UX,0    ! displacement on selected nodes in direction X  is equal 0
! Boundary condition instead of support
Lsel,s,line,,57
Nsll,s,1
```

```
D,ALL,UZ,0      ! displacement on selected nodes in direction Z is equal 0
D,ALL,UX,0      ! displacement on selected nodes in direction X is equal 0
!loading
Lsel,s,line,,10
Nsll,s,1
*GET,POCET,NODE,0,COUNT
F,ALL,FZ,-P/POCET
allsel,all
/solu
solve
EPLOT
FINISH
/POST1
! Central line
Lsel,s,line,,12    ! selecting lines where the nodes are attached for stress syy
Nsll,s,1
nplot
!Line in the flange
Lsel,a,line,,17    ! selecting lines where the nodes are attached !for stress syy
Nsll,s,1
nplot
! RESULTS TO FILE
FILENAME1='PATH_MIDDLE_%W%_%a_W%'
FILENAME2='PATH_FLANGE_%W%_%a_W%'
! Central Line
FLST,2,2,1
FITEM,2,node(B,0,a)          ! nodes coordinates x,y,z
FITEM,2,node(B,0,t)
PATH,cesta,2,50,50,          ! cesta is the name of the path
PPATH,P51X,1
PDEF,sy,S,Y,AVG !stress SY
PAGET,bbb,TABLE              ! values are inserted into a table
PAGET,lll,LABELS
/nopr
/outp,temp,inp
/com, *cfopen,C:\Users\Jorge\Desktop\Jorge-TFG\Results\%FILENAME1%,txt  !filename
/com, *vwrite
/com, (5x,'LENGHT',10x,'SY')        ! label on the top
/com, *vwrite,bbb(1,4),bbb(1,5)     ! position in the table
/com, (3E15.6)                      ! numerical format
```

```
/com, *cfclos
/outp
/inp,temp,inp
/gopr
! Lateral line
FLST,2,2,1
FITEM,2,node(B/2,0,a)                    ! nodes coordinates x,y,z
FITEM,2,node(B/2,0,t)
PATH,cesta1,2,50,50,                     ! cesta is the name of the path
PPATH,P51X,1
PDEF,sy,S,Y,AVG !stress SY
PAGET,ccc,TABLE                          ! values are inserted into a table
PAGET,kkk,LABELS
/nopr
/outp,temp,inp
/com,  *cfopen,C:\Users\Jorge\Desktop\Jorge-TFG\Results\%FILENAME2%,txt  !FILE  NAME
(VYSL)
/com, *vwrite
/com, (5x,'delka',10x,'SY')              ! label on top
/com, *vwrite,ccc(1,4),ccc(1,5)          ! position in the table
/com, (3E15.6)                           ! numerical format
/com, *cfclos
/outp
/inp,temp,inp
/gopr
```

Annex III: APDL Macro for the 3PBT in the UPE profile

```
! Macro for 3D calculation of stresses in Standard UPE beam in a 3PBT<
/clear
/PREP7
/PNUM,KP,1
/PNUM,LINE,1
/PNUM,AREA,1
/PNUM,VOLU,1
/PBC,ALL,,1
! Only one quarter of the specimen will be modelled by using symmetry
W=80        ! height of the specimen
S_W=3       ! S/W ratio
B=50        ! length of the flange
e=4         ! thickness of the web
t=7         ! thickness of the flange
r=10        ! radius of the flange to web
a_W= 0.03   ! a/W
a= a_W*W    ! crack length
S=S_W*W/2 ! 1/2 of the span
P=100/2     ! 1/2 of the load
!--------------------------
! Characteristics of the material
!--------------------------
UIMP,1,EX, , ,210e3,      ! Young's modulus
UIMP,1,NUXY, , ,0.3,      ! Poisson's ratio
!--------------------------
! Element type
!--------------------------
ET,1,SOLID186
KEYOPT,1,2,0
KEYOPT,1,3,0
KEYOPT,1,6,0
KEYOPT,1,8,0
!--------------------------
! Keypoints
!--------------------------
! Cross section in the crack
K,1,0,0,0
K,2,0,0,a
```

K,3,0,0,t

K,4,B/2,0,t

K,5,B-e-r,0,t

K,6,B-e,0,t+r

K,7,B-e-r,0,t+r

K,8,B-e,0,W-t-r

K,9,B-e-r,0,W-t

k,10,B-e-r,0,W-t-r

K,11,0,0,W-t

K,12,0,0,W

K,13,B,0,W

K,14,B,0,t

K,15,B,0,a

K,16,B,0,0

K,17,B/2,0,a

! Cross section located at S/8 from the crack

K,18,0,S/8,0

K,19,0,S/8,t

K,20,B-e-r,S/8,t

K,21,B-e,S/8,t+r

K,22,B-e-r,S/8,t+r

K,23,B-e,S/8,W-t-r

K,24,B-e-r,S/8,W-t

k,25,B-e-r,S/8,W-t-r

K,26,0,S/8,W-t

K,27,0,S/8,W

K,28,B,S/8,W

K,29,B,S/8,0

! Cross section located at 7S/8 from the crack; in the support

K,30,0,7*S/8,0

K,31,0,7*S/8,t

K,32,B-e-r,7*S/8,t

K,33,B-e,7*S/8,t+r

K,34,B-e-r,7*S/8,t+r

K,35,B-e,7*S/8,W-t-r

K,36,B-e-r,7*S/8,W-t

k,37,B-e-r,7*S/8,W-t-r

K,38,0,7*S/8,W-t

K,39,0,7*S/8,W

K,40,B,7*S/8,W

K,41,B,7*S/8,0

! Cross section at the end of the beam

K,42,0,S+1/6*S,0

K,43,0,S+1/6*S,t

K,44,B-e-r,S+1/6*S,t

K,45,B-e,S+1/6*S,t+r

K,46,B-e-r,S+1/6*S,t+r

K,47,B-e,S+1/6*S,W-t-r

K,48,B-e-r,S+1/6*S,W-t

k,49,B-e-r,S+1/6*S,W-t-r

K,50,0,S+1/6*S,W-t

K,51,0,S+1/6*S,W

K,52,B,S+1/6*S,W

K,53,B,S+1/6*S,0

!---------------------------

! Lines

!---------------------------

L,1,2	! L1
L,2,3	! L2
L,3,4	! L3
L,4,5	! L4
ARC,5,6,7,r	! L5
L,6,8	! L6
ARC,8,9,10,r	! L7
L,9,11	! L8
L,11,12	! L9
L,12,13	! L10
L,13,14	! L11
L,14,15	! L12
L,15,16	! L13
L,16,1	! L14
L,15,17	! L15
L,2,17	! L16
L,4,17	! L17
L,1,18	! L18
L,3,19	! L19
L,5,20	! L20
L,6,21	! L21
L,8,23	! L22
L,9,24	! L23

L,11,26	! L24
L,12,27	! L25
L,13,28	! L26
L,16,29	! L27
L,18,19	! L28
L,19,20	! L29
ARC,20,21,22,r	! L30
L,21,23	! L31
ARC,23,24,25,r	! L32
L,24,26	! L33
L,26,27	! L34
L,27,28	! L35
L,28,29	! L36
L,29,18	! L37
L,18,30	! L38
L,19,31	! L39
L,20,32	! L40
L,21,33	! L41
L,23,35	! L42
L,24,36	! L43
L,26,38	! L44
L,27,39	! L45
L,28,40	! L46
L,29,41	! L47
L,30,31	! L48
L,31,32	! L49
ARC,32,33,34,r	! L50
L,33,35	! L51
ARC,35,36,37,r	! L52
L,36,38	! L53
L,38,39	! L54
L,39,40	! L55
L,40,41	! L56
L,41,30	! L57
L,30,42	! L58
L,43,31	! L59
L,44,32	! L60
L,45,33	! L61
L,47,35	! L62
L,48,36	! L63

L,50,38	! L64
L,51,39	! L65
L,52,40	! L66
L,53,41	! L67
L,42,43	! L68
L,43,44	! L69
ARC,44,45,46,r	! L70
L,45,47	! L71
ARC,47,48,49,r	! L72
L,48,50	! L73
L,50,51	! L74
L,51,52	! L75
L,52,53	! L76
L,53,42	! L77
L,5,14	! L78

```
!---------------------------
! Areas
!---------------------------
```

AL,1,16,15,13,14	! A1
AL,2,3,17,16	! A2
AL,17,15,12,78,4	! A3
AL,78,11,10,9,8,7,6,5	! A4
AL,1,2,19,28,18	! A5
AL,19,29,20,3,4	! A6
AL,20,30,21,5	! A7
AL,21,6,22,31	! A8
AL,22,7,23,32	! A9
AL,23,33,24,8	! A10
AL,24,9,25,34	! A11
AL,25,10,26,35	! A12
AL,26,36,27,11,13,12	! A13
AL,37,18,14,27	! A14
AL,28,39,48,38	! A15
AL,39,29,40,49	! A16
AL,30,41,50,40	! A17
AL,41,31,42,51	! A18
AL,42,43,32,52	! A19
AL,43,33,44,53	! A20
AL,44,34,45,54	! A21
AL,45,35,46,55	! A22

```
AL,46,36,47,56                          ! A23
AL,38,37,47,57                          ! A24
AL,58,48,59,68                          ! A25
AL,59,49,60,69                          ! A26
AL,60,50,61,70                          ! A27
AL,61,51,62,71                          ! A28
AL,62,52,63,72                          ! A29
AL,63,53,64,73                          ! A30
AL,64,54,65,74                          ! A31
AL,65,55,66,75                          ! A32
AL,66,76,67,56                          ! A33
AL,58,57,67,77                          ! A34
AL,68,69,70,71,72,73,74,75,76,77        ! A35
!---------------------------
! Volumes
!---------------------------
ASEL,S,AREA,,1
ASEL,A,AREA,,2
ASEL,A,AREA,,3
ASEL,A,AREA,,4
ASEL,A,AREA,,5
ASEL,A,AREA,,6
ASEL,A,AREA,,7
ASEL,A,AREA,,8
ASEL,A,AREA,,9
ASEL,A,AREA,,10
ASEL,A,AREA,,11
ASEL,A,AREA,,12
ASEL,A,AREA,,13
ASEL,A,AREA,,14
ASEL,A,AREA,,15
ASEL,A,AREA,,16
ASEL,A,AREA,,17
ASEL,A,AREA,,18
ASEL,A,AREA,,19
ASEL,A,AREA,,20
ASEL,A,AREA,,21
ASEL,A,AREA,,22
ASEL,A,AREA,,23
ASEL,A,AREA,,24
```

```
ASEL,A,AREA,,25
ASEL,A,AREA,,26
ASEL,A,AREA,,27
ASEL,A,AREA,,28
ASEL,A,AREA,,29
ASEL,A,AREA,,30
ASEL,A,AREA,,31
ASEL,A,AREA,,32
ASEL,A,AREA,,33
ASEL,A,AREA,,34
ASEL,A,AREA,,35
VA,ALL
!---------------------------
! Meshing
!---------------------------
I=W/10      ! coarse meshing
Q=W/25      ! intermediate meshing
L=W/20      ! fine-intermediate meshing
G=W/45       ! fine meshing
Y=0.5        ! finest mesh
Kesize,1,G
Kesize,2,G
Kesize,3,G
Kesize,4,Y
Kesize,5,Y
Kesize,6,G
Kesize,7,G
Kesize,8,G
Kesize,9,G
Kesize,10,G
Kesize,11,G
Kesize,12,Y
Kesize,13,G
Kesize,14,Y
Kesize,15,Y
Kesize,16,G
Kesize,17,Y
Kesize,18,G
Kesize,19,G
Kesize,20,G
```

Kesize,21,G

Kesize,22,G

Kesize,23,G

Kesize,24,G

Kesize,25,G

Kesize,26,G

Kesize,27,G

Kesize,28,G

Kesize,29,G

Kesize,30,Q

Kesize,31,Q

Kesize,32,Q

Kesize,33,Q

Kesize,34,Q

Kesize,35,Q

Kesize,36,Q

Kesize,38,Q

Kesize,39,Q

Kesize,40,Q

Kesize,41,Q

Kesize,42,I

Kesize,44,I

Kesize,45,I

Kesize,46,I

Kesize,47,I

Kesize,48,I

Kesize,49,I

Kesize,50,I

Kesize,51,I

Kesize,52,I

Kesize,53,I

LESIZE,5,G

LESIZE,9,G

LESIZE,50,L

LESIZE,70,L

LESIZE,40,L

LESIZE,41,L

LESIZE,60,L

LESIZE,61,L

LESIZE,52,L

```
LESIZE,72,L
LESIZE,42,L
LESIZE,43,L
LESIZE,62,L
LESIZE,63,L
!--------------------------
! Mesh settings
!--------------------------
! Meshing commands obtained in ANSYS
MSHAPE,1,3D
MSHKEY,0
!*
CM,_Y,VOLU
VSEL, , , ,       1
CM,_Y1,VOLU
CHKMSH,'VOLU'
CMSEL,S,_Y
!*
VMESH,_Y1
!*
CMDELE,_Y
CMDELE,_Y1
CMDELE,_Y2
!--------------------------
! Boundary conditions
!--------------------------
! Boundary conditions for symmetry
ASEL,S,AREA,,2
ASEL,A,AREA,,3
ASEL,A,AREA,,4
NSLA,S,1
D,ALL,UY,0          ! displacement on selected nodes in direction Y is equal to 0
!Boundary conditions instead of support
Lsel,s,line,,57
Nsll,s,1
D,ALL,UZ,0          ! displacement on selected nodes in direction Z is to equal 0
D,ALL,UX,0          ! displacement on selected nodes in direction X is to equal 0
!loading
Lsel,s,line,,10
Nsll,s,1
```

```
*GET,POCET,NODE,0,COUNT
F,ALL,FZ,-P/POCET
allsel,all
/solu
solve
EPLOT
FINISH
/POST1
! Central line
Lsel,s,line,,12              ! selecting lines where the nodes are attached for stress syy
Nsll,s,1
nplot
!Line in the flange
Lsel,a,line,,17              ! selecting lines where the nodes !are attached for stress syy
Nsll,s,1
nplot
! Results to file
FILENAME1='PATH_MIDDLE_%W%_%a_W%'
FILENAME2='PATH_FLANGE_%W%_%a_W%'
! Central Line
FLST,2,2,1
FITEM,2,node(B,0,a)     ! nodes coordinates x,y,z
FITEM,2,node(B,0,t)
PATH,cesta,2,50,50,      ! cesta is the name of the path
PPATH,P51X,1
PDEF,sy,S,Y,AVG          ! stress SY
PAGET,bbb,TABLE         ! values inserted into a table
PAGET,lll,LABELS
/nopr
/outp,temp,inp
/com,   *cfopen,C:\Users\Jorge\Desktop\Jorge-TFG\Results\%FILENAME1%,txt  !FILE   NAME
(VYSL)
/com, *vwrite
/com, (5x,'LENGHT',10x,'SY')                ! label on top
/com, *vwrite,bbb(1,4),bbb(1,5)             ! position in the table
/com, (3E15.6)                              ! numerical format
/com, *cfclos
/outp
/inp,temp,inp
/gopr
```

```
! Lateral line
FLST,2,2,1
FITEM,2,node(B/2,0,a)   ! nodes coordinates x,y,z
FITEM,2,node(B/2,0,t)
PATH,cesta1,2,50,50,     ! cesta is the name of the path
PPATH,P51X,1
PDEF,sy,S,Y,AVG !stress SY
PAGET,ccc,TABLE
PAGET,kkk,LABELS
/nopr
/outp,temp,inp
/com,   *cfopen,C:\Users\Jorge\Desktop\Jorge-TFG\Results\%FILENAME2%,txt   !FILE   NAME
(VYSL)
/com, *vwrite
/com, (5x,'delka',10x,'SY')                  ! label on top
/com, *vwrite,ccc(1,4),ccc(1,5)              ! position in the table
/com, (3E15.6)                               ! numerical format
/com, *cfclos
/outp
/inp,temp,inp
/gopr
```